



*Common Themes, Methods, and Applications
in Multiscale Science*

Los Alamos
NATIONAL LABORATORY

*Los Alamos National Laboratory is operated by the University of California
for the United States Department of Energy under contract W-7405-ENG-36.*

An Affirmative Action/Equal Opportunity Employer

This report was prepared as an account of work sponsored by an agency of the United States Government. Neither The Regents of the University of California, the United States Government nor any agency thereof, nor any of their employees, makes any warranty, express or implied, or assumes any legal liability or responsibility for the accuracy, completeness, or usefulness of any information, apparatus, product, or process disclosed, or represents that its use would not infringe privately owned rights. Reference herein to any specific commercial product, process, or service by trade name, trademark, manufacturer, or otherwise, does not necessarily constitute or imply its endorsement, recommendation, or favoring by The Regents of the University of California, the United States Government, or any agency thereof. The views and opinions of authors expressed herein do not necessarily state or reflect those of The Regents of the University of California, the United States Government, or any agency thereof. Los Alamos National Laboratory strongly supports academic freedom and a researcher's right to publish; as an institution, however, the Laboratory does not endorse the viewpoint of a publication or guarantee its technical correctness.

*Common Themes, Methods, and Applications
in Multiscale Science*

George A. Baker, Jr.

CONTENTS

1. Introduction	2
2. One Spatially-Isolated, Mesoscopic Scale	3
3. One Dispersed, Mesoscopic Scale	9
4. Many Mesoscopic Scales	34
5. No Fixed Scale	61
6. Turbulence	68
7. General Methods	73
8. Applications	94

Common Themes, Methods, and Applications in Multiscale Science

by

George A. Baker, Jr.

ABSTRACT

In 1993, under the leadership of Richard Slansky, the T-Division Director, an initiative was started to facilitate cross communications and interactions between a large number of different workers who were, from their own perspectives and with regard to their own challenges, in fact working on very difficult problems which involved multiple size and time scales. The realization of this common element had the potential for valuable mutual interaction. His initiative led initially to a “competency development initiative” and subsequently to a broadening recognition of the importance of multiscale science and a broadening application of it to problems and concerns inherent in significant fields of endeavor at the Los Alamos National Laboratory. One of the aspects of this effort was a series of meetings which emphasized cross communication between the workers. It was realized early on that this cross communication would be far more effective, considering the difficult technical nature and that the range of the material was well outside the area of specialization of individual members of the group, if notes were taken, written up, and disseminated. This report represents the collection of these notes.

1. Introduction

It seems to me that the various multiscale problems that we have heard about group themselves naturally into four types for the purposes of seeking common elements and possible cross-fertilization of methods. Any such organization is bound to suffer from imperfections of classification as physics problems by their nature tend to overlap each other in various ways. First, however, all the problems share the features of having a well-defined microscopic scale with known equations of motion. Next, they all have mesoscopic scale effects. There may be one, or more, or even an infinite number of mesoscopic scales in the problem. Finally there is the macroscopic scale, which may be either bland, or intrinsically mixed up with infinitely long-ranged, mesoscopic scales, or long-ranged force behavior. These groups of problems are: **(I)** Problems in which there is basically one mesoscopic scale, and it occurs in spatially isolated form. It seems to me that in this case, the various types of adaptive grid methods are rather successful and represent an effective approach. **(II)** Problems in which there is basically one mesoscopic scale, but its effects are dispersed throughout the whole system. So far, these problems are being treated by heroic numerical computation. It seems to me that there are other possible approaches which have some chance of reducing the numerical challenge and can be explored in the future. **(III)** Problems with not just one but several mesoscopic scales. These problems share with those of type **(II)**, the approach of heroic numerical computation. They differ in that it seems to be that the mesoscopic behavior itself is what is of the most direct interest. Here it looks to me like there are good opportunities for cross-fertilization and perhaps some new approaches. **(IV)** Problems without any well-defined scale beyond the microscopic. Here, either through the build-up of long-range correlations via the dynamics, or via a long range force, “all” scales are important. In problems of this character, the ideas of scale-scale interaction, such as found in renormalization group theory should be beneficial.

The problem of turbulence as it is varied through its defining parameters seems to be characterized by types **II–IV**, and so I group it by itself in its own category. Additionally, I have sometimes grouped the presentations on problems which manifestly have many mesoscopic scales in category **II** as those presentations seem to me to be primarily aimed at just one mesoscopic scale (or lumping all the mesoscopic scales into one category).

We have also heard a number of talks which were devoted to methods, and rather than segregate them under an appropriate topic, I have put them in a group by themselves.

Finally, we have heard several discussions on the applications of multiscale science to problems of genuine practical concern. Some of these applications are ongoing, and some of the discussions relate to fertile fields for future endeavor.

2. One Spatially-Isolated, Mesoscopic Scale

Presentation by Joel Dendy

This presentation was on the multigrid methods. This application is to the solution of Poisson's equation

$$\nabla^2 U = F$$

subject to the boundary condition

$$U = g.$$

One could use the Gauss-Seidel method (*i.e.* the method of successive displacements or the relaxation method). The method consists of replacing Poisson's equation with a difference equation on a space lattice. The simplest representation of the difference operator is,

$$\Delta U_{i,j} = 4U_{i,j} - (U_{i,j+1} + U_{i,j-1} + U_{i+1,j} + U_{i-1,j}).$$

Then one selects an order and systematically runs through the lattice successively replacing each U with the average of the U 's from its nearest neighbors sites on the lattice. This procedure is iterated until convergence is obtained. Large-scale initial deviations from the final state relax rather slowly to the answer by this method. The multigrid method approaches this problem by relaxation on successively coarser grids. The \mathbf{V} pattern was recommended. That is, one moves at successive steps from a fine grid to a very coarse one and then back to a fine one. This procedure is repeated until convergence is obtained.

One of the problems which is being studied is the problem of rapid changes in the diffusion constant in an equation of the character

$$-\vec{\nabla} \cdot (D\vec{\nabla}U) = F.$$

It was reported that conservation of flux through an anisotropy was better than linear averaging. This is fine in one dimension. However one must use line relaxation in two dimensions and alternating plane relaxation in three dimensions which was alleged to be a real pain. The relationship between the merits of the multigrid method and those of the "large time step" implicit methods was not discussed.

Another procedure along the same line is to refine the grid in regions where difficulties are detected. The multigrid method was reported to have great flexibility. It can handle "dead regions" and can do logically rectangular grids. The speaker expressed interest in doing reservoir modeling and modeling of contaminant transport.

Presentation by Alan Glasser

This presentation represents joint work with Andrew Kuprat and is on the topic of moving finite elements, which was reported to be a "continuously adaptive method" for computational fluid dynamics. The multiple scales in this problem are the microscopic scale, the region inside a shock (or mesoscopic scale), and the domain (or macroscopic

scale). The problem addressed concerns interacting, moving shocks. The method of approach is an adaptive grid method to resolve the thin, moving fronts. The finite elements are triangles in two dimensions and tetrahedra in three. The grid is flexible, and the elements are irregularly connected. *Linear interpolation is used inside each finite element.* The method was reported to be applicable to very general fluid equations.

A video of some of the results was shown. It showed a “Tsunami in a Bathtub” and graphically illustrated the interaction of shock waves. The general form of the equations describing the fluid motion is

$$\frac{\partial \vec{u}}{\partial t} + \vec{\nabla} \cdot \overleftrightarrow{F} = \vec{S}$$

$$\overleftrightarrow{F} = \overleftrightarrow{C}(t, \vec{x}, \vec{u}) - \overleftrightarrow{D}(t, \vec{x}, \vec{u}) \cdot \overleftarrow{\nabla} \vec{u}$$

$$\vec{S} = \vec{S}(t, \vec{x}, \vec{u}, \overleftarrow{\nabla} \vec{u}),$$

where \vec{x} is the spatial position, \vec{u} is a vector velocity field, and the dyadics \overleftrightarrow{C} and \overleftrightarrow{D} and the source vector \vec{S} are particular to the case under study. The conventional Galerkin methods and the moving finite element method were compared with emphasis on the relative merits of the latter. Mention was made of the need to add artificial internodal viscosity, grid tension, and pressure to cure a singular mass matrix, node jitter, and time step crash. Progress was reported in the area of “graph massage.” Graph is understood here to be a linear graph, which is a collection of vertices and bonds connecting them. This procedure dynamically adds a new node when the finite element either becomes too elongated or when adjacent cells have too much “break.” (I did not hear a precise definition of “break.”) The procedure also deletes nodes when adjacent cells have too little “break.” This procedure has been successful at getting out of “grid tangling.”

The answer sought is the time dependent behavior. There is a need to represent the behavior inside the shocks, or perhaps only the integral over certain aspects of the behavior, because the chemistry is dependent on it in a highly nonlinear manner. Involved is the fully implicit solution of large, sparse Jacobians combining both flow and dissipation. The sparseness is irregular. The need for implicit solutions arises from the fact that the partial differential equations are stiff. (Stiff means, briefly, the existence of at least two highly disparate time scales.)

Presentation by Manjit Sahota

This presentation was on the moving finite volume method. Unstructured grids are used, and the method is reported to be good for modeling a complex geometry, such as the illustrative example of a NASA rocket booster with 6 jet nozzles attached. The problems which are addressed involve turbulence, chemistry, and sprays. The scheme is a “node-centered” scheme and uses tetrahedra or hexahedra. An important aspect for adapting this method to parallel computation is to minimize the inter-processor communication volume. The problem then is how to split up the computations among the different central processors. A physical analogy might be to imagine N immiscible fluids with interfacial tension to minimize their area of contact (the area over which the effects of the computation

in one processor affects that of another). For a long cylindrical problem the different processors would each do a salami slice. For more compact geometries, the solution would be more complex. Computationally one looks at the eigenvector for the smallest eigenvalue of the Laplacian of the connectivity. This sort of optimization leads to a speed-up of a factor of 5–10 on the CM-5. The major obstacles are how to put unstructured grids on a parallel machine and how to do an implicit method on a parallel machine.

Presentation by Joel Dendy

The multigrid method is a nice mechanism to deal with spatially isolated mesoscopic scales. It is usual, in this method, to start with a logically rectangular grid, but one does not have to do so. The competition is the unstructured grid method, where the points are described in a random manner with respect to their address index. That is to say, the indices of neighboring points are not related to the index of the central point. The structure of the grid is contained in a table of neighbors, which is often called the adjacency matrix.

It was reported that at NASA Langley, they use the unstructured grid approach on the Euler equations for flow. In the past they had used the multigrid approach. It is hard to get a good solver for the unstructured grid approach. By a “solver” is meant something that produces the values at the next time step. In a one-dimensional subset of a Laplacian problem, for example, the relevant set of equations is a tridiagonal, inhomogeneous set. The standard lower-left, upper-right triangular-factorization method provides the required solution in relatively few operations and is an example of a “solver.” Not having a good solver in this case seems to mean that the magnitude of the principal error is only reduced by a factor of .9998 in each iteration, which then means that a method which reduced the magnitude of the principal error by a factor of .98 would be a tremendous improvement. The folks at Langley used a Runge-Kutta smoother. The problem is a hyperbolic problem which is unstable. The idea of the smoother is to introduce an artificial time and to use the Runge-Kutta method of intergration for an ordinary differential equation to smooth the problem. Then an explicit method like SOR (Successive Over Relaxation) is used. Another technique is to use a coarse grid to get to the steady state, and then a finer grid to improve the accuracy.

The panelist said that he had been using the multigrid method to get simpler “solvers.” In petro-engineering systems one can’t use implicit-pressure, otherwise-explicit methods, but fully implicit methods must be used. These methods are more difficult to develop, but are required by the interconnections of the variables in this sort of problem.

Presentation by Alan Glasser

The work reported is in collaboration with Kuprat. In this project, the method of an unstructured grid of triangles is used. The work was started with moving finite elements. These triangles had an aspect ratio of 200. The variables are stored at the nodes (vertices) of the triangles. This procedure is good for time-dependent problems. Here use is made of

an adequate representation of the Rankine-Hugoniot jump conditions,* instead of resolving the shock front directly. (This procedure is only valid when the details of the shock front are not otherwise necessary, as may be the case when chemical reactions in the shock front are important.) Originally the panelist thought** that moving finite elements would be a panacea. The key issue is the nature of the flow across the separatrix between the region of closed magnetic field lines and the region of open field lines. There is flow to the core with Mach 1 and Alan gets transport coefficients with a ratio of 10^5 between parallel to and perpendicular to the field lines, whence the aspect ratios of 200. The use of unstructured triangular grids where the structure of the flow is built into the metric leads to a length anisotropy which is proportional to the square root of the transport coefficient anisotropy. There are conflicting requirements between the time-dependent versus the time-independent parts. One wants to advance the shock front by many shock thicknesses per time step, but in the time-independent parts the moving finite elements do not work as efficiently. Thus there is a problem here to combine moving finite elements and the unstructured grid method.

Presentation by Manjit Sahota

This panelist discussed his work on the controlled-volume, finite-element method. Unstructured grids are used, and the variables are node centered. The full 3-dimensional Navier-Stokes equation (with turbulence) is used. The implementation allows various finite elements, but they must have ruled surfaces. (A ruled surface can be visualized by a set of closely spaced tightly stretched strings, like a bent or twisted harp, for example.) Applications are made to automotive design, in the cylinders (combustion), under hood cooling (flow through the radiator, etc.), and external aerodynamics. There is a three-year contract for this work. It uses adaptive grid refinement, and multigrid methods are also being investigated. The work is being framed to a massively parallel computing

* According to Prandtl, in the theory of normal shock waves the simplest case of a discontinuous compression is the normal, steady-state shock wave. Here the gas is initially flowing in parallel lines with a velocity q_1 , pressure p_1 , and volume v_1 . At a plane interface it is compressed into a smaller volume v_2 , the velocity is reduced to q_2 and the pressure increases to p_2 . This phenomenon is governed by (1) the equation of continuity, $m = q_1/v_1 = q_2/v_2$, where m is the mass per second flowing through a unit area, (2) the momentum equation $m(q_1 - q_2) = p_2 - p_1$, and (3) the energy equation, $\frac{1}{2}q_1^2 + i_1 = \frac{1}{2}q_2^2 + i_2$, where i is the enthalpy or total heat. If m and the q 's are eliminated from these equations, then we get the Rankine-Hugoniot condition,

$$\frac{1}{2}(v_1 + v_2)(p_2 - p_1) = i_2 - i_1.$$

This form is completely expressible in terms of the equation of state as enthalpy is a thermodynamic function of p and v , for example. The p, v curve which it gives is called the Hugoniot or dynamic adiabetic.

** See Glasser's previous presentation.

environment. There are multiscale aspects in the cylinders, for example, when the fuel sprays in and also in the flow near the valves and in the gaps of the piston rings.

The geometry of these problems is very complex, which suggests the use of unstructured grids. The method of nested, spectral bisections is very useful in these problems in breaking the problem up among different processors in order to minimize communication costs. The method seems to be as follows: In the adjacency matrix place minus the number of nearest neighbors of the i th grid point in the diagonal element A_{ii} and a one in every A_{ij} for which j is a nearest neighbor of i and zero otherwise. Note that $(1, 1, \dots, 1)$ is always an eigenvector with zero eigenvalue. Now look for the next smallest eigenvalue. Bisect the grid points accordingly as the sign of its eigenvector elements is positive or negative. This procedure divides the system into two such systems and gives the dominant large-scale structure. It has the property that it basically minimizes the communication time. This procedure can be generalized to divide the system into more blocks. One needs one block per processor. In one example, the panelist reported that originally the communication time was 92%, but after applying this method, he got it down to 8%.

Presentation by James Hammerberg

Title: Friction and Nonequilibrium Deformations at Interfaces

The speaker said that the work reported was the result of a collaborative effort involving him and Brad Holian, T-12, Peter Lomdahl, T-11, Joanna Röder, T-11, Alan Bishop, T-11, Shujia Zhou, X-NH, Bard Bennett, X-NH, C. E. Ragan, X-TM, Bob Benjamin, DX-3, and Paul Rightley, DX-3. The goal of this endeavor is a macroscopic model of interfacial slip for use in the Laboratory's "hydro codes." An important concept in this study is that of an interface. More detail on this topic will be given later. A key quantity is the tangential force along the interface, $F_{\text{tangential}}[p, T, \psi, \dot{\psi}, v_{\text{rel}}]$, where p is the pressure, T is the temperature, ψ is the plastic strain, $\dot{\psi}$ is the plastic strain rate, and v_{rel} is the relative tangential velocity of the interface. It was pointed out that the asperities in the two material surfaces meeting at the interface may deform in a ductile manner. The speaker said there was a possibility of adopting a microstructure, relating to some sort of atomic roughness. He also said that the hope is that highly compressed interfaces are dry metal on metal.

Hammerberg said that there are macroscopic theories of friction, and there are microscopic theories, but there are no mesoscopic theories. The regimes of interest for this talk are: pressures less than approximately 300 kilobars and relative velocities less than approximately $\frac{1}{5}$ of the sound velocity. Hammerberg said that there are molecular dynamics simulations and some lower-dimensional Frankel-Kantarova models.

For two ductile metals in contact and flowing plastically, it is expected that the $\langle F_{\text{tangential}} \rangle = A_{\text{eff}} \tau$, where A_{eff} is the effective area of contact and τ is the flow stress of the weaker of the two materials. For flat interfaces, A_{eff} is just the nominal area and $\langle F_{\text{tangential}} \rangle$ is determined by τ in an adhesive model.

The main pressure dependence of the flow stress enters through the shear modulus, $\tau = \tau_0(T, \psi, \dot{\psi})G(T, p)$. For pressures less than $0.5G$, the speaker said that a reasonable approximation to G is $G = G_0(T) \left(1 + \alpha \frac{p}{G_0}\right)$. Thus the pressure dependence of the

coefficient of friction μ may be deduced to be

$$\mu = \frac{\langle F_{\text{tangential}} \rangle}{F_{\text{normal}}} = \frac{[\langle F_{\text{tangential}} \rangle / A]}{[F_{\text{normal}} / A]} = \frac{\tau_0 G_0}{p} \left(1 + \frac{\alpha p}{G_0} \right).$$

Therefore the speaker said we expect that $\langle F_{\text{tangential}} \rangle$ is an increasing function of pressure at fixed velocity and that the coefficient of friction is a decreasing function of pressure.

Next the speaker turned his attention to molecular dynamic simulations (usually on copper). In two-dimensional simulations there are reservoirs of 20 atomic layers each at the top and at the bottom of the simulated region. The atoms in these reservoirs are constrained to move left and right, respectively, at a velocity u_p . The other atoms are unconstrained. Pressure is applied to the top and bottom to keep the average vertical velocity zero. There is an interface in the middle with atomic scale roughness or asperities. Results were displayed for the coefficient of friction μ for various values of u_p . μ tends to decrease as a function of p . The value of $\langle F_{\text{tangential}} \rangle$ is an increasing function of p for fixed u_p and a decreasing function of velocity for fixed density.

Under the heading of microstructure we saw a plot of $F_{\text{tangential}}$ as a function of time. It shows a “bounce phenomenon.” That is to say it can oscillate strongly and even go negative. It was explained that there is a tendency to stick and then to release. In the release phase, a contrary force is necessary to keep the speed uniform. For velocities greater than about $u_p = 0.5$, the applied tangential force scales as $\langle F_{\text{tangential}}^{(t)} \rangle = F_{\infty} f(\lambda t)$, where $\lambda = h^{-1} \sqrt{F_{\infty} / \rho}$ with h the distance between the interface and the reservoir. In this regime, a region of disordered nanocrystallites is formed, and it diffuses inward. At lower velocities, the surfaces stick and slip at the boundary between the reservoir and a work hardened medium with a large dislocation density. Finally we were shown some slides which illustrated the grain structure at various times for a density of $\rho_0 = 1.27$ and for $u_p = 0.49$.

3. One Dispersed, Mesoscopic Scale

Presentation by Shi-Yi Chen

Lattice-gas and lattice-Boltzmann methods are used for microscopic dynamics in a number of systems. These methods are selected in such a way, it is believed, so as to reproduce correctly the macroscopic dynamics, but not necessarily the microscopic dynamics. Three general scales are perceived as important in this problem: the microscopic, the mesoscopic, and the bulk scales. The topic of spinodal decomposition was discussed. The results obtained involve the study of the domain size as a function of “time” (which means the number of steps in the dynamical simulation of the system) when a system is suddenly quenched across a first order phase boundary. If $R(t)$ is the typical domain size, then the scaling law

$$R(t) \propto t^{0.66}$$

was found.

A further topic discussed was the roughen phenomena of a surface. Again simulations using lattice-gas and lattice-Boltzmann techniques were carried out. Here there are the microscopic, roughness of the surface, and bulk scales. (The possible “thickness of the surface or width of the interfacial density-profile” scale was not discussed.). It has been suggested that the surface behavior could be described by the Kadar-Parisi-Zhang equation,*

$$\frac{\partial h^*}{\partial t} = \nu \nabla^2 h^* + \frac{\lambda}{2} \left(\vec{\nabla} h^* \cdot \vec{\nabla} h^* \right) + \eta(x, t),$$

where η is Gaussian white noise, and h^* is the height of the surface. The analysis of this equation leads to $\alpha = \frac{1}{3}$ whereas numerical simulations suggest $\alpha = 0.63(1 \pm 0.05)$. The role of lattice-gas dynamics and lattice-Boltzmann methods versus the true microscopic dynamics was not discussed.

In this study, the scaling indices are sought, and also what differential equations would be appropriate to describe the important aspects of the behavior. One of the anticipated difficulties is the study of problems involving multiphase flow in complicated geometries.

Presentation by Peter Lomdahl

The work reported is joint work with Bishop and Grønbech-Jensen. This project has as its goal the study of the relaxation to an equilibrium distribution at a prescribed temperature from an initial high-temperature state (quenching) of a number of interesting systems. The method employed is the integration in time of the Langevin equations. One

* I remark that this equation can be linearized by the substitution $\psi = \exp(\lambda h^*/2\nu)$ provided λ and ν are constants. The result is $\partial\psi/\partial\tau = \nabla_{\xi}^2\psi + \psi\eta$, which is of the well-known parabolic type with multiplicative noise. The distance is scaled by $\vec{r} = (\sqrt{\lambda/2\nu^2})\vec{\xi}$, and the time by $t = (\lambda/2\nu)\tau$.

such example is a Josephson junction array, whose Hamiltonian is

$$\mathcal{H} = \frac{1}{2} \sum_{i,j} \pi_{i,j}^2 - E_0 \sum_{i,j} [\cos(\theta_{i,j} - \theta_{i-1,j} - A_{i-1,j;i,j}) + \cos(\theta_{i,j} - \theta_{i,j-1} - A_{i,j-1;i,j})],$$

where the θ 's are phase variables, the π 's are their conjugate momenta, and the sum of the A 's around a plaquette is equal to the number of magnetic flux quanta passing through that plaquette and represents a frustration of the system in the sense of a disruption of the order of the ground state.

A second example is multimillion particle ($10^7 - 10^9$) molecular dynamics. Here the Hamiltonian is

$$\mathcal{H} = \sum_{i=1}^N \frac{p_i^2}{2m_i} + \sum_{i < j} V(|\vec{r}_i - \vec{r}_j|),$$

where the potential is a cut-off, Lennard-Jones potential,

$$V(r) = \begin{cases} 4\epsilon \left[\left(\frac{\sigma}{r}\right)^{12} - \left(\frac{\sigma}{r}\right)^6 \right], & r \leq 2.5\sigma, \\ 0, & r > 2.5\sigma. \end{cases}$$

The Langevin equations are just the Hamilton equations of motion with added terms to represent dissipation and the interaction with a heat bath. In both cases, nonlinear effects cause self-organized, coherent, mesoscopic structures to arise which complicates the relaxation phenomena. Examples could be solitons, dendrites, fractals, cracks, *etc.* Their dynamics control a complex macroscopic response, but they themselves are controlled by the microscopic behavior. There are probably three, distinct scales here: the bulk scale, the fracture scale, and the microdynamic scale. The central problem is to understand the various time scales and how they are related to those length scales.

Presentation by Mac Hyman

Three approaches to multiscale problems were discussed. The first is a numerical approach through adaptive grid methods. This method is used for example in the solution of differential equations: the problem is grided, and where accuracy problems are identified, more mesh points are added, but where the solution is smooth, fewer mesh points are used. In principle, any range of *spatially isolated*, different length scales can be accommodated by this method; however, there are surely practical limits in this regard. This sort of method has found appropriate application in problems involving boundary layers, shock fronts, and combustion fronts. There are three distinct scales here: the microscopic, the layer thickness, and the macroscopic.*

The second approach is "homogenization." Examples of problems to which this approach has been applied are turbulent flow and neutron or heat transport with widely varying (with spatial position) diffusion coefficients. For example, in the study of neutron transport, there could be medium, holes, and rods, each with widely (a factor of 1000 was

* These remarks are expounded more fully in Section 2.

mentioned) different diffusion coefficients. A moment's thought shows that the flow of neutrons will adjust itself to pass preferentially through the regions of high diffusivity. When the diffusivity varies much more rapidly than the desired grid size, the idea of this approach is to replace the original highly nonuniform material with an appropriate, homogenized material which will correctly give the macroscopic flows of interest. Even regular patterns, such as a checkerboard with two different diffusivities can lead to a direction-dependent diffusivity in a homogenized medium, calling for a full diffusion tensor with off-diagonal terms. Equations such as

$$u_t = \vec{\nabla} \cdot (d\vec{\nabla}u)$$

have been well studied, and the appropriate procedures are known, but those involving u_{tt} are not yet under control.*

The third approach involves both analytical and numerical methods. The problem approached is for example one of global ocean modeling. Here most of the energy is in eddies whose size is well below the cell size of the grid. The problem is to try to figure out how to incorporate these effects into the model run on the desired cell size, by for example, the use of a better set of mesoscale equations.**

Presentation by Alan Bishop

The work reported here is joint work with Lomdahl and Grønbech-Jensen. It concentrates exclusively on the Josephson junction array and does not discuss the multimillion particle molecular dynamics. Both topics were discussed by Lomdahl and reported in the Notes for the meeting of March 18, 1994. The Josephson junction array can be described as lying on a red-black checkerboard (plane square lattice). There are superconducting squares (grains) on the black squares and the Josephson junctions lie at the corners where the superconducting grains meet. A magnetic field perpendicular to the plane (excluded from the superconductors by the Meissner effect) passes through the red squares. This structure is topologically equivalent to a plane square lattice with superconducting nodes and Josephson junctions for bonds. A typical size that this collaboration can handle is 128×128 or 256×256 . Each superconducting node has associated with it a phase $\theta_{i,j}$ for its order parameter. The equations of motion of the system can be derived from the Hamiltonian.† They are

$$\begin{aligned} \ddot{\theta}_{i,j} = & \sin(\theta_{i,j+1} - \theta_{i,j} - A_{i,j;i,j+1}) + \sin(\theta_{i,j-1} - \theta_{i,j} - A_{i,j;i,j-1}) \\ & + \sin(\theta_{i+1,j} - \theta_{i,j} - A_{i,j;i+1,j}) + \sin(\theta_{i-1,j} - \theta_{i,j} - A_{i,j;i-1,j}) \\ & - \eta(\dot{\theta}_{i,j+1} + \dot{\theta}_{i,j-1} + \dot{\theta}_{i+1,j} + \dot{\theta}_{i-1,j} - 4\dot{\theta}_{i,j}) + \lambda_{i,j}(t), \end{aligned}$$

* The idea behind this approach is closely related to the idea of the renormalization (semi-)group transformation where the smallest scales are integrated out inducing a mapping in the space of Hamiltonians. The analogous statement here is a mapping in the space of equations. If carried out exactly, the description of the larger scales remains precise, but it is likely that only approximate mappings will be practical. The same sort of remarks apply to the presentation of Shi-Yi Chen above.

** This topic is discussed more fully by D. Holm beginning on the next page.

† See the presentation of P. Lomdahl on the previous two pages.

where the sine terms are the tunneling currents, and the non-Hamiltonian terms are the η terms which are the dissipation, and the λ term is thermal noise which is taken to be independent at different times and to have a spatial correlation equal to the product of 2η times the temperature times the inverse lattice Green's function.* The magnetic field can introduce a degree of frustration. The sum of the A 's around a plaquette (a red square) must equal the magnetic flux passing through the plaquette. This effect can make it impossible to assign values to all the θ 's so that the right hand side of the equation of motion vanishes for all i, j . This situation is what is meant by frustration. In order to describe the ground state it is useful to define a "fractional charge" for each black square. It is

$$q_{i,j} = \text{Mod}(\theta_{i,j+1} - \theta_{i,j} - A_{i,j;i,j+1}) + \text{Mod}(\theta_{i,j-1} - \theta_{i,j} - A_{i,j;i,j-1}) \\ + \text{Mod}(\theta_{i+1,j} - \theta_{i,j} - A_{i,j;i+1,j}) + \text{Mod}(\theta_{i-1,j} - \theta_{i,j} - A_{i,j;i-1,j}),$$

where Mod means to subtract (or add) enough multiples of 2π to keep the result in the range $-\pi < x \leq \pi$. The case, called " $f = \frac{1}{2}$ " which leads to maximum frustration was discussed. Here in the ground state values of $q_{i,j} = \pm \frac{1}{2}$ are what occurs. The mesoscopic disruptions have been identified and are domain walls and vortex-antivortex pairs. Here a domain wall means that two antiferromagnetically ordered regions are out of registry with each other by one lattice spacing. That is to say, it is a wall of two adjacent like-charge states. The simplest vortex-antivortex pair is, for example, a simple interchange between a $q = +\frac{1}{2}$ value and a neighboring $q = -\frac{1}{2}$ case. The relaxation of such systems is studied, and these mesoscopic structures significantly affect this process. Decay of the form $\exp[-(t/\tau)^\beta]$ was reported.

This problem has the microscopic scale, the mesoscopic scale of domain walls and vortex-antivortex pairs, and the macroscopic scale. What is sought is a way to bridge over the "mesoscopic barrier" to go from the microscopic to the macroscopic scales. The problem is currently being explored by large scale numerical computation.

Presentation by Darryl Holm

This presentation represents joint work with Roberto Camassa and is on the Hamiltonian asymptotics for coherent structures in ideal shallow-water flows. Suppose that the bottom is level and B is the quiet water depth. Suppose next that there are waves on the surface with crest separation of L and a crest to trough height of h_0 . Suppose further that the parameter $\delta = B/L \ll 1$, which corresponds to shallow water waves. In addition, it will be assumed that $h_0/B \ll 1$. From these two conditions, it follows at once that $h_0/L \ll 1$, which corresponds to small amplitude waves. The upper surface of the fluid is free with a uniform pressure boundary condition, and its position is $z(x, y, t)$ measured from the quiet water level. The velocities in the horizontal and vertical directions will be denoted by \vec{u} and w , respectively, and c is the "natural" wave speed. An important case

* This noise is a correlated random Markov field. Its type is closely related to Boson field theory. Its efficient generation is of interest in itself, but none of these aspects were discussed.

is ocean modeling. For the wave motion corresponding to the dominant eddies,* we have the following characteristic values:

$$\begin{aligned}
u &\sim 10'\text{s of cm/sec}, & w &\sim 1 \text{ cm/sec} \sim u\delta, \\
L &\sim 10'\text{s of km}, & B &\leq 5 \text{ km} \sim L\delta, \\
c &\sim \sqrt{g \times 4 \text{ km}} = 200 \text{ m/sec}, & u/c &\leq 0.005 = \epsilon \sim \delta^2, \\
h_0 &\sim 10'\text{s of cm}, & h_0/B &\sim 0.00002 \sim \epsilon^2, \text{ and} \\
\text{time scale: } & \frac{L}{\delta\epsilon c} = \frac{1}{\delta\epsilon} \frac{20 \text{ km}}{200 \text{ m/sec}} = \frac{1}{\delta\epsilon} \times 3 \text{ min} \sim 2 \text{ days.}
\end{aligned}$$

Thus for these purposes, the ocean represents a shallow water system with $\delta \approx 0.07$. Relaxing the condition on a level bottom, we allow for the bottom to be given by $z = -b(x, y)$. The system is described by the Euler equations, which are, in dimensionless form,

$$\begin{aligned}
\frac{D\vec{u}}{Dt} + \vec{\nabla}P &= 0, & \frac{D}{Dt} &= \frac{\partial}{\partial t} + \vec{u} \cdot \vec{\nabla} + w \frac{\partial}{\partial z}, \\
\delta^2 \frac{Dw}{Dt} + \frac{\partial P}{\partial z} &= 0, & (\delta \rightarrow 0, \text{ hydrostatic}), & \text{ and} \\
\vec{\nabla} \cdot \vec{u} + \frac{\partial w}{\partial z} &= 0,
\end{aligned}$$

subject to boundary conditions involving $\epsilon = |\vec{u}|/c$, $c = \sqrt{Bg}$, with g the acceleration due to gravity. The case $\epsilon \rightarrow 0$ corresponds to a rigid lid, and $h_0/B = O(\epsilon^2)$.

By expanding in the small quantities appropriate for small-amplitude, shallow-water waves, the equation for the motion of the free surface has been derived as

$$u_t + c_0 u_x - \epsilon \left[\frac{1}{3} u_{xxt} + \frac{3}{2} u u_x + \frac{1}{6} c_0 u_{xxx} \right] = \frac{\epsilon^2}{3} \left[u_x u_{xx} + \frac{1}{2} u u_{xxx} \right].$$

The method of derivation for this equation is reported to be able to retain the basic properties of Euler's equations with a free surface, *i.e.*, the action principal, energy conservation, Kelvin's Theorem, and Galilean invariance for the flat bottom case. As far as this initiative is concerned, we now see only the scale of order L , the mesoscopic scale, and are no longer compelled to work on the scale of order $B = L\delta$, the microscopic scale. This result is an apparently successful effort to breach the mesoscopic barrier.

Presentation by Alan Bishop

Micro \longrightarrow Meso \longrightarrow Macro

* See the presentation by C. Zemach in Section 6.

There are a lot of buzz words attached to the mesoscopic scale such as emergent structure, multiple space, and time scales. It was suggested that local or regional balance is the key, as otherwise one regime will dominate. This would be described by a lower level of approximation. There are three important questions.

1. What are the microscopic mechanisms driving “complexity”? (Examples: competing interactions and coupled fields.)
2. How can mesoscopic structure be described? [Examples: collective modes/reduced models, coupled space and time, relevant “statistical” descriptions such as collective modes plus fluxations (compare with $f(\alpha)^*$), or perhaps image resolutions.] $K - \epsilon$ turbulence modeling of diffusive fluxes was mentioned here.
3. There is interest in “What do the vortex-antivortex pairs, and domain walls *etc.*, do to the macroscopic ‘functionality’?”

Presentation by Gary Doolen

This discussion was on laying-down patterns on two-dimensional surfaces. It seems that electro-deposition of aluminum can form a pattern of cylindrical voids of the order of 10 nanometers in diameter and arbitrary heights which occur at regular intervals. The voids form a hexagonal lattice, and the spacing changes with the voltage. There are a lot of questions. For example what if we vary the substrate? It was mentioned that DARPA will fund laying-down chemistry on 2D surfaces and the growth of these patterns.

If the electric field is varied in time, then we get a cheap, uniform layered-material in this way. One can lay down incredibly complex patterns. Some pictures of chlorine and starch were shown where blobs would grow and bifurcate. Study is also being made of the growth of tubulene. It grows tubes. It will grow and shrink, perhaps in response to local electrical gradients, and it samples space to see where it can grow. All these various phenomena are on the mesoscopic scale. The holy grail of this area is to try to explain mitosis.

Presentation by Neils Grønbech-Jensen

This presentation reflects work by A. Bishop, D. Dominguez, P. Lomdahl, and S. Shenoy as well as the speaker.** The system under study is a three-dimensional network of superconductors connected by Josephson junctions. The system is topologically equivalent to a space lattice with superconducting nodes and Josephson junctions for bonds, but is not one such. Each superconducting node has associated with it a phase θ_{ijk} for its order parameter. The model being discussed is the 3-D RSJ (XY) system. Its equations of motion are

$$\gamma \ddot{\theta}_{ijk} + \sum_{\epsilon} a_{\epsilon} (\dot{\theta}_{ijk} - \dot{\theta}_{ijk+\epsilon}) + \sum_{\epsilon} i_{\epsilon} \sin(\theta_{ijk} - \theta_{ijk+\epsilon}) = \sum_{\epsilon} \lambda_{ijk,\epsilon} + \eta(\delta_{0j0} - \delta_{NX-1,j,0}).$$

* By $f(\alpha)$ is meant the distribution of lengths in a fractal which are greater than α .

** See also the previous presentations by P. Lomdahl and A. Bishop.

The first term is a capacitance term, the sum over ϵ is a sum over nearest neighbors, the second term is a damping term, the third term is the Josephson term, the fourth term is the noise term and the last term is a bias term reflecting a current put in at the bottom and taken out at the top of the system (rectangular parallelepiped). The various relevant parameters and average values are

$$\begin{aligned}\tau &= \frac{\hbar}{2e} \frac{1}{R_{ab} I_{ab}}, \quad \gamma = \frac{2e}{\hbar} C_0 R_{ab}^2 I_{ab}, \quad \eta = I_{\text{bias}}/I_{ab}, \\ a_\epsilon &= R_{ab}/R_\epsilon, \quad i_\epsilon = I_\epsilon/I_{ab}, \quad \langle \lambda_{ijk,\epsilon} \rangle = 0, \quad \text{and} \\ \langle \lambda_{ijk,\epsilon}(t) \lambda_{i'j'k',\epsilon'}(t') \rangle &= 2 \frac{kT}{I_{ab}} \frac{2e}{\hbar} a_\epsilon \delta_{(ijk,\epsilon)(i'j'k',\epsilon')} \delta(t-t').\end{aligned}$$

The subscript ab refers to the horizontal plane. The fundamental ac-Josephson relation is

$$\Delta V_{ij,kl}(t) = \frac{\hbar}{2e} \frac{d}{dt} [\theta_{ij}(t) - \theta_{kl}(t)].$$

The speaker said that he is allowing both dissipative I^R and capacitive I^C currents in addition to the supercurrent I^S , both of which are given in units of I_c as

$$I_{ij,kl}^R = \frac{\Delta V_{ij,kl}}{I_c R} = \frac{\hbar}{2e I_c R} (\dot{\theta}_{ij} - \dot{\theta}_{kl}) \quad \text{and} \quad I_{ij,kl}^C = \frac{C}{I_c} \frac{d}{dt} \Delta V_{ij,kl} = \frac{\hbar C}{2e I_c} (\ddot{\theta}_{ij} - \ddot{\theta}_{kl}).$$

Up to this point, there is no intra-plane coupling in the equations, and one might have been wondering how this work differs from a bunch of independent, one-dimensional problems. The answer is in the electromagnetic field. If we start with the equations

$$\begin{aligned}\frac{\partial \phi}{\partial t} &= \frac{2e}{\hbar} V = \frac{2e}{\hbar} \int_1^2 E_z dz, \\ \frac{\partial \phi}{\partial x} &= \frac{2e}{\hbar} \int_1^2 B_y dz = \frac{2ed}{\hbar} B_y, \quad \text{and} \quad \frac{\partial \phi}{\partial y} = -\frac{2e}{\hbar} \int_1^2 B_x dz = -\frac{2ed}{\hbar} B_x,\end{aligned}$$

where 1 lies in the lower plane below the gap plus the penetration depth, and 2 similarly lies in the upper plane above the gap plus the penetration depth, and d is the gap plus twice the penetration depth. By treating the horizontal directions as continuous for the moment and then by taking some partial derivatives and using Maxwell's equations, we come to the basic equation

$$\frac{\hbar}{2ed\mu} \left(\frac{\partial^2 \phi}{\partial x^2} + \frac{\partial^2 \phi}{\partial y^2} \right) = J_0 \sin \phi + I_b G_\alpha \frac{\hbar}{2e} \frac{\partial \phi}{\partial t} + \frac{\epsilon \hbar}{2et_0 x} \frac{\partial^2 \phi}{\partial t^2}.$$

In addition, the surface losses in the superconductors must be considered, which will modify the above results. One could write,

$$\frac{\partial \phi}{\partial x} + \beta \frac{\partial^2 \phi}{\partial x \partial t} = B_y, \quad \Rightarrow \quad \frac{\partial \phi}{\partial t} + \beta \frac{\partial^2 \phi}{\partial t^2} = V,$$

which is a modified Josephson relation. It is only correct to first order in β and is only self-consistent to that order as well. The quantity β is the ratio of the number of particles to quasi-particles. The equations

$$\frac{\partial\phi}{\partial t} = V + \beta\frac{\partial V}{\partial t}, \text{ and } \frac{\partial\phi}{\partial x} + \beta\frac{\partial V}{\partial x} = B_y = -i_x$$

lead to self-consistency.

Computer simulations of these equations have been applied to Giaever's DC flux transformer, which has a horizontal current applied to a primary (horizontal) layer, separated by an insulating layer from a secondary layer. There are two electrical contacts, top and bottom, to measure the results. Also a pseudo DC flux transformer was studied which was a layer of superconductor with the CuO planes lying horizontally. There were 4 contacts top and bottom, and current was inserted in the first and withdrawn from the fourth top contact. The simulations were carried out on a $48 \times 48 \times 8$ lattice system using second-order Runge-Kutta time integration (Greenside-Helfand). The speaker explained that these results were compared with experimental results on $\text{Bi}_2\text{Sr}_2\text{CaCu}_2\text{O}_{8-y}$ single crystals with good agreement. A video was shown which illustrated the behavior of the simulation and showed, it was pointed out, that the picture of a rigid object being dragged through the system is not valid here, but rather things unfold from the top down. It is these structures that occur on the mesoscopic scale (and block progress from the microscopic scale to the macroscopic scale) that are what is relevant to this initiative.

Presentation by Darryl Holm

This presentation was on the subject of self-consistent, Hamiltonian dynamics of wave, mean-flow interaction for a rotating stratified incompressible fluid, and it reported joint work with Ivan Gjaja. First, the speaker gave a description of various types of waves in the ocean and some of the things that affect them. Briefly, sunshine causes wind which exerts a force on the surface of the water. The water near the surface moves in a superposition of various motions to produce waves. In addition, there are currents in the ocean which in turn are affected by the Coriolis force due to the rotation of the earth. At the bottom of the ocean, there is an uneven lower surface, which can vary significantly in depth. The flow past the unevenness, as well as past promontories, *etc.*, can cause eddies and various other motions.

The speaker said that our current capability in the heroic effort to produce a global climate model on a computer is a horizontal grid system of about 20 kilometers spacing, which is an important advance over previous horizontal spacings of about 100 kilometers because it captures much more of the ocean's kinetic energy—in particular, the eddies. In the atmosphere, the bulk of the kinetic energy is in gyres around 1,000 kilometers in size. However, in the ocean a lot of the kinetic energy resides in eddies about 15 kilometers in size. The peak in the kinetic energy spectrum varies with latitude and arises from a balance between hydrostatic pressure and the Coriolis force on the free surface. This feature makes numerical ocean modeling computationally difficult because about half the kinetic energy is below the previously used grid sizes of 100 kilometers spacing or more.

The speaker also reported that, as has been known for twenty years, the power spectrum of vertical displacement lies between about 0.04 cycles per hour and about 3 cycles per hour and has an ω^{-2} decay.

The first results of the speaker's method were reported to be the derivation of new equations for the wave, mean-flow interaction. The first case studied was for a single frequency wave train. These equations are then expanded* in a ratio of time scales, ϵ , and the wave amplitude, α . In addition, a phase averaging in Hamilton's principle for the three-dimensional Euler equations is used. The results are new equations for the "ray optics" limit for the wave, mean-flow, interaction equations. A further step would extend the theory to describe an ensemble of waves which have a spectral distribution in wave number \vec{k} .

In answer to a question about the relation of the Laboratory's numerical ocean modeling efforts to experimental data, the speaker pointed out that our efforts are benchmarked by various measurements performed in the ongoing World Ocean-Circulation Experiment (WOCE) and the TOPEX-Poseidon joint experiment. The latter involves cooperation between France and the U.S. to measure sea-surface height variability with great accuracy and over long times using satellite altimetry. Our efforts are supported by a U.S. DOE program called Computer Hardware, Advanced Mathematics and Modeling Physics (CHAMMP). Measurements of opportunity were also discussed in connection with the famous rubber ducky experiment. Apparently, a ship loaded with hundreds of thousands of rubber duck bathtub toys sank off Japan and released its cargo. Being bathtub toys, the rubber duckies float, and it was possible to use them to track the transport by ocean currents when they washed up on various shores across the Pacific ocean at various times. This transport is significant, and it was stated that the ocean currents carry at least half of the heat from the equator to the poles.

In order to proceed, we were reminded of Lord Kelvin's theorem (see the Appendix), which is, the speaker said, a geometrical statement of fluid dynamics. If the ocean is considered as a stratified, rotating, incompressible fluid in a conservative force field (namely gravity), Kelvin's theorem is expressed as

$$\frac{d}{dt} \oint_{\gamma(t)} (\vec{u} + \vec{R}(\vec{x})) \cdot d\vec{x} = \oint_{\gamma(t)} \left[\vec{\nabla}(u^2/2 - p) \cdot d\vec{x} - g\rho dz \right],$$

where the contour $\gamma(t)$ moves with the fluid velocity, \vec{u} . Hence,

$$\oint_{\gamma(t)} \left[\vec{u}_t + (\vec{u} \cdot \vec{\nabla})\vec{u} + u_j \vec{\nabla} u^j - \vec{u} \times (\vec{\nabla} \times \vec{R}) \right] \cdot d\vec{x} = \oint_{\gamma(t)} \left(u_j \vec{\nabla} u^j - \vec{\nabla} p - g\rho \vec{e}_z \right) \cdot d\vec{x},$$

where the subscript t means time differentiation, the subscript j and superscript j refer, respectively, to covariant and contravariant components of a vector, and the Einstein summation convention is employed. Finally, \vec{e}_z is the unit vector in the vertical direction, and g is the acceleration due to gravity. Equating the integrands in the above expression of Kelvin's theorem gives the equations of motion for the fluid in the approximation considered

* See the previous presentation by Darryl Holm for related work.

by the speaker. In “coordinate-free” notation, the speaker wrote the content of the previous equation as

$$(\partial_t + \mathcal{L}_u) \left((\vec{u} + \vec{R}(\vec{x})) \cdot d\vec{x} \right) = d\left(\frac{1}{2}u^2 - p\right) - g\rho dz,$$

where \mathcal{L}_u denotes the Lie derivative with respect to the vector field $\vec{u} \cdot \vec{\nabla}$. Such ideal fluid dynamics in Eulerian variables possesses a Hamiltonian principle, *i.e.*, $\delta L = 0$. The Lagrangian which yields the motion equations under consideration is given by

$$L = \int dt \int d^3x \left[\frac{1}{2}D|\vec{u}|^2 + D\vec{u} \cdot \vec{R}(\vec{x}) - D\rho(\vec{l})gz - p(D - 1) \right],$$

where

$$\frac{\partial l^A}{\partial t} = -\vec{u} \cdot \vec{\nabla} l^A, \quad D = \det \left(\frac{\partial l^A}{\partial x^i} \right).$$

Now to obtain the equations of motion, one varies the Lagrangian with respect to the $l^A(\vec{x}, t)$, $A = 1, 2, 3$ at fixed \vec{x} and t . These steps yield

$$\begin{aligned} \delta l^A &\Rightarrow (\partial_t + \mathcal{L}_u) \left(\frac{1}{D} \frac{\delta \mathcal{L}}{\delta \vec{u}} \cdot d\vec{x} \right) - d \left(\frac{\delta \mathcal{L}}{\delta D} + \rho gz \right) + g\rho dz = 0, \\ \delta p &\Rightarrow D - 1 = 0, \text{ (incompressibility),} \quad \rho = \rho(\vec{l}) \Rightarrow \frac{\partial \rho}{\partial t} = -\vec{u} \cdot \vec{\nabla} \rho, \end{aligned}$$

where the equation that results from δl^A is Lord Kelvin’s theorem in geometrical form for an arbitrary Lagrangian $L[\vec{u}, D, \rho]$!

With this formalism finally before us, the strategy is now to make approximations in the fluid Lagrangian, L . Specifically we will decompose the total fluid trajectory denoted $\vec{X}(l^A, t)$ for a fluid element with label l^A into the sum $\vec{x}(l^A, t) + \alpha \vec{\xi}(\vec{x}, t)$, where \vec{x} is the trajectory of the fluid element along the mean flow, which is to be determined self-consistently along with the motion due to the waves. The ratio of wave amplitude to wavelength, α , is regarded as small ($\alpha \ll 1$), and $\alpha \vec{\xi}$ represents the displacement of the fluid due to the presence of the wave. Thus we regard the waves as riding on the mean flow which it also influences self-consistently. If we write $\vec{\xi} = \vec{a} \exp(i\phi/\epsilon) + \vec{a}^* \exp(-i\phi/\epsilon)$, then the Lagrangian may be expanded as

$$L^{(\epsilon, \alpha)}(\vec{X}) = L^{(0,0)} + \alpha^2 \left[L^{(2,0)} + \epsilon L^{(2,1)} + \epsilon^2 L^{(2,2)} \right] + O(\alpha^4),$$

where the α^0 term describes the mean flow, the α^2 term describes the wave, mean-flow interaction, and the α^4 term describes the wave-wave interactions.

Next, Holm explained that if we set $\alpha = 0$, then the variation of the mean-flow quantities leads to the Euler equations for the mean flow. If instead we vary the wave quantities, evaluated at $\delta L^{(0,0)} = 0$, then we get the linearized spectral equations. On the other hand, if we phase-average (over ϕ), then vary the wave quantities and evaluate the mean flow at $\delta L^{(0,0)} = 0$, then we get Whitham’s modulation equations at order

$O(\alpha^2, \alpha^2 \epsilon)$, and the WKB* stability equations at order $O(\alpha^2 \epsilon^2)$. If we phase-average, and then vary both the wave and the mean-flow quantities (omitting the order α^4 terms in the action), we arrive at the wave, mean-flow interaction equations. The speaker remarked that he wanted to avoid analyzing the wave-wave interactions, as too many people had failed on this in the past. The averaged Lagrangian was given by the speaker in compact notation as

$$\begin{aligned}\bar{L} &= \bar{L}_{\text{hydro}} + \alpha^2 \bar{L}_{\text{wave}} \\ &= \int dt \int d^3x \left\{ D \left[\frac{1}{2} |\vec{u}|^2 - \rho(l(\vec{x}, t))gz + \vec{u}_L \cdot \vec{R}(\vec{x}) \right] + p_0(1 - D) \right\} \\ &\quad + \alpha^2 \int dt \int d^3x F^{*\mu} D_{\mu\nu} F^\nu.\end{aligned}$$

The following notation has been employed:

$$\begin{aligned}\vec{\Omega} &= \frac{1}{2} \vec{\nabla} \times \vec{R}, \quad F^\mu = (\vec{a}, b), \quad k_\mu = (\vec{k}, -\omega), \quad x^\mu = (\vec{x}, t), \quad \tilde{\omega} = \omega - \vec{u} \cdot \vec{k}, \quad (D_{\mu\nu})^\dagger = D_{\mu\nu}, \\ D_{ij} &= D\tilde{\omega}^2 \delta_{ij} - \frac{1}{2}(D+1)p_{0,ij} - 2iD\tilde{\omega}\epsilon_{ijk}\Omega_k, \quad D_{4j} = -iDk_j = -D_{j4}, \quad \text{and } D_{44} = 0.\end{aligned}$$

In this form, the variations

$$\frac{\delta \bar{L}}{\delta F^{*\mu}} = D_{\mu\nu} F^\nu = 0$$

imply the dispersion relation for the waves, $\det D_{\mu\nu} = 0$. The resulting dispersion relation governs internal waves propagating in the slowly varying oceanic mean flow. It generalizes the dispersion relation for internal waves linearized around a steady, stably stratified, equilibrium flow. In addition, \bar{L} invariance under $\phi \rightarrow \phi' + \text{const}$ implies the conservation law

$$\partial_{\epsilon t} N + \frac{\partial}{\partial \epsilon \vec{x}} \cdot (\vec{v}_g N) = 0, \quad \text{and } \vec{v}_g N = N \vec{u}_L + 2D\Im(b^* \vec{a})$$

for the wave action density

$$N = D\tilde{\omega} |\vec{a}|^2 + 2i\vec{\Omega} \cdot \vec{a} \times \vec{a}^l.$$

Next the speaker made the observation, which is interesting from the structural point of view, that the wave, mean-flow interaction equations are Hamiltonian with a Lie-Poisson bracket. He writes duality relations for the variables as

$$\mu = \{\vec{m}, D, \rho; \vec{P}, N\} \quad \text{is dual to} \quad \underbrace{V(\mathbb{S}) (\Lambda^0 \oplus \Lambda^n)}_{\text{mean-flow}} \oplus \underbrace{V(\mathbb{S}) \Lambda^0}_{\text{waves}},$$

where \mathbb{S} represents the semidirect-product Lie algebra of vector fields acting amongst themselves by the Lie commutator and on differential forms by the Lie derivative, and \oplus

* The letters stand for G. Wentzel, H. A. Kramers, and L. Brillouin.

represents the direct sum. With this understanding of the Hamiltonian structure, we may express the self-consistent wave, mean-flow dynamics as

$$\dot{\mu} = \{\mu, \bar{\mathcal{H}}\}_{LP} = -ad^*_{(\delta H/\delta \mu)}, \quad \{F, H\}_{LP} = \left\langle \mu, \left[\frac{\delta F}{\delta \mu}, \frac{\delta H}{\delta \mu} \right] \right\rangle.$$

Here $\langle \cdot, \cdot \rangle$ denotes the pairing between elements of the Lie algebra and its dual. The dual variables μ are expressed in terms of the original fluid variables as

$$\vec{m} = D \left(\vec{u}_L + \vec{\Omega} \times \vec{x} \right) - \alpha^2 N \vec{k}, \text{ and } \vec{P} = N \vec{k}, \text{ (wave momentum density),}$$

and the Hamiltonian has the following variational derivatives with respect to these variables:

$$\frac{\delta H}{\delta \vec{m}} = \vec{u}_L \text{ (Lagrangian - mean fluid velocity), and } \frac{\delta H}{\delta \vec{P}} = \vec{v}_g \text{ (group velocity).}$$

These Hamiltonian wave, mean-flow interaction equations may be expressed in coordinate-free form as

$$\begin{aligned} (\partial_t + \mathcal{L}_{\vec{u}_L}) \left((\vec{m}/D) \cdot d\vec{x} \right) &= d \left(-\frac{\delta \bar{\mathcal{H}}}{\delta D} + \rho d \frac{\delta \bar{\mathcal{H}}}{\delta \rho} \right) - \rho d \frac{\delta \bar{\mathcal{H}}}{\delta \rho}, \quad (\text{Lord Kelvin's theorem}) \\ (\partial_t + \mathcal{L}_{\vec{u}_L}) \rho &= 0, \quad (\text{buoyancy}) \\ (\partial_t + \mathcal{L}_{\vec{u}_L}) (D d^3 x) &= 0, \quad (\text{continuity}), \text{ and} \\ \left. \begin{aligned} (\partial_t + \mathcal{L}_{\vec{v}_g}) \left((\vec{P}/N) \cdot d\vec{x} \right) &= -d (\delta \bar{\mathcal{H}}/\delta N) \\ (\partial_t + \mathcal{L}_{\vec{v}_g}) (N d^3 x) &= 0 \end{aligned} \right\} \partial_t \vec{k} = -\vec{\omega}, \quad \begin{aligned} &(\text{wave transport equation}), \\ &(\text{wave action conservation}), \end{aligned} \end{aligned}$$

where, e.g., $\mathcal{L}_{\vec{u}_L}$ denotes Lie derivative with respect to the vector field $(\vec{u}_L \cdot \partial/\partial \vec{x})$.

We now come to the high point of the talk. Darryl explained that *these equations separate into equations for a two-fluid model. Each fluid carries its own momentum density. The mean-flow fluid carries mass and volume along the Lagrangian mean fluid velocity, \vec{u}_L . The wave "fluid" carries wave action along the wave group velocity, \vec{v}_g . This two-fluid model is analogous to the Landau model for superfluid He⁴, except in the Landau theory the wave-excitation fluid carries mass, whereas here the rectified wave fluid carries momentum and wave action density, but no mass.*

As a final remark, the speaker pointed out that the leading order effect of the waves on the fluid is the Coriolis force on the fluid due to the passage of the wave. This force causes an Eulerian mean acceleration given by

$$\frac{d\vec{u}}{d\epsilon t} = -\frac{\alpha^2}{\epsilon} N \vec{k} \times 2\Omega \vec{e}_z,$$

and appears in the leading-order Eulerian mean-motion equation as,

$$\frac{\partial \vec{u}}{\partial(\epsilon t)} + \left(\vec{u} \cdot \vec{\nabla}_{\epsilon \vec{x}} \right) \vec{u} - \frac{\alpha^2}{\epsilon} N \vec{k} \times 2\Omega \vec{e}_z + \frac{1}{\epsilon} \left(-\vec{u} \times 2\Omega \vec{e}_z + g\rho \vec{e}_z + \vec{\nabla} p_0 \right) = O(\alpha^2).$$

Title: A Discussion of Kelvin's Theorem

This theorem is really one of vector analysis. I follow the presentation of H. Lass in his "Vector and Tensor Analysis." First, let us consider the velocity of particles occupying an element of volume of a fluid. Let P be a point in that region and let \vec{v}_P be the velocity of the fluid at P . The velocity at a nearby point Q is just $\vec{v}_Q = \vec{v}_P + (d\vec{r} \cdot \vec{\nabla})\vec{v}_P$ to first order in the separation $d\vec{r}$. Here it is meant that the derivatives are to be evaluated at P . For convenience, we will now write \vec{r} as shorthand for $d\vec{r}$. There is a vector identity which says

$$\vec{\nabla}(\vec{r} \cdot \vec{w}) = \vec{r} \times (\vec{\nabla} \times \vec{w}) + (\vec{r} \cdot \vec{\nabla})\vec{w} + \vec{w}.$$

Let us now choose, $\vec{w} \equiv (\vec{r} \cdot \vec{\nabla})\vec{v}_P$. Thus,

$$(\vec{r} \cdot \vec{\nabla})\vec{w} = x \frac{\partial x}{\partial x} \frac{\partial \vec{v}}{\partial x} \Big|_P + y \frac{\partial y}{\partial y} \frac{\partial \vec{v}}{\partial y} \Big|_P + z \frac{\partial z}{\partial z} \frac{\partial \vec{v}}{\partial z} \Big|_P = \vec{w}.$$

Note that the $\partial \vec{v} / \partial x$ is evaluated at P and does not depend on $d\vec{r}$ which we have shortened to \vec{r} , and so was not differentiated in the above equation. Therefore for this choice of \vec{w} , we have the result

$$\vec{w} = \frac{1}{2} \vec{\nabla}(\vec{r} \cdot \vec{w}) + \frac{1}{2} (\vec{\nabla} \times \vec{q}) \times \vec{r}.$$

Since $\vec{v}_Q = \vec{v}_P + \vec{w}$, we have $\vec{\nabla} \times v_Q = \vec{\nabla} \times \vec{w} = (\vec{\nabla} \times \vec{v})_P$, where the last equality follows by direct computation using our definition of \vec{w} . If we define $\vec{\omega} = \frac{1}{2} (\vec{\nabla} \times \vec{v})_P$, then we may write

$$\vec{v}_Q = \vec{v}_P + \vec{\omega} \times \vec{r} + \frac{1}{2} \vec{\nabla}(\vec{r} \cdot \vec{w}).$$

There is a geometrical interpretation of this form. The velocity at Q is (i) the velocity at P , plus (ii) the rigid body rotation about a line through P in the direction of $\vec{\omega}$, plus the motion of Q relative to P in this translating and rotating framework. The first two parts of the velocity also occur in a rigid body, and the third is related to the fluid character.

The next step toward Lord Kelvin's theorem, is to compute the circulation around any closed curve Γ moving with the fluid. It is

$$C = \oint_{\Gamma} \vec{v} \cdot d\vec{r} = \int_S \int (\vec{\nabla} \times \vec{v}) \cdot d\vec{\sigma},$$

where the second inequality is true by Stokes' better-known theorem. Here S is the surface bounded by Γ , and $d\vec{\sigma}$ is the area of a surface element with the direction of the normal to the surface. Notice that as $\vec{\nabla} \times \vec{\nabla} \equiv 0$, only the second term in our expression just given for the velocity makes a nonzero contribution to the circulation. A curve which is parallel to ω at every point is called a vortex line. It is convenient to write the circulation as

$$C = \oint_{\Gamma} \vec{v} \cdot \frac{d\vec{r}}{ds} ds,$$

where s is an integration parameter along the curve Γ . Let us now see how the circulation changes in time if we let the particles which compose the curve Γ move with the motion of the fluid. As time goes on, assuming continuity of the flow, the closed curve remains closed. Therefore,

$$\frac{dC}{dt} = \oint_{\Gamma} \frac{d\vec{v}}{dt} \cdot \frac{d\vec{r}}{ds} + \oint_{\Gamma} \vec{v} \cdot \frac{d}{dt} \left(\frac{d\vec{r}}{ds} \right) ds = \oint_{\Gamma} \frac{d\vec{v}}{dt} \cdot \frac{d\vec{r}}{ds} + \oint_{\Gamma} \vec{v} \cdot \frac{d}{ds} \left(\frac{d\vec{r}}{dt} \right) ds.$$

Euler's equation of motion for the fluid is

$$\frac{d\vec{v}}{dt} = \vec{f} - \frac{\vec{\nabla}p}{\rho},$$

where p is the pressure and ρ is the density. If we have a conservative field, then $\vec{f} = -\vec{\nabla}\chi$, and if ρ is a function of p alone, then we can write

$$V = \chi + \int \frac{dp}{\rho}, \quad \frac{d\vec{v}}{dt} = -\vec{\nabla}V.$$

Substituting this result into the equation for the time derivative of the circulation, we get Lord Kelvin's theorem

$$\frac{dC}{dt} = - \oint \vec{\nabla}V \cdot d\vec{r} + \oint \frac{1}{2} \frac{dv^2}{ds} ds = - \oint d(V - \frac{1}{2}v^2) \equiv 0$$

for a conservative field and for the density a function of pressure alone. In other words, the circulation is a conserved quantity with these restrictions.

Presentation by David Sherrington

Title: Non-Equilibrium Macrodynamics of Disordered and Frustrated Systems

The work reported is joint work with Ton Coolen and Stephen Laughton.

$$\begin{array}{lcl} \text{Microdynamics} & \longrightarrow & \text{Macrodynamics} \\ \text{Many variables} & \longrightarrow & \text{Few variables} \\ \text{Possibly stochastic} & \longrightarrow & \text{deterministic?} \end{array}$$

Interest in the above transitions, the speaker said, was not just confined to long-time equilibrium. Various questions regarding these matters arise, such as: How many macroscopic variables are needed? Are there closed autonomous equations for these macroscopic variables? Are there specific results?

The speaker would like a general theory with the following characteristics. One starts with the microscopic state which is described by \vec{S} , a vector variable of high dimension and a time-dependent distribution $p_t(\vec{S})$. There would be stochastic dynamics defined by a master equation

$$\frac{d}{dt} p_t(\vec{S}) = f(p_t(\vec{S})).$$

One would then derive from this information a set of order parameters $\vec{\Omega}$ of lower (hopefully low) dimensionality, and a distribution

$$P_t[\vec{\Omega}] = \sum_{\vec{S}} p_t(\vec{S}) \delta(\vec{\Omega} - \vec{\Omega}(\vec{S})).$$

The form of the dynamics was not clear, but it should be that the master equation for $p_t(\vec{S})$ implies the equations of motion for $P_t[\vec{\Omega}]$, which may or may not be closed.

By way of further introduction the speaker said that eventually he has obtained what he believes to be a very good description/theory, but that he prefers first to guide us through the thinking which led to it.

Sherrington then turned to a specific example. Consider a system in which the microscopic variables are $\sigma_i = \pm 1$, for example, Ising spins. Impose Glauber dynamics, *i.e.*, the spins are updated in a random sequential manner according to the transition probabilities,

$$p(\sigma_i \rightarrow \sigma'_i) = \frac{1}{2} \{1 + \sigma'_i \tanh \beta h_i\}, \quad \text{where} \quad h_i = \sum_j J_{ij} \sigma_j + \theta_i.$$

The h_i represent local fields, the J_{ij} represent the exchange energies, and the θ_i represent an external field. David then explained that range-free interactions imply no spatial dependence on $\vec{\Omega}$. Examples would be: (i) the J_{ij} are independently randomly distributed variables drawn from $P(J_{ij})$ (a Sherrington-Kirkpatrick or Viana-Bray spin glass), or (ii) $J_{ij} = f\{\xi_i^\mu; \xi_j^\mu\}$ with the ξ_i^μ independent and randomly distributed [a Hopfield neural network storing patterns, $\{\xi_i^\mu\} = \{\pm 1\}$; $\mu = 1, \dots, p$].

The plan is now random sequential dynamics. That is, the Glauber dynamics implies a master equation, which in turn implies the equations of motion for $P_t[\vec{\Omega}]$. The master equation for $p_t[\vec{\sigma}]$ is

$$\frac{d}{dt} p_t(\sigma) = \sum_i [p_t(F_i \vec{\sigma}) W_i(F_i \vec{\sigma}) - p_t(\vec{\sigma}) W_i(\vec{\sigma})].$$

Then the equation of motion for $P_t[\vec{\Omega}]$, where the Ω 's are the macroscopic order parameters, becomes

$$\frac{d}{dt} P_t[\vec{\Omega}] = \sum_{l \geq 1} \frac{(-1)^l}{l!} \sum_{k_1}^K \cdots \sum_{k_l}^K \frac{\partial^l}{\partial \Omega_{k_1} \cdots \partial \Omega_{k_l}} \left\{ P_t[\vec{\Omega}] F_{k_1, \dots, k_l}^{(l)}[\vec{\Omega}; t] \right\},$$

where

$$F_{k_1, \dots, k_l}^{(l)}[\vec{\Omega}; t] \equiv \left\langle \sum_j W_j(\vec{\sigma}) \Delta_{j k_1}(\vec{\sigma}) \cdots \Delta_{j k_l}(\vec{\sigma}) \right\rangle_{\Omega; t}$$

$$\Delta_{jk}(\vec{\sigma}) \equiv \Omega_k(F_j \sigma) - \Omega_k(\vec{\sigma}).$$

These equations in their turn imply the behavior at finite times, t , for the limit as the system size, N , tends to infinity. Next we get a Liouville equation for $P_t[\vec{\Omega}]$ and lastly a deterministic equation for $\vec{\Omega}(t)$, namely,

$$\frac{d}{dt}\vec{\Omega}(t) = \left\langle \sum_i W_i(\vec{\sigma}) \left[\vec{\Omega}(F_i\vec{\sigma}) - \vec{\Omega}(\vec{\sigma}) \right] \right\rangle_{\vec{\Omega};t},$$

where the notation $\langle \rangle_{\vec{\Omega};t}$ is called a sub-shell average, and

$$\begin{aligned} W_k(\vec{\sigma}) &= \frac{1}{2} [1 - \sigma_k \tanh \beta h_k(\vec{\sigma})], \\ F_k \Phi(\vec{\sigma}) &= \Phi(\sigma_1, \dots, -\sigma_k, \dots, \sigma_N), \text{ and} \\ \langle f(\vec{\sigma}) \rangle_{\vec{\Omega};t} &= \frac{\sum_{\vec{\sigma}} p_t(\vec{\sigma}) \delta[\vec{\Omega} - \vec{\Omega}(\vec{\sigma})] f(\vec{\sigma})}{\sum_{\vec{\sigma}} p_t(\vec{\sigma}) \delta[\vec{\Omega} - \vec{\Omega}(\vec{\sigma})]}. \end{aligned}$$

Since $p_t(\vec{\sigma})$ depends on the whole distribution for the microscopic variables, the equations are not closed.

By way of clarifying remarks, the speaker said “No loops are relatively easy, and no disorder is easy, but strong disorder together with loops is difficult.” An example of an easy problem is the mean-field Ising model, which he called an “infinite-ranged, Ising ferromagnet.” Here in terms of variables previously defined, we set $J_{ij} = J_0/N$ and $\theta_i = \theta$. One macroscopic variable suffices, and it is $m = N^{-1} \sum_i \sigma_i$. The distribution $p_t(\vec{\sigma})$ depends on $\vec{\sigma}$, only via m in this case. The equation of motion is

$$\frac{dm}{dt} = \tanh(\beta(J_0 m + \theta)) - m,$$

and the equilibrium solution $dm/dt = 0$ is, of course, the usual mean-field theory result, $m = \tanh(\beta(J_0 m + \theta))$.

A hard example which contains both disorder and frustration is as follows. Select

$$J_{ij} = \frac{J_0}{N} + \frac{J z_{ij}}{\sqrt{N}}, \quad \text{where} \quad \langle z_{ij} \rangle = 0, \text{ and} \quad \langle z_{ij}^2 \rangle = 1.$$

Sherrington then remarked that this problem is much more difficult if $J \sim O(1)$. Examples of this case are the Sherrington-Kirkpatrick spin-glass, where the z_{ij} are independently distributed Gaussian random variables, and the Hopfield neural network within the basin of attraction of one pattern. This basin is to be gauged to $\xi_i^1 = 1$ for $i = 1, \dots, N$. The other patterns are $\{\xi_i^\mu\}$ for $\mu = 2, \dots, p = \alpha N$. Here, the variables are selected to be,

$$z_{ij} = \frac{1}{\sqrt{p}} \sum_{\mu>1}^p \xi_i^\mu \xi_j^\mu, \quad J_0 = 1, \text{ and} \quad J = \sqrt{\alpha} = \sqrt{\frac{p}{N}},$$

which in line with the previous remarks is only difficult for $\alpha \sim O(1)$, *i.e.*, for an extensive number of patterns.

David next began a discussion of “Hopfield neural nets.” First, patterns are stored,

$$\{\xi_i^\mu = \pm 1\}; \quad \mu = 1, \dots, p; \text{ and } i = 1, \dots, N.$$

Next “synapses” are defined by

$$J_{ij} = \frac{1}{p} \sum_{\mu} \xi_i^\mu \xi_j^\mu,$$

and the overlap of the microscopic variable state with a pattern μ is defined as

$$m^\mu = N^{-1} \sum_i \xi_i^\mu \sigma_i.$$

The dynamics of this model are as described before, with the J_{ij} being used in the definition of h_i , which in turn is used in the definition of W_i and so forth through the previously described dynamic equations. A microscopic state is said to be in the “basin of attraction” of a pattern μ if the flow under the dynamics is such that, with the passage of time, $m^\mu \sim O(1)$ and for all $\nu \neq \mu$, $m^\nu \sim O(N^{1/3})$. The overlap with μ is expected to increase with time in such a case, and the overlap with other patterns to decrease, or at least not to increase. Basins of attraction so defined, do not necessarily fill the whole of state space. There may be other attractors which are not patterns.

A “phase diagram” was displayed for the Hopfield model in equilibrium. The coordinates were temperature and $\alpha = p/N$. Three phase regions were shown. The first region, which was bounded by the coordinate axes and a convex line from $(0, T_c)$ to $(\alpha_c, 0)$ was labeled “retrieval of memorized patterns, ‘ferromagnet’.” The second region was bounded by the temperature axis and a line of positive slope starting from $(0, T_c)$ and was labeled “no restricted attractors, ‘paramagnet’.” Finally the third region was bounded by the two aforementioned lines plus part of the α -axis and was labeled “restricted attractors not related to memorized patterns, ‘spin glass’.”

Next Sherrington discussed the order parameters of interest. In the first case, the set consisted of the magnetization and the overlap with a “nominated” pattern:

$$m = N^{-1} \sum_i \sigma_i, \quad \text{and} \quad m^\mu = N^{-1} \sum_i \xi_i^\mu \sigma_i.$$

Other order parameters needed to describe equilibrium might be deduced from

$$p_\infty(\vec{\sigma}) \sim \exp(-\beta H(\vec{\sigma})),$$

where the Hamiltonian could be written as

$$H(\vec{\sigma}) = f(m(\vec{\sigma})) + R(\vec{\sigma}).$$

The function f is meant to absorb all the direct dependence on $m(\vec{\sigma})$. The speaker said that an additional order parameter would be needed if $R(\vec{\sigma}) \sim O(1)$. He said that we will now consider the case where

$$H/N = -\frac{1}{2}J_0m^2(\vec{\sigma}) - Jr(\vec{\sigma}) + O(N^{-1}), \text{ and } r(\vec{\sigma}) = N^{-3/2} \sum_{i<j} \sigma_i z_{ij} \sigma_j,$$

where the z_{ij} are as before. Here the minimal set of order parameters is, for this simple version of the theory,

$$\vec{\Omega}(\vec{\sigma}) = \{m(\vec{\sigma}), r(\vec{\sigma})\}.$$

If one works through from the microscopic variables to the Liouville equations to the macroscopic variables, one gets deterministic flows described by

$$\begin{aligned} \frac{dm}{dt} &= \int dz D_{m,r;t}(z) \tanh[\beta(J_0m + Jz + \theta)] - m, \\ \frac{dr}{dt} &= \int dz D_{m,r;t}(z) \tanh[\beta(J_0m + Jz + \theta)] - 2r, \end{aligned}$$

where

$$D_{m,r;t}(z) = \lim_{N \rightarrow \infty} \left\langle N^{-1} \sum_i \delta(z - z_i(\vec{\sigma})) \right\rangle_{\vec{\Omega};t}$$

is the sub-shell average as defined before. In this case he denotes

$$h_i(\vec{\sigma}) = J_0m(\vec{\sigma}) + Jz_i(\vec{\sigma}), \quad \text{and} \quad z_i(\vec{\sigma}) = N^{-1/2} \sum_j z_{ij} \sigma_j,$$

where $Jz_i(\vec{\sigma})$ is the noisy contribution to the local field.

So far, these equations are not closed.* Sherrington proposed making two Ansätze to obtain closure. These are (i) *self-averaging* over the specific microscopic realization of disorder, and (ii) *equi-partitioning* of the microscopic state probability $p_t(\vec{\sigma})$ within each (m, r) sub-shell. This second assumption is only made during the calculation of the D 's and eliminates $p_t(\vec{\sigma})$ from $D_{r,m;t}$ and with it the time dependence, so we have only the static $D_{r,m}$ instead of a dynamic variable. The speaker said that the resulting expression can be evaluated by replica theory.** Even so we were told, the evaluation is nontrivial, but after several manipulations the results can be expressed in the form

$$D_{m,r}(z) = \lim_{n \rightarrow 0} \int \prod_{i,j} \prod_{\alpha, \beta=1, \dots, n} dx_i^\alpha dy_j^{\alpha\beta} \exp[-N\Phi(m, r, z; \{x_i^\alpha\}, \{y_j^{\alpha\beta}\})],$$

* This is the usual type of bugbear in this sort of work in statistical mechanics. For example, the exact equations for a few particles always involve the behavior of at least one more particle, and so on up the line.

** According to the speaker, we are confronted with the problem of averaging an expression of the form

$$\langle f(\sigma) \rangle = \frac{\text{Tr}[f(\sigma)W_{\{J\}}(\sigma)]}{\text{Tr}[W_{\{J\}}(\sigma)]}$$

over a probability distribution for J . In this work, the denominator is difficult to deal

where the number of indices i, j is finite, Φ is $O(N^0)$, and n is the number of replicas. The D 's are in general non-Gaussian. The reader will notice from the product structure that n is necessarily an integer, so one might wonder about taking its limit as $n \rightarrow 0$. The replica method involves developing a straightforward type of expression for general n and then extrapolating it to zero.* Since the exponent is proportional to N (and hopefully there are not too many maxima), the method of steepest descents is useful to evaluate this expression. These procedures lead to a closed set of equations.

The speaker then showed some plots in the m - r plane of numerical simulations of this problem for $\alpha = 0.1$. Time trajectories were displayed for zero temperature with the starting points $(m, r) = (0.1, 1), (0.2, 1), \dots, (0.8, 1)$ and for $N = 2,000 - 16,000$. The construction of these trajectories also involved a replica-symmetry hypothesis. There appeared to be attractors at $(m, r) = (1, 1)$ and $(0, 11)$. These curves started with a positive slope and lay in two roughly triangular regions. For $m \leq 0.3$, they tended to the $(0, 11)$ attractor, and the other trajectories to the other attractor. These two triangular regions are bounded by the lines $m = 0, r = 1$, a convex curve joining the two attractors, and a line of positive slope starting from about $(0.35, 1)$ and running up to the concave curve just mentioned. Mention was made of the de Almeida-Thouless line (limit of replica-symmetry stability) in this regard. A plot was displayed for $N = 32,000$ to compare the results of this simple theory with a numerical simulation. The theory did pretty well (as a function of time) before the trajectories crossed the de Almeida-Thouless line, but not too well afterwards.

In order to improve the comparison of the theory with the numerical simulations, Sherrington elaborated on a more advanced theory. In essence, he now abandons the *raison d'être* which he had been advocating heretofore. Instead of trying to reduce the description of the system to the use of a "few" macroscopic variables, he proposes instead to use an *order function*. A function, in fact, is equivalent to an (if analytic countable) infinite number of parameters. His justification was that he thought that the addition of any finite number of extra observables would not give more than just minor improvements.

with. The method of replicas removes the denominator by considering instead

$$\lim_{n \rightarrow 0} \text{Num.}(\text{Den.})^{n-1},$$

which can be expressed as

$$\langle f(\sigma) \rangle = \lim_{n \rightarrow 0} \left\{ \text{Tr}_{\sigma^\alpha; \alpha=1, \dots, n} \left[f(\sigma^1) \prod_{\alpha=1}^n W_{\{J\}}(\sigma^\alpha) \right] \right\},$$

and is relatively easier to average.

* Some care must be exercised in this step because the values for $n = 1, 2, \dots$ are insufficient to uniquely determine the value at zero as can be seen by considering the function $(\sin \pi n)/n$.

The order function is introduced to be

$$\mathcal{D}[\zeta, h; \vec{\sigma}] = N^{-1} \sum_i \delta_{\zeta, \sigma_i} \delta(h - h_i(\vec{\sigma})).$$

It turns out that the quantities m, r used in the simpler version are just moments of this distribution, so that theory is a true simplification of this one, and this one should retain all the virtues (except simplicity of course) of the simpler one. The probability distribution of this order function is given by

$$P_t[\mathcal{D}[\zeta, h]] = \sum_{\vec{\sigma}} p_t(\vec{\sigma}) \delta\{\mathcal{D}[\zeta, h] - \mathcal{D}[\zeta, h; \vec{\sigma}]\},$$

which, of course, involves microscopic quantities, and a delta function of delta functions! By the same type of techniques as used before, one can obtain an equation of motion for $P_t[\mathcal{D}]$. By discretizing h , one can run through (although with increased difficulty) a good share of the step recounted above, again making the same sort of hypotheses. As an example of the results, the following dynamical equation was obtained for the Sherrington-Kirkpatrick model with $J_0 = 0$:

$$\begin{aligned} \frac{\partial}{\partial t} \mathcal{D}[\sigma, h] &= \frac{\partial}{\partial h} \left\{ \mathcal{D}[\sigma, h] \sum_{\sigma^1} \int dh^1 A(\sigma, h; \sigma^1, h^1) (\sigma^1 - \tanh \beta h^1) \mathcal{D}[\sigma^1, h^1] \right\} \\ &+ \frac{\partial^2}{\partial h^2} \left(\mathcal{D}[\sigma, h] \left\{ 1 - \sum_{\sigma^1} \int dh^1 \sigma^1 \tanh \beta h^1 \mathcal{D}[\sigma^1, h^1] \right\} \right) \\ &+ \frac{1}{2} \sigma \tanh \beta h \{ \mathcal{D}[\sigma, h] + \mathcal{D}[-\sigma, h] \} - \frac{1}{2} \{ \mathcal{D}[\sigma, h] - \mathcal{D}[-\sigma, h] \}, \end{aligned}$$

where the A 's are solved for from a set of complicated saddle-point equations. We then saw a graph that showed the time evolution of the binding energy for the Sherrington-Kirkpatrick model at $T = 0$, which compared the simple theory and the advanced theory with a numerical simulation using $N = 8,000$. The advanced theory was a great improvement for all the times shown. We also saw some more plots for other cases and histograms of the distributions \mathcal{D} .

At this point, Sherrington gave us a whirlwind tour of some results of Normand Mousseau.

The question at hand is the way an example of parallel microdynamics leads to interesting macrodynamics. It starts with a cellular automata model. There are two general cases. The microscopic variables reside on either a hypercubic lattice or a randomly connected network. The microscopic scale variables are $S_i(t) = 0, 1$ for $i = 1, \dots, N$. The rule is that

$$S_i(t+1) = f\left(\sum_{j \in \mathcal{J}_i} S_j(t)\right),$$

where the set \mathcal{J}_i consists of all the nearest neighbor sites j to the site i . The form of $f(x)$ considered is $f(x) = 1 \forall x_{\min} \leq x \leq x_{\max}$ and zero otherwise. The macroscopic variable is

$$c(t) = N^{-1} \sum_i S_i(t).$$

The idea seems to be to begin with a random configuration $\vec{S}(t = 0)$ which yields an intermediate value of $c(0)$, *e.g.*, $\frac{1}{4} \leq c(0) \leq \frac{3}{4}$. Then one iterates the dynamics and observes the relation between $c(t)$ and $c(t + 1)$. What one sees is an attractor. The type depends on the rule employed and the connectivity of the underlying lattice or network. The various types observed are fixed points, periodic cycles, quasi-periodic cycles, and chaotic attractors. For a randomly quenched mixture of incompatible rules, one sees all of the above plus glassiness for cases with sufficient frustration. Here

$$C(t - t') = N^{-1} \sum_i (S_i(t) - c(t)) (S_i(t') - c(t'))$$

was said to decay slowly.

The work of Chaté and Manneville was mentioned. We then viewed a series of plots of $c(t + 1)$ vs. $c(t)$, which mainly looked sort of like harp-shaped figures, a bit fuzzed out. There is no theory, but simulations still give quasi-three cycles. We saw one figure in which a spray of dots seemed to be approaching the exact solution, a bell-shaped curve. This feature indicates chaotic systems. In the case of quenched random mixtures, we saw a fuzzy harp (quasi-three cycle), a fixed point, and a two cycle. Finally we saw a plot of $\log \log C(t)$ vs. $\log t$. The speaker said that it showed a stretched exponential, *i.e.*, $C(t) \asymp A \exp(-\lambda t^{0.4})$, which was a signal of glass. Thus he said the middle phase is glassy.

Sherrington ended his presentation with some remarks about generalizations, the possible applications of his methods to problems of aging, a plea for more experiments in this area, and a couple of plots of the auto-correlation functions for the three-dimensional Edwards-Anderson model.

Presentation by Len Margolin

Title: The Application of Nonlinear Enslavement to Global Ocean Modeling

This work was reported to have been in collaboration with Darryl Holm, Don Jones, Drew Poje, and Edriss Titi. It concerns dissipative systems. The speaker started with a color plot of the ocean surface temperature done with a grid spacing of 30 kilometers. He said that his talk would cover the ocean's multiscales, the enslavement method (which, he said, leads to a better stochastic flow or chaotic flow), and a more complicated example. The ocean has a huge range of scales and 95% of the energy is subgrid at the currently feasible grid spacing.* Margolin is currently able to calculate stretches of 30 years of time, but that period is short for oceans and doesn't resolve the physics.

* See also the immediately previous presentation of Darryl Holm.

The speaker quoted E. N. Lorenz as saying, “Climate is what you expect; weather is what you get.” Len said that about half the equatorial heat is transported towards the poles by the ocean, of which half is by the western boundary currents and the other half by mesoscale eddies. (The rest of the heat is transported by the atmosphere.) He further said that the climate of the earth has multiple equilibria, and he wants to understand how you get from one equilibrium to another. A fundamental length scale for rotating fluids is the Rossby radius,

$$\mathcal{R} \equiv \frac{\sqrt{gH}}{|f|},$$

where g is the acceleration due to gravity, H is the depth of the ocean, and $|f|$ is the Coriolis force.

Some of the time scales in the ocean are, (i) the transit time of a gravity wave, about 10 hours, (ii) the variability of insolation, ice, and run-off forcing, about 1 year, and (iii) the natural scales for climate variability, about 1,000 years. Some of the spatial scales in the ocean are (i) convective instabilities, 1 km., (ii) peak of the horizontal energy spectrum, 20 km., (iii) width of the western boundary currents 100 km., and (iv) the width of the ocean 10,000 km. Clearly this problem is a multiscale one.

Margolin then describe the current state of the art. For high-resolution runs, the mid-latitude cells are 18 km. on an edge; the problem time is 30 years and the wall clock time to do the run is about 3 months. For climate runs, the mid-latitude cells are about 150 km. on an edge, and the problem time is about 1,000 years. The issue is that the high-resolution runs do not resolve the Rossby radius (but are close to doing so). Can the accuracy be improved without changing the cell size or the associated time step, and even if we do improve the accuracy, how do we measure the improvement?

Margolin next discussed the approximate inertial manifold (AIM) method. It is a methodology which was developed for solving nonlinear, dissipative partial differential equations. It is based on ideas from nonlinear dynamics, including asymptotic balance, the theory of attractors and inertial forms. The underlying idea is nonlinear enslavement. That is, the small scales are slaved to the large scales by the nonlinearity of the problem. These schemes are most often implemented in Galerkin procedures.* Since oceans are not dissipative (in their principal balance) and ocean models are based on finite difference approximations, the issue is the following: do AIM methods apply to the oceans?

Burger’s equation was presented as an example. For this example, the problem is recovering a solution on a coarse mesh with the accuracy of a fine mesh. The equation is

$$\frac{\partial u}{\partial t} + u \frac{\partial u}{\partial x} - \lambda \frac{\partial^2 u}{\partial x^2} = f(x, t).$$

Consider two meshes, one with half the mesh spacing of the other. On the fine mesh label the values of u at successive mesh points $\alpha_k, \beta_k, \alpha_{k+1}, \beta_{k+1}, \dots$, and call the corresponding right-hand sides $f_k, g_k, f_{k+1}, g_{k+1}, \dots$. Then start with the difference

* expansion in orthogonal polynomials

scheme:

$$\frac{\alpha_k^{n+1} - \alpha_k^n}{\delta t} + \frac{(\beta_k^n)^2 - (\beta_{k-1}^n)^2}{2 \delta x} - 4\lambda \frac{\beta_k^n + \beta_{k-1}^n - 2\alpha_k^n}{\delta x^2} = f_k, \text{ and}$$

$$\frac{\beta_k^{n+1} - \beta_k^n}{\delta t} + \frac{(\alpha_{k+1}^n)^2 - (\alpha_k^n)^2}{2 \delta x} - 4\lambda \frac{\alpha_{k+1}^n + \alpha_k^n - 2\beta_k^n}{\delta x^2} = g_k.$$

Next consider the change of variables*

$$a_k \equiv \alpha_k + \beta_k \sim O(u), \quad \text{and} \quad b_k \equiv \beta_k - \alpha_k \sim O\left(\frac{\partial u}{\partial x} \Delta x\right).$$

Back substitution for α and β in terms of a and b leads to the re-expression of the above equations in terms of a and b . The result is to express in terms of variables defined on the coarser mesh equations which are so far exactly equivalent to those on the finer mesh. Of course, there are now twice as many variables per mesh point as before. These equations are

$$\frac{a_k^{n+1} - a_k^n}{\delta t} - 2\lambda \frac{a_{k+1}^n + a_{k-1}^n - 2a_k^n - b_{k+1}^n + b_{k-1}^n}{\delta x^2} + \frac{(a_{k+1}^n)^2 - (a_{k-1}^n)^2}{4 \delta x}$$

$$+ \frac{-2a_{k+1}^n b_{k+1}^n + 4a_k^n b_k^n - 2a_{k-1}^n b_{k-1}^n + (b_{k+1}^n)^2 - (b_{k-1}^n)^2}{4 \delta x} = f_k^+, \text{ and}$$

$$\frac{b_k^{n+1} - b_k^n}{\delta t} - 2\lambda \frac{a_{k+1}^n - a_{k-1}^n - 6b_k^n - b_{k+1}^n - b_{k-1}^n}{\delta x^2} + \frac{(a_{k+1}^n)^2 + (a_{k-1}^n)^2 - 2(a_k^n)^2}{4 \delta x}$$

$$+ \frac{-2a_{k+1}^n b_{k+1}^n + 2a_{k-1}^n b_{k-1}^n + (b_{k+1}^n)^2 + (b_{k-1}^n)^2 - 2(b_k^n)^2}{4 \delta x} = f_k^-.$$

The idea now is somehow or other to eliminate the small scale represented by the variables b , and to obtain an expression, $b_k = \Phi(a_k)$, so that the resulting equation on the coarse scale no longer depends on the set of auxiliary variables b_k . This representation of the b 's in terms of the a 's is what is meant by the speaker when he speaks of the small scales being enslaved to the large scales (by nonlinearity).

In order to provide a rationale to justify his method of approach to the achievement of these ends, Len gave a scaling analysis of Burger's equation. Taking out the dominant scale of each variable, he got

$$\left[\frac{U}{T}\right] \frac{\partial u}{\partial t} + \left[\frac{U^2}{L}\right] u \frac{\partial u}{\partial x} - \left[\frac{\lambda U}{L^2}\right] \frac{\partial^2 u}{\partial x^2} = [\mathcal{F}]f(x, t).$$

He then assumes that the primary balance of terms is between the forcing, advection, and diffusion. This assumption is presumably appropriate for the applications he has in mind.

* The idea of averaging out the scale of the highest frequency also appears in the theory of the renormalization group. See, for example, the presentation by George A. Baker, Jr. in Section 5.

The forcing determines the velocity scale U , and thus we have the order of magnitude relations,

$$\mathcal{F} \sim \frac{\mathcal{U}^2}{\mathcal{L}}, \quad \mathcal{U} \sim \frac{\lambda}{\mathcal{L}}, \quad \text{and} \quad \mathcal{U} \gg \frac{\mathcal{L}}{\mathcal{T}}.$$

He also performed a scaling analysis of the difference equation for the u 's and found that a linear stability analysis shows that

$$\Lambda = \frac{\lambda \delta t}{\delta x^2} \leq \frac{1}{2}, \quad \text{and} \quad U = \frac{u \delta t}{\delta x} \leq \frac{1}{2}$$

are necessary (and hopefully sufficient although this part wasn't said) for the stability of his explicit, numerical equations. He further noted that

$$\frac{U}{\Lambda} = \frac{\mathcal{U} \mathcal{L} \delta x}{\lambda \mathcal{L}}.$$

The ratio

$$\epsilon \equiv \frac{\delta x}{\mathcal{L}} = \frac{1}{N} \ll 1,$$

being one over the number of points in the grid, is a small parameter. The stability is controlled by the viscous condition and the condition $\delta t \sim \delta x^2 / \lambda$ (but of course, necessarily $\leq 0.5 \delta x^2 / \lambda$). Thus the new variables introduced have the scales

$$a_k \sim \mathcal{U}, \quad \text{and} \quad b_k \sim \frac{\partial u}{\partial x} \delta x = \frac{\mathcal{U}}{\mathcal{L}} \delta x = \mathcal{U} \epsilon.$$

There then followed the scaling of the “ b ” equation, to limited order in ϵ . Matching terms to the second order in ϵ leads to the enslavement expression sought,

$$b_k = \frac{a_{k+1} - a_{k-1}}{8} - (a_{k+1}^2 - 2a_k^2 + a_{k-1}^2) \frac{\delta x}{64\lambda} \\ + \left[a_{k+1} \left(\frac{a_{k+2} - a_k}{8} \right) - a_{k-1} \left(\frac{a_{k+2} - a_k}{8} \right) \right] \frac{\delta x}{32\lambda},$$

where the superscripts n are suppressed. Note that in this derivation, in addition to the stability requirements, the requirement that ϵ be small, there is also the requirement that $b_k^{n+1} - b_k^n \sim b \delta t / \mathcal{T}$.

Margolin concluded his presentation with the example of the 2-dimensional, shallow water equations. They are

$$\frac{\partial h}{\partial t} + \vec{\nabla} \cdot (h\vec{u}) = 0, \quad \text{and} \quad \frac{\partial \vec{u}}{\partial t} + (\vec{u} \cdot \vec{\nabla})\vec{u} = -g\vec{\nabla}h + f(1 + \beta\vec{r} \cdot \vec{e}_y)(\vec{u} \times \vec{e}_z) + \nu \nabla^2 \vec{u} + \vec{F},$$

where h is the thickness of the fluid and \vec{F} is the forcing term (winds).

The example system computed was 2,000 km north to south and 1,000 km east to west. It was subject to winds which varied sinusoidally (north to south). The flow in the “idealized ocean basin” resolved into two counter-rotating gyres. Various solutions were

presented: the solution on a fine grid, the solution on a coarse grid, and the enslaved difference approximation on a coarse grid, for example. The enslaved difference approximation on a coarse grid seemed to agree very well with the solution on a fine grid, while the coarse-grid solution differed noticeably. What makes it work is that, in this case, the flow is almost steady. The kinetic energies as a function of time were also compared. The statistical moments and the heat transport were compared as well. The overall picture was that the enslaved coarse-grid solution compares well with the standard fine-grid solution.

4. Many Mesoscopic Scales

Presentation by Lee Collins

The general topic here is cluster dynamics and this presentation reports joint work with Joel Kress. The goal is the modeling of hot, dense, disordered media. Examples would be systems of ions and electrons, dense plasmas, and alkali liquids. The sought answers are transport properties, both material and radiation. Additional results of interest are thermodynamic properties, the pair correlation functions, conductivity, diagnostics, *e.g.*, line broadening mechanisms, and cluster formation rates and their size distribution. The interest in the cluster properties stems from the fact that the radiation transport is very sensitive to them. A number of time scales of importance have been identified in the dense plasma case. Densities of the order of 10^{10} to 10^{17} to 10^{18} (or perhaps only to 10^{14} electrons/cc.) were mentioned. There is the electron time scale of about 10^{-17} seconds, the motion scale of the nuclei of about 10^{-15} to 10^{-14} seconds, the cluster formation scale of about 10^{-13} to 10^{-11} seconds, and the transport scale of about 10^{-12} to 10^{-11} seconds which overlaps the cluster scale. There is not a direct analogy between the time scales and the distance scales. The distance scale for transport is in the range of 100 to 1,000 Bohr (1 Bohr = 5.2917×10^{-9} cm). The approach that has been used to attack this problem is (approximate) quantum, molecular-dynamical simulation applied to a periodically replicated cell of N atoms. Classical equations are used for the nuclei, and density functional and empirical methods are used for the electrons. Problems of size $N = 50$ have been treated using density functional method and $N = 1,000$ with semi-empirical methods. The major obstacle here is that the equations of motion of the system are on the microscopic time scale and answers on the macroscopic scale are sought.

Presentation by Salman Habib

The methods discussed in this presentation were all computer based, and in particular, parallel computation is emphasized and the Thinking Machines CM5 is used. One of the procedures used is solving field theoretic Langevin equations. This is a molecular dynamics type of approach.

One example of the sort of problem under study is the statistical mechanics of kinks. This problem can be thought of as a version of one-space and one-time dimensional $\lambda : \phi^4$ theory. For simplicity it can be viewed as a chain of classical particles each of which is in its own, two-equivalent-minima potential, together with interactions between the particles along the chain. When the temperature is low, each particle will sit, subject to small thermal vibrations, at one of its two possible minima. A kink is where one particle is in the positive-value-of-the-coordinate minima and the next particle along the chain is in the other minima. An antikink is where the particles are vice versa. The possibility is present, when the temperature is not too low, that the transition from one minima to the other may require a span of several particles along the chain. These particles, of course, would not be particularly near to their respective potential minima. Thus there are three length scales in this problem: (1) the length scale of the phonons, (2) the length scale,

or width, of the kinks, and (3) the length scale between kinks, or the distance along the chain that the particles are all in one minima. The answers sought in this investigation are correlation functions, density of kinks, *etc.* There is an (approximate) analytical theory of these phenomena based on a dilute gas theory. As one runs a computer simulation forward, the kinks and antikinks can annihilate each other, and also kink–antikink pairs can be formed. If $n_k(t)$ denotes the number of kinks at time t , then the autocorrelation function, $\langle n_k(t)n_k(t + \tau) \rangle - \langle n_k(t) \rangle \langle n_k(t + \tau) \rangle$, is expected to decay like the sum of two exponentials in “computer time.” There have been problems with previous simulations *e.g.*, a recent PRL in which, the speaker said, the wrong correlation between kinks was reported. Mention was made of multiplicative noise.* The most important obstacle was reported to be the nonlinearity of the field equations.

There are, or potentially are, applications of these methods to (1) Nonequilibrium dynamics in general and those near phase transitions in particular, (2) beams and galactic dynamics, (3) quantum dynamics, and (4) shaped-memory problems.

Presentation by Fred Cooper

The problem described in this presentation concerns heavy-ion collisions as calculated from quantum chromodynamics (QCD), but the work is also relevant to the problem of the early universe. There are three time scales: (1) the oscillation scale, (2) the plasma frequency scale, and (3) the electric-field to quantum-field equilibration time. There is also a fourth or relaxation time scale, but it has not yet been incorporated. The oscillations referred to are caused by the impossibility of constructing solutions to (for example) the Dirac equation from the basis of positive energy states alone, particularly when the density is enough to crowd particles into regions smaller than their Compton wavelength. The admixture of these negative energy states causes very high frequency real oscillation, larger than $2mc^2/\hbar \approx 2 \times 10^{21} \text{s}^{-1}$ for electrons. This phenomenon is called *Zitterbewegung*. The plasma frequency is the usual plasma frequency expected in a gas of positive and negative charges. There is a bimodal distribution in the power spectrum. One peak is for the *Zitterbewegung* and the next for the plasma frequency. The third scale refers to the rate of transfer of energy from the electromagnetic field to the quantum field. The results displayed look like a damped oscillator with high-frequency static. That is to say, there are the static frequency, the oscillator frequency, and the rate of damping.

The object is to predict the distribution of the quarks in the quark-gluon plasma phase, and from that to determine the distribution function for the rates of lepton production. The principal obstacles are the multiple time scales and the chaotic behavior. The type of chaotic behavior referred to here was described as being characterized by a single square-wave-shaped portion of the power spectrum. The approach is through the numerical integration of, among other things, classical oscillator equations on the Thinking Machines CM5. The appropriate Lagrangian is

$$\mathcal{L} = \frac{1}{2}\dot{x}^2 + \frac{1}{2}\dot{A}^2 - \frac{1}{2}(m^2 + e^2 A^2)x^2$$

* See also the footnote to the presentation by S.-Y. Chen, Section 3.

subject to

$$\langle x(t) \rangle = 0, \quad \text{and} \quad \langle x(t)x(t) \rangle = G(t).$$

Presentation by Lee Collins

The physical problem under discussion is that of dense plasmas with temperatures of the order of volts. These conditions occur in lots of places. There are multiple scales in this problem. The smallest in space and the quickest in time is the motion of electrons on the atomic scale. Next there is the scale of nuclear motion. There is the cluster formation scale, and somewhat overlapping it, is the transport properties (e.g., diffusion and viscosity) scale. The clustering of say 3, 4, or 5 particles has a strong effect on the radiation properties, but not particularly on the transport properties. The radiation properties are quite sensitive to changes in the density. There are several types of quantum molecular dynamical methods to approach these problems. One group is the Car-Parrinello methods. In these methods, a self-consistent, calculation is not done, but basically pseudo-particles are used, *i.e.*, nucleons dressed with electrons. Alternatively, as used by the panelist and his coworkers, there is the density functional approach. The codes used were developed with Norm Troullier of the University of Minnesota. One fixes the nuclei and finds the time asymptotic distribution of the electrons by density functional methods. A full matrix diagonalization of the electronic Hamiltonian is used, but maybe not at every step. From this distribution, the forces on the nuclei are computed. *These procedures peel off the microscopic scale, at the expense of more computation per mesoscopic scale time step.* These sort of procedures are effectively equivalent to integrating out the fast nodes. Could they be applicable to the problems involving the “mesoscopic barriers” of the previous panel discussions supposing the fundamental pseudo-particles or structures can be identified? Discussions during the course of this meeting also led to the question, are there regions of interest such as in inertial confinement fusion in which the opacity problem could be treated by finite-temperature, quantum many-body perturbation theory (plus series summation methods)?

Presentation by Fred Cooper

Work has concentrated on two things. One is the distribution of quarks in a quark-gluon plasma. The other is a simple model of $N + 1$ coupled quantum oscillators. Analytic results can be obtained for this model, and it is thought to exemplify the basic character of the other model. How does the large N expansion work here? Consider N phase-locked copies satisfying

$$\ddot{x} + (m^2 + e^2 A^2)x = 0$$

plus one copy of

$$\ddot{A} + e^2 x^2 A = 0.$$

In lowest-order approximation (in $1/N$), you get

$$\ddot{A} + e^2 \langle x^2 \rangle A = 0,$$

$$\ddot{x} + [m^2 + e^2 A^2(t)]x = 0.$$

The trick is to make A a classical field ($\mathbf{A} \sim \sqrt{N}A_0$, $\hat{e}^2 = e^2/N$). Alternatively, the Hamiltonian approach gives

$$H = N \frac{\dot{x}^2}{2} + \frac{\dot{A}^2}{2} + Nm^2 x^2 + e^2 A^2 N x^2, \quad \text{and}$$

$$\frac{H}{N} = \frac{\dot{x}^2}{2} + \frac{\dot{A}^2}{2N} + m^2 x^2 + e^2 A^2 x^2,$$

where we have the restrictions

$$\langle x \rangle = 0, \quad \text{and} \quad \langle x^2 \rangle \sim 1.$$

The A field behaves as if it had a very large mass, and it is centered about a big value (see above), but its fluctuations are of order unity. The lowest-order problem turns out to be chaotic and is very sensitive to the initial conditions. The time scale for which chaos sets in is governed by the Lipanov exponents. There is also the time scale for the order $1/N$ quantum corrections. If this time scale isn't longer than the chaos time scale, then this method doesn't work, and this approach is out of luck. This approach has similarities to a mean-field theory for the electric field carried by A . The question of whether the quantum dynamic corrections swamp the fastest motion of the resultant equations should also be investigated in the problem described by the previous panelist. A further question is whether the methods of dressed quarks and/or self-consistent field methods could be usefully applied here as they were in the problems studied by the first panelist.

Presentation by Salman Habib

This presentation began with the fundamental question, "How do the scales arise and what are they?" The answer is hard to discover a priori. Suppose that the microscopic physics is known, or only partially known, then you may miss things like gels. Here is an example* which illustrates some of the complexities. Consider N -point masses with a $1/r$ potential, for example, a globular cluster. It was stated that N -body codes are very dangerous because the error control is bad. Energy errors of the order of one percent occur. Gravitational systems are unstable.** Very complicated things happen, and one can't follow the motion. It was reported that there is a big argument about whether such a system is integrable or not. Whether the orbits are chaotic or not, or whether

* This example is closely related to problems with no fixed scale. See the presentation of Mike Warren in Section 5.

** This point is important. Since energy is conserved, one might think that a bound (negative energy system) could not disperse, and this lack of dispersion is assumed in the usual proof of the virial theorem. However, a moment's reflection shows that near-collision processes could lead to two mass points becoming more tightly bound and a third being given enough energy to be ejected.

by scattering they might go into a stochastic orbits,* or when they might be trapped in periodic (or quasi-periodic) orbits is poorly understood. The addition of a very small amount of noise can cause the orbits to leak through the Cantori** and cause the diffusion time scale to change from linear to exponential.

AOT Division wants to build a proton LINAC (linear accelerator) at an energy of 1 GeV and a current of 100 mA. The behavior of the proton beam shares much in common with the above described gravitational problem.†

The relaxation time for a galaxy was computed by Chandrasekar to be about 100 times the age of the universe. However, there is a much faster time scale hidden in the N -body system that he missed. The mean-field potential problem is nonintegrable, and we get a new time scale governed by the Lipanov exponents which tends rapidly to a quasi-equilibrium, rather than the true equilibrium with which Chandrasekar was concerned. This time scale is about one-tenth the age of the universe.

An example of systems for which the appropriate physics is not known comes from nanotechnology and is a metascopic gold wire about 20 microns long. The resistance in this wire in a magnetic field changes in a random way. If the wire is long enough, quantum interference effects stop these changes, but how the phase-breaking length comes out of the fundamentals is not known.

Another example is gravity wave detectors. One-ton aluminum bar detectors are made. They have very high Q . Single crystal detectors will ring for about a year at about 1 kHz. The quantum coherence time is much smaller, and the dissipative mechanism in this problem is not understood.

Referring to the kink-nucleation problem,†† the panelist said that noise can change the time scale. When the heat bath is multiplicative, the time scale can be changed by orders of magnitude. One must be careful of the color of the noise as well. An important question is “What is the role of fluctuations, or what aspect is it of fluctuations, that can change the time scales by orders of magnitude?” The panelist also said that certain expansions go bad after some time and that the $1/N$ expansion is sort of like the BBGKY truncation scheme because they both treat 3- or 4-body and higher effects in an averaged way. Another time scale found in many body studies is the long time tails of Cohen and Dorfman in dense gases.

Presentation by Emil Mottola

In this talk, of interest are problems in which there is a rapid (basically uninteresting)

* By a stochastic orbit, as distinguished from a regular orbit, is meant that if one considers a Poincaré section of phase space, a region of this section [bounded by a KAM-tori (Kolmogorov, Arnold, Moser)] is randomly penetrated by successive passage of the orbit, more or less filling the region.

** These are generalized tori in phase space that, without the noise which causes the leaks, would have contained the orbits of the system. They are named after G. Cantor.

† Except of course, there are no bound states because the sign of the interaction is purely repulsive.

†† See the previous presentation by S. Habib.

microscopic scale fluctuation plus interesting mesoscopic and macroscopic behavior. In this series we have previously heard of some examples of such microscopic scales. For instance, the *Zitterbewegung* described by Fred Cooper or the phonon length scale in the kink problem discussed by Salman Habib. Two methods of approach are described. The first one, Gaussian dynamics, is able, with considerable computational effort, to deal with the microscopic and mesoscopic scales. Unfortunately, the involved approximations break down at the longer times of the macroscopic scale. The second method is a kinetic theory approach. Cross comparison of this method with the first shows that the kinetic theory approach gives results in which the mesoscopic scale behavior is well reproduced, and the microscopic-scale variations are smoothed out. Thus, the kinetic theory approach takes a big step forward by not having to work at the microscopic scale.

First, the speaker described the *Gaussian dynamics* method. Consider a wave function which is a general Gaussian,

$$\psi(x, t) = \mathcal{N} \exp \left\{ -(x - \bar{q})^2 \left[\frac{1}{4G} - i\Sigma \right] + i\bar{p}(x - \bar{q}) \right\},$$

where \bar{q} , \bar{p} , G , and Σ are real functions of time. They are, for the moment, arbitrary, but as the formalism develops, choices will be made so that they will obey a set of Hamilton's equations. These quantities can be expressed in terms of expectation values:

$$\begin{aligned} \bar{q}(t) &= \langle \psi | \hat{q} | \psi \rangle = \int_{-\infty}^{\infty} x \psi^* \psi dx, \\ \bar{p}(t) &= \langle \psi | \hat{p} | \psi \rangle = \int_{-\infty}^{\infty} \psi^* \left(-i \frac{\partial}{\partial x} \right) \psi dx, \\ G(t) &= \langle \psi | \hat{q}^2 | \psi \rangle - \bar{q}^2 = \int_{-\infty}^{\infty} (x - \bar{q})^2 \psi^* \psi dx, \\ 4G(t)\Sigma(t) &= \langle \psi | \hat{p}\hat{q} + \hat{q}\hat{p} | \psi \rangle - 2\bar{q}\bar{p}, \quad \text{and} \\ \frac{1}{4G(t)} + 4\Sigma^2(t)G(t) &= \langle \psi | \hat{p}^2 | \psi \rangle \equiv K(t). \end{aligned}$$

Alternatively, and *this idea is crucial*, one may use these expectation values to define a Gaussian approximation to the wave function. This procedure was called the *mean-field approximation*. The idea then is to follow a set of 5 parameters in time rather than to deal with a wave function. (Of course this is an approximation, as the wave function in most problems does not retain a Gaussian shape.) The parameters in such a Gaussian wave function, however, are not sufficiently general to encompass the full range of such expectation values for the first and second moments of the operators \hat{q} , \hat{p} (their mean values and their variance), but as noted in the last of the above equations, there must be a relation between K , G , and Σ . In order to overcome this problem and have 5 independent quantities, the speaker next moved to the corresponding density matrix, which he writes

as,*

$$\rho(x', x, t) \equiv \langle x' | \hat{\rho}_{\text{Gauss}}(t) | x \rangle = (2\pi\hbar G)^{-\frac{1}{2}} \exp \left\{ \frac{i\bar{p}(x' - x)}{\hbar} - \frac{1}{2} \frac{(K - 4G\Sigma^2)}{\hbar^2} (x - x')^2 - \frac{i\Sigma}{\hbar} [(x - \bar{q})^2 - (x' - \bar{q})^2] - \frac{1}{8G} (x + x' - 2\bar{q})^2 \right\}.$$

This form of the density matrix permits all five parameters to be independent.**

With malice aforethought, the speaker next introduced the following equations to describe the time dependence of 5 time-dependent parameters in the density matrix,

$$\dot{\bar{q}} = \bar{p}, \tag{1}$$

$$\dot{\bar{p}} = -\omega^2(t)\bar{q}, \tag{2}$$

$$\dot{G} = 4\Sigma G, \tag{3}$$

$$\dot{\Sigma} = -\frac{\omega^2(t)}{2} - 4\Sigma^2 + \frac{K}{2G}, \tag{4}$$

$$\dot{K} = -4\omega^2(t)G\Sigma, \tag{5}$$

with $\omega(t)$ a definite function of time depending on the application. A directly calculable consequence of these equations of motion is that $\frac{d}{dt}[GK - 4G^2\Sigma^2] = 0$ so that $GK - 4G^2\Sigma^2 \equiv \hbar^2\mu^2/4$ is a constant of the motion. (It is just the quantity which we found from the Cauchy-Schwartz inequality.) The quantity μ is called the mixing parameter since $\text{Tr } \hat{\rho}(t) = 1$, but $\text{Tr } \hat{\rho}^2(t) = \mu^{-1} \leq 1$ follows by direct calculation. It follows in the usual way that, as a density matrix defined from a pure state is a projection operator,

* This equation differs from that for a pure state by replacing the coefficient of the $(x - x')^2$ with that displayed, instead of the pure state value of $1/8G$. This replacement has the effect of multiplying the density matrix by the factor

$$\mathcal{C} = \exp \left[\frac{1}{2} \left(\frac{1}{4G} - K + 4\Sigma^2 G \right) (x - x')^2 \right].$$

This term can be expanded in a sum of products of function $\phi_n(x)\phi_n(x')$, and so the density matrix represents an ensemble instead of a pure state. The ϕ_n 's are themselves each expressible as a finite sum of Hermite polynomials times a Gaussian. The set of Hermite polynomials times their Gaussian weight function is a complete set. While it is true that the ensemble so generated has component states which span the whole space, it nevertheless only represents a one-dimensional subset of an infinite dimensional set of density matrices.

** In order to maintain normalizability, it must be that $K \geq 4G\Sigma^2$. For values of the parameters determined by taking expectations with respect to a general wave function, this inequality, in the form, $GK \geq 4G^2\Sigma^2$, can be derived by an application of the Cauchy-Schwartz inequality, $(\int f^2 dz \int g^2 dz \geq (\int fgdz)^2)$, provided $G \neq 0$.

the trace of its square is also unity, and so $\mu = 1$ for any pure state. As we saw above, the general, mean-field approximation can be represented by a one-dimensional family of Gaussian density matrices which in turn are appropriate to an ensemble of (not purely Gaussian) states.

The next step in the setup of the Gaussian dynamics formalism is to convert the equations into a classical form. Let us define

$$\begin{aligned}\xi^2(t) &\equiv G(t), \text{ and} \\ \dot{\xi}(t) &= 2\xi(t)\Sigma(t),\end{aligned}$$

where the second equation follows from the first by virtue of Equation (3) above. We may now eliminate K in favor of ξ and μ as $K = \frac{1}{4}\hbar^2\mu^2/\xi^2 + \dot{\xi}^2$. In this form, the equations of motion (1-5) above can be derived as Hamilton's equations for the Hamiltonian,

$$\begin{aligned}H_{\text{eff}}(\bar{p}, \bar{q}; p_\xi, \xi) &= \frac{\bar{p}^2}{2} + \frac{p_\xi^2}{2} + V_{\text{eff}}(\bar{q}, \xi), \text{ and} \\ V_{\text{eff}}(\bar{q}, \xi) &= \frac{\omega^2(t)}{2} (\bar{q}^2 + \xi^2) + \frac{\hbar^2\mu^2}{8\xi^2}.\end{aligned}$$

Here the Gaussian dynamics of certain density matrices has been re-expressed as strictly classical dynamics, and the only appearance of \hbar is as a central repulsion in the effective potential.* In this formulation, \hbar comes purely from the initial data, *e.g.*, that for $\text{Tr } \hat{\rho}^2(0)$ and $G(0)K(0) - 4G(0)^2\Sigma(0)$. These equations of motion are identical to those for a *Gaussian* phase-space distribution of a cloud of independent particles. For such a Gaussian distribution under these equations of motion, direct computation shows that the second moment of the distribution, $\int dx \int dp f^2(x, p) = \sigma_2 \equiv 1/(h\mu)$, is a time-independent constant. The only role of \hbar here is to normalize this distribution.

Next Emil presented a simple example. It was the two-well, anharmonic oscillator. The Lagrangian of the system is $\mathcal{L} = \frac{1}{2}\dot{q}^2 - \lambda(q^2 - v^2)^2/8$. In the example, the large- N method** or mean-field method is used. In this method, $q \rightarrow \sum_{i=1}^N q_i q_i$. The notation $\chi = -\lambda v^2/2 + (\lambda/2N) \sum_{i=1}^N q_i q_i$ is needed, and so is the definition of the f 's as mode functions in the expansion

$$q = \bar{q} + af(t) + a^\dagger f^*(t), \quad p = \bar{p} + a\dot{f}(t) + a^\dagger \dot{f}^*(t),$$

with a, a^\dagger the usual creation and annihilation operators. With the further definition $\xi^2(t) \equiv \langle (q - \bar{q})^2 \rangle$, when this problem is worked out in this approximation, it leads to

$$\left[\frac{d^2}{dt^2} + \bar{\chi}(t) \right] \bar{q}(t) = 0, \tag{1'}$$

* To make a full connection with quantum mechanics, it would be necessary also to give the quantum Hamiltonian for which $\mathcal{H}\psi = i\hbar(\partial/\partial t)\psi$ yields the same equations of motion. The speaker did not address this issue, but in the context of the mean-field approximation the time dependent quantities $\bar{q}, \bar{p}, G, \Sigma$ were supposed to have come from the solution of some such more fundamental equation.

** See also the above presentation of Fred Cooper regarding the large- N method.

$$\bar{\chi}(t) = \frac{\lambda}{2} [-v^2 + \bar{q}^2(t) + \xi^2(t)], \quad (2')$$

$$\left[\frac{d^2}{dt^2} + \bar{\chi}(t) \right] f(t) = 0, \quad (3')$$

$$\xi^2(t) = (2n + 1)|f(t)|^2, \text{ and} \quad (4')$$

$$f \frac{d}{dt} f^* - f^* \frac{d}{dt} f = i\hbar. \quad (5')$$

These equations are the Heisenberg representation. The usual commutation relation $[a, a^\dagger]$ implies by (5') the expected results $[p, q] = i\hbar$. Finally, the speaker pointed out that these equations are *identical* with (1-5) given earlier when we identify $\omega^2(t) \rightarrow \bar{\chi}(t)$ and $\mu \rightarrow 2n + 1$, so that the large- N method applied to this example reproduces the mean-field Heisenberg equations which are equivalent to the Gaussian density matrix evolution in the Schrödinger picture.

This same procedure can also be applied to *systems with many degrees of freedom which is where the method is of interest to this initiative*. The problem described was the Schwinger problem. In this problem, one has a large condenser with a high charge on the plates. This produces a very strong electric field. The quantum electro-dynamics problem is to study the system of electrons and positrons which are pulled out of the vacuum in the space between the condenser plates. A plot of the solution (including 60,000 modes and run on the CM5) reveals that the current shows plasma oscillations, but riding on top of them is a small amplitude, very high-frequency jitter (Zitterbewegung). It was pointed out by the audience that there is an analogous problem in solid-state physics involving an applied-field, the Stark effect, and excitons, *etc.* There is also a longer-term time scale which is related to Landau (collisionless) damping. In this problem, it is manifest by “dephasing” or “decoherence.” The approximations in the Gaussian dynamics prevent it from accurately describing the solutions over such long times, however.

Next, *the kinetic theory approach was discussed by the speaker. The Boltzmann equation, to the lowest order, is*

$$\left[\frac{\partial}{\partial t} + e\vec{E} \cdot \vec{\nabla}_{\vec{p}} \right] N(\vec{p}, t) = ?$$

for the spatially homogeneous case. We have the time dependence

$$\dot{E}_z = -\dot{j}_z = -2e \int \frac{d^3 \vec{p}}{(2\pi)^3} \left(\frac{p_z}{\omega_{\vec{p}}} \right) N(\vec{p}, t).$$

If ? = 0, then there is no particle creation, no entropy production, but only dissipationless plasma oscillations. Since we know that QED does lead to particle creation, Emil suggested the Schwinger-inspired source term,

$$? = - \underbrace{(1 - 2N)}_{\text{}} \underbrace{|eE| \ln \left\{ 1 - e^{-\pi m^2 / |eE|} \right\}}_{\text{}} \underbrace{\delta(p)}_{\text{}}.$$

The first factor is the Pauli blocking term, the second the Schwinger rate term, and the last assumes creation at rest. We were shown a graph comparing the solutions for the current which illustrated the result that the kinetic theory method produces a nonjittery version which agrees quite well with the actual solution as generated by Gaussian dynamics, at least for the first few cycles.*

The speaker claimed that these equations of motion (*i.e.*, for the Gaussian density-matrix) are *chaotic*, and that this feature can easily be seen even in the simple anharmonic oscillator case discussed above. The reason, he said, was that while chaos is impossible with one degree of freedom, these equations describe a distribution, and so they can be chaotic. The Lyapanov exponent is

$$\lim_{t \rightarrow \infty} \lim_{\Delta \rightarrow 0} \frac{\ln \left[\frac{\Gamma_p(t) - \Gamma_{p+\Delta}(t)}{\Delta} \right]}{t} = \gamma_L > 0,$$

where $\Gamma_p(t)$ is the phase space trajectory with initial data p , and Δ is an infinitesimal. This inequality means that the orbits are exponentially diverging which feature leads, of course, to decoherence. (An analogy in solid state physics is polaron tunneling.) We were shown graphs of the results for $eE/m^2 = 1.000, 0.999$ to illustrate this point. They were quite similar at first, even down to the jitter. In the Gaussian approximation, different initial conditions lead to different $\omega(t)$ functions. This effect, in turn, leads to the rapid phase decoherence between different states.

Altogether then, we see in the Schwinger problem what we can call a microscopic (fast decoherence time), a mesoscopic (plasma or collective excitation time), and a macroscopic scale (plasmon damping time) in this problem. The kinetic theory method gives a good, nonjittery solution as displayed at the mesoscopic time scale. The Gaussian approximation method succeeds in representing the first two time scales, but the third is a time scale on which the approximation breaks down, and it is not unreasonable for this to be the Lyapanov time scale. This last idea is not proven in general, but does hold for the comparison of Schrödinger dynamics with Gaussian dynamics. One result along this line, which is known, is that the maximal Lyapanov exponent of classical $SU(N_c)$ gauge theory is just twice the quantum plasmon damping exponent.

Presentation by Lee Collins:

Title: Transient Quantum Mechanical Processes

This problem has multiple time scales. It involves hitting a molecule with a laser. Laser pulses can now be generated in the range of femtoseconds rather than nanoseconds, which was the previous state of the art. This time scale is of the same order as some of the molecular processes. If you can hit during such a process, you can probe deeply, or maybe control the molecular process. Special shaped pulses are required for some of these applications. As an example, HCl vibrates, and one could use such a laser to control the excited-state populations.

* Emphasis added.

The time scales are as follows:

1. Electrons in the molecule move very fast.
2. Vibrations of the electron cloud are of the order of 10s to 100s of femtoseconds.
3. Rotations are of the order of 1000 femtoseconds.

Experiments have been conducted in MST Division on K_2 . Here the experimenters can probe, on a 50 femtosecond time scale, where the molecule is during the vibrations. They get plots of the energy versus distance. By pulse shaping techniques, you can force the molecule into one configuration or another. One of the questions of interest here is an “inverse scattering type question,” *i.e.*, given a process rate what is the laser pulse required to produce it? (The solution need not be unique.) The basis is the time-dependent Schrödinger equation. Time-dependent perturbation theory doesn’t work well here because the perturbation is not small and the process is transient. The method being used is a version of optimal control theory. All three of (i) the penalty properties, (ii) the optimization properties, and (iii) the constraints, which here are the time-dependent Schrödinger equation, feed into a measuring functional. The resulting output would be the necessary electric field.

Presentation by Hans Frauenfelder

Title: Energy Landscapes

This talk focused on biomolecules, and in particular, on the problems of protein folding. He explained that there is a primary structure of the protein molecule in which the molecule is like a somewhat wavy line, there is a secondary structure in which the molecule looks like an α -helix or a coil spring, and a tertiary structure in which the molecule looks like a coil spring that is all wadded up. This structure was referred to as space filling. He showed plots of properties which one might have naively expected to decay exponentially but which seemed to decay in a power-law manner. This behavior is thought to reflect a multitude of time scales. From here, the discussion moved to the energy landscape. This phrase refers to a semiclassical description of the energy of a protein in terms of the conformation of the molecule. To some limited extent, it seems to be like a phonograph record. When viewed from a distance, it seems fairly smooth. When viewed more closely, it has a lot of very similar grooves. When the grooves are examined in detail, one finds various internal structures. So it is with the energy landscape of a protein. When the free energy is plotted against the conformation coordinates, one sees valleys. These are called “substates.” Looked at in more detail, the surface is rough with small valleys in the valley floor. If we look here in more detail, we see “folding funnels.” As the funnel narrows down, we come to the region called a “molten globule.” With further narrowing, we reach the bottom of the funnel, where we have the “native protein.” Here however, we again find a rough bottom. The valleys in this rough bottom are called taxonomic CSs (conformational substates) and if we now look at the valleys in the bottom of these valleys, we find again more roughness. The new tiny valleys so discovered are called statistical CSs.

New results were also discussed. Hole burning was mentioned: if you have a broad line, you can burn a hole in it with a laser. Myoglobin was reported to have a structure

which bifurcates (actually, multifurcates) to a depth of 7 levels. You see different effects as the temperature goes up. The various motions have been classified. The ones on the largest scale are called vibrations. Some concluding remarks were the following: Proteins can unfold in nanoseconds, and the x-ray structure that one sees is just the resting state and not the working state. The phenomena extend over 6 orders of magnitude in time. Lastly, light has an enormous effect.

Presentation by Alan Glasser

Glasser talked to us about NIMROD (NonIdeal Magneto-hydrodynamics, Rotation, Open Discussion) which is a team effort involving D. C. Barnes, A. H. Glasser, R. A. Nebel, C. R. Sovinec, and a number of outsiders. They are developing a new computer code. They have talked to the potential customers and are dealing with conflicting requirements. This project involves parallel computing. He reported that fusion funding was down one-third this year but not dead, and he expects this will be mostly paid for by Europe and Japan. The code is for numerical simulation of a Tokamak, which is basically an axisymmetric torus, whose purpose is to confine a sufficiently hot plasma in order to induce a thermonuclear fusion reaction to generate heat energy. This energy, in turn, is to be used to drive a generator for the production of electric power. These objects are pretty good sized. We saw a picture of one with a man standing up inside it. There were several more pictures including one at General Atomics and one at the Massachusetts Institute of Technology. The constructors of these machines tend to have lots of inspection ports and equipment all over the outside. They have toroidal coils to produce a toroidal field plus central coils to produce a poloidal field. There is a proposal to build one which will stand 30 meters high and cost 6 billion dollars. It is hoped the Japanese will pay for it.

The confinement time τ in a tokamak is given by $\tau \propto a^2/D$, where a is the linear dimension of size, and D is the diffusion constant. The volume over area $V/A \propto a$ scales as the linear size. The stored energy scales like the volume, but the structure to receive the energy is only proportional to the area A . Thus the problems of disruptions become more acute as the size increases. An important parameter with regard to disruptions is $\beta = f/E$, where f is the plasma frequency and E is the magnetic field energy. Not all modes are unstable, and not all unstable modes lead to a disruption, but they can lock onto the walls and cause a disruption.

The transport coefficients can differ by a factor of a million from along the magnetic field lines to across them. This anisotropy leads directly to multiscale phenomena. There is also the alphen time which is of the order of megahertz and the plasma frequency which is of the order of gigahertz, among other important scales. The confinement time is of the order of seconds, so many, many computer time steps are required.

A second problem is the heat load on the diverter plates. (It was explained that the escaping material is swept against the diverter plates.) There is worry about burning out the diverter plates.

The equations governing the behavior inside a tokamak are as follows. First, the fluid

equations are

$$\begin{aligned} \frac{\partial n_j}{\partial t} + \vec{\nabla} \cdot (n_j \vec{v}_j) &= 0, \\ \rho_j \left(\frac{\partial \vec{v}_j}{\partial t} + \vec{v}_j \cdot \vec{\nabla} \vec{v}_j \right) + \vec{\nabla} P_j + \vec{\nabla} \cdot \overset{\leftrightarrow}{\Pi}_j &= n_j q_j \left(\vec{E} + \frac{1}{c} \vec{v}_j \times \vec{B} \right) + R_j, \text{ and} \\ \frac{3}{2} \left(\frac{\partial P_j}{\partial t} + \vec{v}_j \cdot \vec{\nabla} P_j \right) + \frac{5}{2} P_j \vec{\nabla} \cdot \vec{v}_j + \vec{\nabla} \cdot \vec{q}_j + \overset{\leftrightarrow}{\Pi}_j : \vec{\nabla} \vec{v}_j &= Q_j, \end{aligned}$$

where n_j is the particle density for species j , ρ_j is the mass density, P is the scalar part of the pressure, Π is the linear part of the pressure tensor, R_j is the force on species j by the other particles, q_j is the charge, \vec{q}_j is the flux, and Q_j is the heat source term. The speaker remarked that the mean free path along the field is of the order of kilometers, so the fluid equations are not quite valid. The quiet implicit method developed by Barnes is used. Note was also taken that the fluid equations alone don't close. It is assumed that the bulk of the material is Maxwellian plus a Δf for the particles; \vec{q} and $\overset{\leftrightarrow}{\Pi}$ are given by higher moments of the particle distribution.

The Maxwell equations are

$$\begin{aligned} \vec{\nabla} \cdot \vec{B} &= \vec{\nabla} \times \vec{E} + \frac{1}{c} \frac{\partial \vec{B}}{\partial t} = 0, \\ \vec{B} &= \vec{\nabla} \times \vec{A}, \quad \vec{E} = -\vec{\nabla} \phi - \frac{1}{c} \frac{\partial \vec{A}}{\partial t}, \\ \nabla^2 \vec{A} &= -\frac{4\pi}{c} \vec{J}, \text{ and} \\ \vec{\nabla} \cdot \vec{A} &= \vec{\nabla} \cdot \vec{J} = 0. \end{aligned}$$

The constitutive equations are

$$\vec{J} = \sum_j \vec{J}_j = \sum_j n_j q_j \vec{v}_j.$$

An important part, the speaker said, is the numerical grid. First of all, it is to be uniform in the angle θ , the angle in cylindrical coordinates about the axis of symmetry. In an r - Z cross section, the grid is sort of like a (distorted) set of polar coordinates about the core of the confined material, except that a patch of rectangular coordinates is placed in the very center. This is a nonorthogonal coordinate system, although it is a logically rectangular grid. Glasser then remarked that nonlinear instabilities and their time evolution lead to disruptions. He also mentioned finite elements in the flux core and the use of bilinear elements represented by bicubic splines (The product of a cubic spline in each of the two dimensions.) Glasser also spoke of exact conservation laws, finite-element conservation laws, and implicit time steps.

The exact conservation laws are

$$\begin{aligned}\frac{\partial u}{\partial t} + \vec{\nabla} \cdot \vec{F} &= 0, \\ U(\Omega, t) &\equiv \int_{\Omega} u(\vec{x}, t) d\vec{x}, \text{ and} \\ \frac{dU(\Omega, t)}{dt} &= - \int_{\partial\Omega} \vec{F} \cdot \vec{n} d\vec{x}.\end{aligned}$$

The finite-element conservation laws are

$$\begin{aligned}u(x, t) &= u_i(t)\alpha_i(\vec{x}), \quad (f, g) \equiv \int_V f(\vec{x})g(\vec{x}) d\vec{x}, \quad \phi(\Omega, \vec{x}) = \sum_i \alpha_i(\vec{x}), \\ (\alpha_i, \alpha_j) \frac{du_j}{dt} &= -(\alpha_i, \vec{\nabla} \cdot \vec{F}) = \int_V \vec{F} \cdot \vec{\nabla} \alpha_i d\vec{x}, \text{ and} \\ U(\Omega, t) &\equiv \int_{\Omega} u(\vec{x}, t)\phi(\Omega, \vec{x}) d\vec{x}.\end{aligned}$$

For Ω bounded by grid lines and $\phi(\Omega, x) \rightarrow 0$ on the boundary $\partial\Omega$,

$$\frac{dU(\Omega, t)}{dt} = \int_{\partial\Omega} \vec{F} \cdot \vec{\nabla} \phi(\Omega, \vec{x}) d\vec{x}.$$

Presentation by Mark Herant

Title: Supernovae and How They Blow Up

There are two types of supernova and the speaker said that he would confine his remarks to Type II. This type involves the death of a massive star, which has a mass greater than $10M_{\odot}$, *i.e.*, ten solar masses. Supernovae of this type yield the most powerful explosions releasing of the order of 10^{53} ergs of which the order of 10^{51} is in kinetic energy. They eject heavy elements and energize the interstellar matter. They occur at the rate of about one per 30 to 100 years per galaxy. Previously, computer simulations had yielded a black hole instead of an explosion. The famous 1987 supernova, imaginatively named SN1987A, showed evidence of mixing of material from the deeper layers and the surface layers. The problem with previous simulations seems to be that, as they were one-dimensional, the symmetry of this solution did not allow for convective mixing which is necessarily an asymmetrical behavior. We see experimental evidence that this asymmetry occurs in nature because we see high-velocity neutron stars which are believed to be kicked out of an asymmetrical supernova explosion.

We pick up the description of the calculation in the red giant phase. The star is the size of the orbit of Jupiter, but the core is about the size of Earth. One notices that there is a ratio of almost 6 orders of magnitude between the star size and the core size. This

certainly qualifies as a multiscale problem. The core is mainly iron.* When the nuclear production of energy ends, there is no more pressure generated to hold up the star, and the core collapses in about 1 second to a neutron star with a diameter of about 20 km. This leaves the core about 8 orders of magnitude smaller in diameter (or 24 orders of magnitude in volume) than the star, on a times scale, say less than 10^{-14} , of that of the life of the star. The time scale of the nuclear reactions is similarly short compared with the collapse time. As the density goes up, the reaction, $p + e \rightarrow n + \nu + \text{energy}$, takes place. The collapse results in a neutron star which is so dense that it is opaque to neutrinos, and it takes several seconds to bleed this reaction heat and the reaction heat of compression out of the core. The neutron degeneracy provides pressure support at the center, but the original collapse produced an inward-moving shock wave, as the outside doesn't know about this change at the center yet. Near the center, the colder gases fall in and are heated by convection and rise out against the shock. This effect then forces the shock out. One needs at least two dimensions to model this convection process. After the explosion (about 100 seconds), you get instabilities which lead to mixing (on a scale of 10^6 kilometers). The time scale is now about one hour (3,600 seconds), and one sees the characteristic, mushroom-shaped caps.** To do things properly, one really needs to do a three-dimensional calculation, on, as we have seen, a wide range of time (0.1 milliseconds to minutes or hours) and length scales.

Continuation of the Presentation by Mike Warren

Using particle hydrodynamics algorithms to integrate the equations of motion for every particle means that there is a need to find each particle's neighbors which are nearer in distance than say R . Here we range from a very dense region in the center to a very dilute region outside, and the usual neighbor finding schemes are poor for this situation. We use tree data-structures. That is to say, the region is broken into octants, and then each octant is further subdivided. The process is continued until, on average, there is one particle per cell. Obviously, the number of levels of subdivision will be greater in the dense regions than in the dilute regions. On a parallel machine, domain decomposition is used so that the number of particles is roughly equal on each processor. A one-page C-code was flashed up to illustrate the load-balancing procedure with 16 processors. The building of the data structure and the load balancing are very quick, and they are done for each time step. The two-dimensional problems can be run on a large workstation in a day or so. For a three-dimensional problem, much more computational time is required. The programs have been written so that the same code plus a special machine-dependent file run on any message-passing machine.

* The reason that it is iron comes from nuclear physics. Iron has given up the maximum energy per particle so that further nuclear reactions do not yield more energy.

** The calculation is two-dimensional, and the mushroom shape is characteristic in the two-dimensional, version of the famous "bubble problem." The bubble problem is as follows: Consider a motionless sphere of heated gas in an ambient atmosphere of cool gas. Assuming no mixing across the boundary, describe the subsequent motion. The trouble with this problem is that the bottom rises faster than the top, and it may or may not eventually form a torus.

Presentation by Avadh Saxena

Title: Multiscale Issues in Low-Dimensional Electronic and Magnetic Materials

Saxena said that the following aspects of his subject will be of particular importance: (i) Competing interactions (*e.g.*, electron-phonon, e-e, J, *etc.*), (ii) The case of two coupled fields. Here one integrates one of them out, and nonlinearity implies length and/or time scales, (iii) Competition with intrinsic length and times scales (*e.g.*, lattice, external field periodicity), (iv) Pattern evolution, (v) Nonadiabatic effects (*e.g.*, quantum lattice fluctuations), (vi) Multiple length and/or time scales, and (vii) Complexity.

The speaker explained the emergence of multiple scales in the following way. Electronic filling of bands implies incommensurability which in turn implies the “polaron” lattice. There are then the length scales: a , the lattice spacing, ξ , the correlation length, and d , the macroscopic sample size. Also, fine-scale structure (*e.g.*, twinning) couples to the polaron lattice in electronic materials (striped phases in high-temperature superconductors).^{*} In addition, there is competition with internal degrees of freedom (*e.g.*, shape modes). Finally, the speaker pointed to the melting of phases due to (i) quantum fluctuations, (ii) thermal effects, (iii) external field, (iv) discommensurations (or topological defects), and (v) impurities/disorder.

In a further laying out of the general ground, Avadh pointed to the modeling of nanostructures in materials. In this regard, he mentioned MX (metal-halogen) chains, doped polymers, and some coaxial graphitic microtubules which he said are quasi-one-dimensional. There are high- T_c superconductors, other coaxial graphitic microtubules, and some fullerenes which are reported to be quasi-two-dimensional. Other fullerenes and quantum dots were described as quasi-zero-dimensional. In addition, he mentioned self-assembly on surfaces, inorganic-organic stacks, and the self-organization of large Josephson junction arrays. He next described in a qualitative manner his modeling strategy. It is to develop a new synergism of (i) statistical and quantum mechanics, (ii) nonlinear and nonequilibrium techniques, and (iii) pattern recognition and computational strategies. There are important issues at the boundaries between (i) solid state physics and organic chemistry, (ii) physics, organic/macromolecular chemistry and biology, and (iii) condensed matter and materials science. Next, the speaker gave a list of important effects. With regard to the ground states, he mentioned (i) charge density waves, (ii) bond order waves, (iii) spin density waves, (iv) spin-Peierls phases, and (v) long-period “superlattice” phases. With regard to excitation, he listed (i) solitons, (ii) polarons, (iii) bipolarons, (iv) excitons, (v) breathers, and (vi) soliton and (bi)polaron lattices.

Saxena next turned his attention to solitons in degenerate systems such as *trans*-polyacetylene. He showed us pictures of the chemical diagrams. They looked like footprints marching across the screen from left to right. Each footprint was labeled with a C with a line sticking up from a left footprint and down from a right footprint. On the first row (R), the left-right footprints were connected with a single line and the right-left footprints with a double line. In the second row (L), these connecting lines were interchanged. He also showed a plot of the energy per unit length versus the band gap. It had a double

^{*} See also the following presentation by P. Swart.

minimum at $\pm\Delta_0$, where $2\Delta_0$ is the Peierls gap. If doped, the system will create polarons. The Hamiltonian for the Takayam, Lin-Liu, Maki (TLM) continuum model was given as

$$\mathcal{H}_{\text{TLM}} = \frac{1}{2\pi\lambda v_F} \int dx \Delta^2(x) + \sum_s \int dx \psi^\dagger(x) \left\{ -i\hbar v_F \sigma_3 \frac{\partial}{\partial x} + \Delta(x) \sigma_1 \right\} \psi(x),$$

where

$$\psi(x) = \begin{bmatrix} u(x) \\ v(x) \end{bmatrix}$$

is a two-component spinor, and the σ_i are the Pauli matrices. This formula leads to the eigenvalue problem,

$$\begin{aligned} \epsilon_n u_n(x) &= -i\hbar v_F \frac{\partial}{\partial x} u_n(x) + \Delta(x) v_n(x), \text{ and} \\ \epsilon_n v_n(x) &= i\hbar v_F \frac{\partial}{\partial x} v_n(x) + \Delta(x) u_n(x). \end{aligned}$$

There is a self-consistency condition,

$$\Delta(x) = -\lambda\pi v_F \sum'_{n,s} \{u_n^*(x)v_n(x) + v_n^*(x)U_n(x)\},$$

and the total energy is given by

$$E_T = \sum'_{n,s} \epsilon_n + \frac{1}{2\pi\lambda v_F} \int dx \Delta^2(x).$$

These spinor fields can be decoupled by the change of variables

$$f_n^\pm(x) = u_n(x) \pm i v_n(x), \quad \text{as} \quad \epsilon_n f_n^\pm(x) = -i\hbar v_F \frac{\partial}{\partial x} f_n^\mp(x) \pm i\Delta(x) f_n^\mp(x),$$

which by back substitution yields the Schrödinger-like equations,

$$\left\{ \epsilon_n^2 + \hbar^2 v_F^2 \frac{\partial^2}{\partial x^2} - \left(\Delta^2(x) \mp \hbar v_F \frac{\partial}{\partial x} \Delta(x) \right) \right\} f_n^\pm(x) = 0.$$

Next the speaker showed a plot of the order parameter (Peierls distortion, boson field). In the first of these figures, there was a single polaron which looked like an upside-down Gaussian curve. With more doping, a polaron lattice was displayed. It looked like the sum of a whole set of single polarons with their centers regularly spaced with a spacing d .

The speaker next gave us a taste of the connections with a (solvable) field theory, specifically, with the Gross-Neveu (Larkin), coupled, N-flavor, massless Fermion model. Here the Lagrangian is

$$\mathcal{L}(x) = \sum_{\alpha=1}^N \bar{\psi}^{(\alpha)}(x) \left(i\gamma_\mu \frac{\partial}{\partial x_\mu} \right) \psi^{(\alpha)}(x) + \frac{1}{2} g_{GN} \left[\sum_{\alpha=1}^N \bar{\psi}^{(\alpha)}(x) \psi^{(\alpha)}(x) \right]^2,$$

where γ_μ for $\mu = 0, 1$ are the two-dimensional Dirac γ matrices. That is

$$\gamma_0 = \sigma_3, \quad \gamma_1 = i\sigma_1, \quad \psi^{(\alpha)} = \begin{pmatrix} \psi_1^{(\alpha)} \\ \psi_2^{(\alpha)} \end{pmatrix}, \quad \text{and} \quad \bar{\psi} = \psi^\dagger \gamma_0.$$

This model has a number of properties. It has discrete chiral symmetry, $\psi \rightarrow \gamma_0 \gamma_1 \psi$. The index $\alpha = 1, \dots, N$ labels the particle type, and in this regard there is internal $SU(N)$ symmetry. The introduction of an auxiliary meson field $\sigma(x)$ results in a system of non-interacting fermions plus bosons. The model has spontaneous dynamical symmetry breaking which leads to “mass generation.” In the adiabatic static limit, one gets the same fermion and self-consistency equations as for the continuum Peierls systems. The Peierls gap corresponds to the mass in this model.

Avadh followed that with a structural diagram of a halogen-bridged transition metal complex (MX chain) which was a line of bivalent and tetravalent platinum, each surrounded by a ring of four nitrogens and with a chlorine between each on the central line. Between each such ring there are also two ClO_4 structures. The chemical formula is $[\text{Pt}(\text{en})_2][\text{Pt}(\text{en})_2\text{X}_2](\text{ClO}_4)_4$, where X stands for Cl, Br, or I, and en stands for ethylenediamine. Of interest here was how time scales with energy. We then saw a number of plots of computer results. In one plot for a photoexcited hole polaron, starting with an initial polaron we get intragap levels which correspond to a soliton. We also got to see a plot of “breathers,” which in this mode of presentation, look like crinkled wrinkles.

In a final sample of his work, Saxena discussed the role of spin anisotropy. For his model, he took a cylinder covered with classical Heisenberg spins all over. How does spin-anisotropy affect deformation? For the anisotropic part of the Hamiltonian, he uses

$$\mathcal{H}_{\text{anisotropy}} = Jw_0^2 \sin^2 \theta.$$

If there is no spin anisotropy, then a Sine-Gordon equation results for the spin part, and it doesn't affect the deformation, but if there is anisotropy, then it does affect the deformation. The characteristic length of the deformations is ρ_0 , the radius of the cylinder. In the simple cases, there appears a periodic slight squashing of the cylinder as the deformation. If the winding number is greater than zero, then much more contorted-looking shapes were obtained.

Presentation by Pieter Swart

Title: Martensitic Mesostructure

Martensitic phase transitions are displacive, first-order, solid-solid, diffusionless, and reversible. An example would be the following: a system is in a high-temperature, high-symmetry phase like a face-centered-cubic structure for temperatures above the transition temperature, and the system goes into a low-temperature, low-symmetry phase for lower temperatures, such as a face-centered-orthorhombic phase of which there are three variants. Classic examples of martensitic transitions occur in Steel, NiTi (Nitinol), and LiNiO_3 (lithium niobate). There can be recoverable local strains as large as 10%. Large crystals

(bigger than a cubic micron) form characteristic and hierarchical mesostructures for temperatures below the transition temperatures. The crystal, when cooling down, forms its own composite. Refinement is driven by incompatibility, *e.g.*, austenite-martensite interfaces. Surprisingly enough, the resulting geometries can be extremely well predicted by continuum-based theories.* We saw a number of pictures illustrating the interesting things that can happen. Sometimes temperature changes the length scale. We saw needle domains and microstructure within microstructure. We saw pictures of a material built out of blocks of material which had its own distinct microstructure. It was pointed out that the interfaces are typically sharp and coherent (not grain boundaries). There are severe constraints on (i) which variant can join with which (rotated) variant, (ii) orientation, (iii) Y junction geometry, *etc.* Junctions can occur between (mirror-image) twins. The boundaries between twins can be highly mobile (although they need not be, as, for example, in steel). This feature, plus the huge strains involved, implies the possibility of effective actuators, sensors, and many other unique applications.

Example Sensor and Actuator Materials

Class	Property	Material	Switching Field
Ferroelectric	Piezoelectric	Pb(Zr, Ti)O ₃	E
	Electrostrictive	Pb(Mg ₁₃ Nb _{2/3} O ₃	E
Ferromagnetic	Magnetostrictive	Terfenol	H
Ferroelastic	Shape Memory	Nitinol, NiAl	Stress, Strain

There are a number of applications for this type of physics. Under the heading of *Shape Memory Alloys* (CuZn, CuZnAl, AuCd, NiTi, NiAl, FePd, ...) there are the following: hydraulic couplings and fasteners, guidewires for medical applications, orthodontic braces, temperature regulators, thermally/current driven actuators, and dampers. Under the heading of *Ferro & Piezoelectrics* (BaTiO₃, PZT, PLZT, ...) there are the following: sensors & actuators (medical, sonar, ...), surface acoustic wave devices (surfing, analog filters), damping patches, micromechanical devices (MEMS), and real-time optical control (deformable telescope mirrors). The speaker projects a \$10 billion market here by 1998. Under the heading of *Magnetostrictive Devices* (Terfenol, FeTbDy) there are the following: high-power actuators, vibration isolators, induction and stepping motors, high-power sonar, and maybe even memory storage devices. The speaker said that Terfenol is under-exploited. We saw a picture of a sonar dome on a navy ship. This was claimed to be the largest application, at least in terms of physical size. Finally, under the heading of *Composites* there are "smart materials."

The major problems in this area were reported to be the following: (i) These materials exhibit aging, albeit slowly. (ii) The materials have a limited temperature range. (iii) They are difficult to machine. (iv) They are expensive. And (v) they are poorly understood because of a lack of experimental evidence at the mesoscopic and microscopic levels. Martensitic microstructures are a result of dynamics acting on a complicated energy surface. Swart

* See the presentation by David Kinderlehrer in Section 7 for related material.

says the total, “stored-elastic” energy can be expressed as $E = \int \phi(\overleftarrow{\nabla} \vec{u}, \dots) dx$ for some ϕ , *nonconvex* in $\overleftarrow{\nabla} \vec{u}$, so that, using this continuum picture, the martensitic mesostructure should be just the solution to $\min \int \phi(\overleftarrow{\nabla} \vec{u}, \dots) dx + \text{constraints}$. It is important to pay attention to the following issues: (i) When does one expect many ground states with fine structure? (ii) What is the homogenized energy of such ground states, *i.e.*, energy minimizers? (iii) What is the role of dynamics in selecting the observed mesostructures? And (iv) what is the role of thermodynamics and noise?

The nature of the energy landscape was next discussed briefly under the assumption of constant temperature, sharp interfaces, and statics. Let $\overleftrightarrow{F} = \overleftarrow{\nabla} \vec{u}$, a 3×3 matrix. It should have the properties of (1) frame invariance, *i.e.*,

$$\phi(\overleftrightarrow{F}) = \phi(\mathcal{R} \overleftrightarrow{F}), \quad \forall \mathcal{R} \in \mathbf{SO}_3,$$

of (2) material symmetry, which implies that

$$\phi(\overleftrightarrow{F}) = \phi(\overleftrightarrow{F} \mathcal{G}), \quad \forall \mathcal{G} \in \mathbf{P},$$

where \mathbf{P} is the point symmetry group, and for coherent interfaces

$$\overleftarrow{\nabla} \vec{u} = \overleftrightarrow{F}_1 \quad \Big| \quad \overleftarrow{\nabla} \vec{u} = \overleftrightarrow{F}_2, \quad \text{with} \quad \overleftrightarrow{F}_1 - \overleftrightarrow{F}_2 = a \otimes n = \text{rank } 1.$$

Hence Swart concludes that in 9-dimensional matrix space there exist several isolated energy wells.

In conclusion, the speaker propounded questions which have been a recurrent theme in this initiative: What is the macroscopic (or homogenized) nature of fine mesostructures and how do solutions to nonlinear partial differential equations arising from the variational settings blow up because of the highly oscillatory (or singular) behavior? He further said that this area represents a renaissance in the dusty topic of the variational calculus. Interfacial physics is needed to understand going from the mesoscopic level to the microscopic level, and we must be very careful here. Lastly he addressed the question, “Why is this class of problems a suitable candidate for the combined micro+meso+macro (3M) attack?” In answer, he listed a number of the reasons which have been advanced to establish this initiative: (i) There is important physics and a large and growing number of applications. (ii) All the levels are important, with strong interactions. (iii) The experimental roadblocks are serious barriers to progress. (iv) Even the engineering community concedes that a detailed understanding of mesodynamics is the key to success (translation, they have worked hard and failed without it.) As a last example, he cited the problem of what happens in tip propagation when it meets a different phase or microstructure of the material.

Presentation by Salman Habib

Title: Nonequilibrium Phases and Transitions

This talk gives an added perspective* on a Laboratory Directed Research and Development-funded project to explore future possibilities. The participants in this group are E. Mottola (principal investigator), A. Bishop, F. Cooper and the speaker. The idea is to get a focused program.

Some of the topics of interest were listed as: nonequilibrium phases such as metastable phases and stable nonequilibrium states; nonequilibrium transitions such as quenches, spinodal decomposition, transitions in driven systems, defect formation, and heavy ion collisions; and related topics such as the statistical mechanics of nonlinear coherent structures, low-temperature transport and mesoscopic quantum tunneling. Habib said that the participants were interested in how microscopic physics implies relevant phenomenology and in the analytic and computational techniques applicable to both.

Next the speaker cited the $O(3)$ nonlinear σ -model as an example. First however, he introduced a quantum mechanical toy model, the pendulum. It is defined by a potential $V(\theta) = \omega^2(1 - \cos \theta)$. There is a static, unstable solution to this equation with energy $E_{\text{sph}} = 2\omega^2$. It was explained that the “sphaleron” rides over the top of the potential, while the “instantons” and “periodic instantons” tunnel through the potential barriers between the potential minima. The tunneling factors for instantons was reported to be $\Gamma_{\text{tunnel}} \sim \exp(-2S_0) = \exp[-2(16\omega)]$, where 16ω is the instanton action, and the thermal “tunneling” factor was reported to be $\Gamma_{\text{thermal}} \sim \exp(-2\omega^2/kT)$. A figure was shown of the behavior in the (S/ω) - $(\beta\omega)$ plane. In the plane, the sphaleron solutions form a straight line through the origin with a positive slope. For $\beta\omega$ less than some critical value, there is classical hopping and when it is greater there is quantum tunneling. There is a line, roughly parabolic opening to the right for the instanton solutions. It was shown as tangent to the sphaleron at the critical value of $\beta\omega$. The portion of this curve for $\beta\omega$ less than about 1.5 times the critical value was marked “periodic instanton,” and the rest “instanton.”

The nonlinear σ -model is defined by the equation,

$$S = \frac{1}{2g^2} \int dx d\tau (\partial_\mu n^a)^2 + \frac{m^2}{g^2} \int dx d\tau (1 + n_3),$$

where the Einstein summation convention is used and the range of a is 1 to 3. The normalization $n^a n^a = 1$ is imposed, and the second term (mass or magnetic field term) breaks the conformal symmetry. Salman next explained that there are “winding number” transitions in the $O(3)$. The point seems to be that, in the σ -model, the spins live on a sphere, $\therefore \vec{n} \cdot \vec{n} = 1$. If one picks the boundary conditions that the n^a tend to constants as $(x, t) \rightarrow (\infty, \infty)$, then it follows that $\mathbf{R}^2 \mapsto \mathbf{S}^2$, and so we have a mapping from $\mathbf{S}^2 \mapsto \mathbf{S}^2$ which is characterized by the winding number. A similar plot to that for the pendulum problem was then displayed. It showed the $g^2 S$ - $m\beta$ plane. Here again, for a critical value of $m\beta$, there is a sharp dividing line between the classical (left-side) and the quantum (right-side) portions. Again there is a diagonal line whose value at the critical value of

* See also the presentation by Alan Bishop in Section 8.

$m\beta$ gives a critical value of $g^2 S$ which divides the quarter plane into upper and lower parts. Presumably, this diagonal line again corresponds to the sphaleron. Here as in the pendulum case, the calculations can be done, but they are much harder, and the behavior is very different. Next we were treated to a graph of ΔW versus time. Here the value of ΔW oscillated with small amplitude about various integer values and then made a relatively big jump (up or down) to the next integer value where it remained for a fair period of time, until it made its next jump.

Habib next turned his attention to “kinks” in the $\lambda : \phi^4$: statistical mechanics.* (The $:\phi^4$: notation means a normal ordered product.) This work was reported to be with F. J. Alexander and A. Kovner, and also with A. Saxena on the $\lambda : \phi^6$: case. The model being considered is in one-space and one-time dimension. The Lagrangian is

$$\mathcal{L} = \frac{1}{2}\dot{\phi}^2 - \frac{1}{2}(\partial_x \phi)^2 + \frac{1}{2}m^2\phi^2 - \frac{1}{4}\Lambda\phi^4,$$

which leads to the equation of motion,

$$\ddot{\phi} = \partial_x^2 \phi + m^2\phi - \Lambda\phi^3.$$

This equation has the “kink” solution,

$$\phi_k = \frac{m}{\sqrt{\Lambda}} \tanh \left[\frac{m}{\sqrt{2}}(x - x_0) \right], \quad \text{with the energy } E_k = \sqrt{\frac{8}{9}} \frac{m^3}{\Lambda}.$$

There are nonequilibrium aspects to this problem. The standard (naive) approach is, if $n_k(t)$ denotes the density of kinks at a time t , then the autocorrelation function, $\langle n_k(t)n_k(t + \tau) \rangle - \langle n_k(t) \rangle \langle n_k(t + \tau) \rangle$ is expected to decay like an exponential $e^{-t/\tau}$ in “computer time,” t , with τ the kink lifetime. In fact, Habib has found that it decays like the sum of two exponentials! He said that they are the result of two distinct processes going on in the system. If one plots the kink locations as a function of time, Salman was led to the concept of “geminate” and “nongeminate” recombination of kinks. The geminate type corresponds to closed loops in this sort of picture and the nongeminate type does not. The effects of the geminate recombination is dominant in the early stages and leads to the more rapidly decaying exponential. The nongeminate processes lead to the more slowly decaying term and are dominant at longer times. These latter terms were described as diffusive effects. Thus with multiple time scales present, it was the speaker’s view that no simple analysis is possible. He then discussed the effect of the type of noise present, for example, multiplicative or additive noise. He presented results on the nucleation problem [here $n(t = 0) = 0$], which demonstrated that the equilibrium value of $n(t)$ depends on the noise type, being greater for nonlinear than for linear noise type.

He concluded that the strong dependence on noise type implies that the *whole* theory of kink nucleation and dynamics may have to be rethought and that more numerical data are needed. He said that he felt that the equilibrium statistical mechanics of kinks is now

* See also the first presentation by Habib in this section.

well understood, but the nonequilibrium behavior is still far from being understood. He plans to undertake heroic calculations in the future and to work on an analytic theory for the nucleation problem, perhaps an inhomogeneous mean-field type of theory.

Presentation by Fred Cooper

Title: Is Chaos a Limiting Factor in Numerically Simulating Time-Dependent Quantum Mechanical Systems and Time Evolution in Quantum Field Theory Using Dirac's Time-Dependent Variational Method?

Subtitle: (Semi) Quantum Chaos and Variational Methods

Cooper said that the work he is reporting was done in collaboration with Salman Habib, Rob Ryne, and John Dawson. By way of introduction, he said that the long time average is not sensitive to the distributional behavior of the expectation values. He will approximate a quantum mechanical problem in a very reasonable way. It will turn out, however, that the approximation will be sensitive to the initial conditions. The Lipanoff time scale gives an estimate of how long you can believe the approximation. One can do the quantum mechanical problem on the computer for comparison with the approximation, but the field theory problem is too hard to do this way. The problem considered will be a purely Hamiltonian system and thus not dissipative.

For the action,

$$S = \int_{t_1}^{t_2} dt \langle \Psi | \left(i \frac{\partial}{\partial t} - H \right) | \Psi \rangle / \langle \Psi | \Psi \rangle,$$

Dirac's action principle ($\delta S = 0$, $\delta |\Psi(t_1)\rangle$, $\delta |\Psi(t_2)\rangle$) leads to the time-dependent Schrödinger equation,

$$\left(i \frac{\partial}{\partial t} - H \right) | \Psi \rangle = 0.$$

If we minimize the action within a restricted variational basis, then

$$\Psi \mapsto \Psi_v(y_i(t)), \quad \text{and} \quad \int dx \Psi_v^* \Psi_v = 1$$

leads to an effective action functional defined on the variational parameters, $y_i(t)$, as

$$\Gamma[y_i(t)] = \int dt \langle \Psi_v | \left(i \frac{\partial}{\partial t} - H \right) | \Psi_v \rangle.$$

Lagrange's equations for the variational parameters follow from $\delta \Gamma[y_i] = 0$. We now have a variational wave function which is dependent on just a few parameters.

The structure of the action leads to symplectic Hamiltonian dynamics.* The Dirac form of the actions with the above described variational ansatz leads to

$$\Gamma[\vec{y}] = \int dt \int_{-\infty}^{+\infty} dx \Psi(x, \vec{y}) \left\{ i \frac{\partial}{\partial t} - H \right\} \Psi(x, \vec{y}(t)) = \int dt L(\vec{y}, \dot{\vec{y}}),$$

* For a discussion of symplectic methods, see Section 7. It was pointed out there that, for symplectic Hamiltonian dynamics, the Jacobian of the transformation of phase space in Liouville's theorem is just unity. Put otherwise, symplectic Hamiltonian dynamics means

where H is chosen to be

$$H = -\frac{1}{2} \frac{d^2}{dx^2} + V(x).$$

It follows directly from the above structure of the equations that

$$L(\vec{y}, \dot{\vec{y}}) = \sum_{i=1}^N \pi_i(\vec{y}) \dot{y}_i - h(\vec{y})$$

is the most general form allowed. The quantities in this form are

$$\pi_i(\vec{y}) = \frac{i}{2} \int_{-\infty}^{+\infty} \left\{ \Psi^*(x, \vec{y}) \frac{\partial}{\partial y_i} \Psi(x, \vec{y}) - \Psi(x, \vec{y}) \frac{\partial}{\partial y_i} \Psi^*(x, \vec{y}) \right\},$$

and

$$h(\vec{y}) = \int_{-\infty}^{+\infty} dx \Psi^*(x, \vec{y}) H \Psi(x, \vec{y}).$$

If we now minimize the action, $\Gamma[\vec{y}]$ given above, we get Lagrange's equations,

$$\frac{d}{dt} \frac{\partial L}{\partial \dot{y}_i} - \frac{\partial L}{\partial y_i} = 0, \quad \text{for } i = 1, \dots, N.$$

For the general form of L for our case given above, the equations of motion are derived from

$$\sum_{j=1}^N M_{ij}(\vec{y}) \dot{y}_j = \frac{\partial h(\vec{y})}{\partial y_i},$$

where $M_{ij}(\vec{y})$ is given by

$$M_{ij}(\vec{y}) = \frac{\partial \pi_i}{\partial y_j} - \frac{\partial \pi_j}{\partial y_i} = -M_{ji}(\vec{y}),$$

which is immediately seen to be an antisymmetric matrix. Now if the inverse of M_{ij} exists, the equations of motion can be put into a symplectic form:

$$\dot{y}_i = \sum_{j=1}^N M_{ij}^{-1}(\vec{y}) \frac{\partial h(\vec{y})}{\partial y_j}.$$

that the system possesses the Poisson bracket structure of classical dynamics. The notion of symplectic refers to the symplectic group. The orthogonal group in n dimensions $O(n)$ is the group of linear transformations $A_{i,j}$ which leave the scalar product $\vec{x} \cdot \vec{y} \equiv \sum_{i=1}^n x_i y_i$ invariant. More generally, we could have chosen $\vec{x} \star \vec{y} \equiv \sum_{i,j=1}^n x_i S_{i,j} y_j$, where $S_{i,j}$ is any positive definite quadratic form. The symplectic group in n dimensions $Sp(n)$ is the set of all linear transformations $A_{i,j}$ which leave invariant a nondegenerate bilinear form $\{\vec{x}, \vec{y}\} = \sum_{i,j=1}^n x_i M_{i,j} y_j$, where $M_{i,j} = -M_{j,i}$ is antisymmetric. It follows directly that $\det M = (-1)^n \det M$ so that if n is odd, then $\det M = 0$, and so the bilinear form is degenerate. Thus the symplectic group can only be defined in even dimensions.

Since M_{ij}^{-1} is necessarily also antisymmetric, $h(y)$ is a conserved quantity because

$$\frac{dh(y)}{dt} = \sum_i \frac{\partial h}{\partial y_i} \dot{y}_i = \sum_{i,j} \frac{\partial h}{\partial y_i} M_{ij}^{-1} \frac{\partial H}{\partial y_j} = 0.$$

It is convenient at this point, the speaker said, to introduce Poisson brackets for our system using the definition

$$\{A, B\} \equiv \sum_{i,j} \frac{\partial A(\vec{y})}{\partial y_i} M_{ij}^{-1} \frac{\partial B(\vec{y})}{\partial y_j}.$$

This definition satisfies Jacobi's identity.* In terms of this notation, the equations of motions can be rewritten as,

$$\dot{y}_i = \{y_i, h(y)\} = \sum_j M_{ij}^{-1} \frac{\partial h}{\partial y_j} = \sum_j \{y_i, y_j\} \frac{\partial h}{\partial y_j},$$

and so these equations of motion are symplectic in structure. The point of all this formal work is to show that the approximation of the original quantum mechanical problem by wave functions which depend on a few parameters can be cast in the form of a Hamiltonian system with symplectic dynamics, which in its turn is suitable for finite-difference approximation.

Cooper next described an example. It is the case of the $N + 1$ oscillator problem (scalar electrodynamics). The Hamiltonian for the $N + 1$ oscillator system is

$$H = \frac{1}{2} \left[p_A^2 + \sum_{i=1}^N p_i^2 + (m^2 + e^2 A^2) \sum_{i=1}^N x_i^2 \right],$$

where m is the mass and e is the electron charge. We have introduced an $N + 1$ component oscillator x_μ , $\mu = 0, 1, \dots, N$ with $x_0 = A$ and the other N oscillators labeled by the Roman indices, $i = 1, \dots, N$.

In this example, the operator equations of motion are

$$\ddot{x}_i + (m^2 + e^2 A^2)x_i = 0, \quad \text{and} \quad \ddot{A} + \left(e^2 \sum_i x_i^2 \right) A = 0.$$

Taking the expectation values, we get

$$\langle \ddot{x}_i \rangle + m^2 \langle x_i \rangle + e^2 \langle A^2 x_i \rangle = 0, \quad \text{and} \quad \langle \ddot{A} \rangle + e^2 \sum_i \langle x_i^2 A \rangle = 0.$$

* $\{u, \{v, w\}\} + \{v, \{w, u\}\} + \{w, \{u, v\}\} = 0$

The choice made by the speaker for a trial wave function is

$$\Psi_v(x_\mu) = \mathcal{N} \exp \left[-\frac{1}{\hbar} (x - q(t))_\mu (x - q(t))_\nu \left(\frac{1}{4} G^{-1} - i\Pi \right)_{\mu\nu} + \frac{i}{\hbar} p_\mu(t) (x - q(t))_\mu \right],$$

where repeated subscripts are to be summed over, and the normalization constant is given by*

$$\mathcal{N} = \exp \left[-\frac{1}{4} \text{Tr} \{ \ln(2\pi\hbar G_{\mu\nu}) \} \right].$$

The variational parameters in this trial wave function are

$$\begin{aligned} q_\mu(t) &= \langle \Psi_v | x_\mu | \Psi_v \rangle, \\ p_\mu(t) &= -\langle \Psi_v | i\hbar \frac{\partial}{\partial x_\mu} | \Psi_v \rangle, \\ G_{\mu\nu}(t) + q_\mu(t)q_\nu(t) &= \langle \Psi_v | x_\mu x_\nu | \Psi_v \rangle, \text{ and} \\ 2q_\mu(t)p_\nu(t) + 4 \sum_\lambda \Pi_{\mu\lambda} G_{\lambda\nu} &= \langle \Psi_v | (x_\mu p_\nu + p_\nu x_\mu) | \Psi_v \rangle. \end{aligned}$$

Note is taken that the number of parameters is always even. The effective action is given by

$$\Gamma = \int dt \left\{ \sum_{i=1}^N p_i \dot{q}_i + p_A \dot{A} - \hbar \text{Tr} \left[\dot{\Pi}_{\mu,\lambda} G_{\lambda,\nu} \right] - H_{\text{eff}} \right\},$$

where the effective Hamiltonian is

$$\begin{aligned} H_{\text{eff}} &= \langle \Psi_v | H | \Psi_v \rangle \\ &= \sum_{i=1}^N \frac{p_i^2}{2} + \frac{p_A^2}{2} + \frac{\hbar}{8} \text{Tr}[G^{-1}] + 2\hbar \text{Tr}[\Pi G \Pi] + \frac{1}{2} [m^2 + e^2(A^2 + G_{0,0})] \sum_{i=1}^N (q_i^2 + G_{ii}). \end{aligned}$$

Next, Cooper specialized these general equations to the case $q(t) = p(t) = 0$ and remarked that, in this case, both G and Π are diagonal. Making the further specialization to $N = 1$, he denotes $G_{1,1} = G(t)$ and $G_{0,0} = D(t)$. In Hartree approximation, the effective Hamiltonian becomes

$$H_{\text{H}}^{(0)} = \frac{1}{2} p_A^2 + 2\hbar (\Pi_G^2 G + \Pi_D^2 D) + \frac{\hbar}{8} \left(\frac{1}{G} + \frac{1}{D} \right) + \frac{\hbar}{2} [m^2 + e^2(A^2 + \hbar D)] G.$$

In addition, the speaker described the other special case where $N \rightarrow \infty$. Here we define the average effective Hamiltonian as

$$\begin{aligned} \tilde{H}_{\text{eff}}^{(0)} &= \lim_{N \rightarrow \infty} H_{\text{eff}}^{(0)} / N \\ &= \frac{1}{2} p_A^2 + 2\hbar \Pi_G^2 G + \frac{\hbar}{8G} + \frac{\hbar}{2} (m^2 + e^2 A^2) G. \end{aligned}$$

* See also the presentation by Emil Mottola starting on page 38.

In the Hartree approximation, Hamilton's equations for the expectation values are

$$\begin{aligned} \dot{A} &= p_A, & \dot{p}_A &= -e^2 \hbar A G, & \dot{G} &= 4\hbar \Pi_G G, & \dot{D} &= 4\hbar \Pi_D D, \\ \dot{\Pi}_G &= \frac{\hbar}{8G^2} - 2\hbar \Pi_G^2 - \frac{m^2}{2} - \frac{1}{2} e^2 \hbar (A^2 + \hbar D), & \text{and} & & \dot{\Pi}_D &= \frac{\hbar}{8D^2} - 2\hbar \Pi_D^2 - \frac{1}{2} e^2 \hbar^2 G. \end{aligned}$$

To the leading order in large N , $D = 0$, and there is no equation for Π_D .

Next Fred showed us some of the numerical results in graphical form. First, there was a Poincaré recurrence map in the $\langle xp + px \rangle$ $\langle x^2 \rangle$ plane. It looked like a smiley conehead. Next, we had a plot of A versus t . All the curves start out at about +4 with a small negative slope and then move sharply downward. At a little past unit time, the exact curve parted company with the other two curves. The curve labeled $1/N$ reversed slope at about time 4 and parted company with the curve labeled H which reversed slope at around 5. Subsequently, the curves continued to oscillate and bore little resemblance to each other. This feature was explained as being due to the sensitivity of the approximations to the initial conditions, a feature not shared by the exact solution. A plot of the Lipanoff exponent at large times shows that for the $1/N$ curve to be about 0.7, while that for the H curve was about 0.5. Then we saw a couple of graphs that demonstrated that the frequency distribution as a function of x or A , while quite Gaussian in shape initially, is definitely non-Gaussian for later times. This shape error represents a significant difference from the assumed shape of the trial wave functions being used.

At this point in the presentation, the speaker switched from dynamics to statics. The connection with the above work is to explore methods to treat non-Gaussian wave functions. In this regard, he considered the anharmonic oscillator, for which the Hamiltonian is

$$H = -\frac{d^2}{dx^2} + \frac{1}{4}(x^2 + \epsilon x^4), \quad \text{and} \quad (H - E)\psi(x) = 0.$$

Using conventional Rayleigh-Schrödinger perturbation theory, one can deduce that

$$\psi(x, \epsilon) \asymp \exp(-x^2/4) \sum_{n=0}^{\infty} \epsilon^n P_n(x) \quad \text{and} \quad E(\epsilon) \asymp \sum_{n=0}^{\infty} \epsilon^n E_n,$$

where the P_n are polynomials of degree $2n$ in x^2 , and $P_0 = 1$. For all $n > 0$, $P_n(0) = 0$. Using these results, the speaker proposed for the more general case than the anharmonic oscillator a wave function of the same structure, but with the coefficients now being adjustable parameters. He found that if we compute the cumulants (also called connected parts), $W[2n]$, and demand, as was the case for the anharmonic oscillator, that $W[2n] = O(\epsilon^{\frac{1}{2}n-1})$, then through N th order in ϵ , there are $N + 1$ free parameters. Note was taken that to get a scattering correction, a quartic polynomial is required. Fred then said that what he proposed to do in the dynamic case was to treat the free parameters as variational parameters. He concluded by saying that chaos provides an upper bound on the validity of the variational computation.

5. No Fixed Scale

Presentation by Rajan Gupta

The work reported here is joint work with Pablo Tamayo. Three topics were mentioned: (1) QCD, (2) the statistical mechanics of spin models at and near the critical point, and (3) nonequilibrium statistical mechanics in the critical region. The first topic was not discussed.

Concerning topic two, the XY -model has been studied in two dimensions. It has a Kosterlitz-Thouless transition at temperature T_c . Here the spin-spin correlation length behaves as

$$\xi \propto \exp\left(-\frac{b}{(T - T_c)^{\frac{1}{2}}}\right).$$

In addition, the $O(3)$, nonlinear σ -model was studied. This model is asymptotically free. Here the critical temperature is $T_c = 0$, and the spin-spin correlation length behaves as

$$\xi \propto \exp\left(\frac{2\pi}{T}\right).$$

In three dimensions, the spin- $\frac{1}{2}$ Ising model was studied. Here the spin-spin correlation length behaves as

$$\xi \propto \left(\frac{T}{T_c} - 1\right)^{-\nu}.$$

Thus, in these three cases we get a considerable spectrum of behaviors. What these problems share is that *all length scales contribute to the problem* and, according to renormalization group theory, in an asymptotically self-similar manner. The contribution by all scales is the major obstacle to the solution of the problem. The approach used here is that of Monte Carlo techniques. The effects of the contribution by all scales is made manifest by what is called “critical slowing down.” That is to say, that larger and larger structures are generated as one approaches the critical point, and it takes progressively longer times for them to relax to an equilibrium distribution. Modern Monte Carlo algorithms adapted to respond to this problem have very greatly ameliorated this problem. The answers sought here are the behavior of the various thermodynamic functions and critical exponents.

Under the third topic, a two-temperature Ising model was studied using the Metropolis Monte-Carlo algorithm. Here the Hamiltonian is

$$\beta\mathcal{H} = \frac{J}{kT} \sum_{\text{bonds}} S_i S_j, \quad \text{and} \quad T = T_1 \text{ or } T_2$$

randomly at each time step with probabilities p and $1 - p$, respectively.

Presentation by Mike Warren

This presentation concerns the N -body problem and reports joint work with Wojciech Zurek. It concerns the dynamical motion of large numbers of particles interacting via long-range forces, *e.g.*, gravity. A problem of astrophysical interest might be one with a system

size of 100 megaparsecs (5.82×10^{34} Bohr). On this scale, a galaxy would be the size of a computer screen pixel. A problem of interest here would be structure formation on a cosmological scale. Other problems of interest in this project are collisions between stars, merger of galaxies, accretion of black holes, *etc.* These problems involve enormous density contrasts, and very irregular time-dependent structures. The approach used builds on the result proved by Newton (*Principia*) for the $1/r^2$ gravitational force that for a spherical distribution of mass, the force on a test particle is the same as if all the mass inside a sphere passing through the test particle were concentrated at the center point of the sphere and all the mass outside of that sphere were not there. On this basis, the multipole expansion is started and is useful for more complicated forces than $1/r^2$. In this project, the problem space is decomposed into boxes, and for each box, the potential can be expanded as

$$\sum_j \frac{Gm_j m}{|\vec{r} - \vec{r}_j|} \approx \frac{GMm}{|\vec{r} - \vec{r}_{\text{cm}}|} + K(\theta, \phi) \frac{GMm}{|\vec{r} - \vec{r}_{\text{cm}}|^2} + \dots,$$

where \vec{r} is outside the smallest circumscribed sphere about \vec{r}_{cm} containing all the \vec{r}_j , $M = \sum_j m_j$, \vec{r}_{cm} is the center of mass, and $K(\theta, \phi)$ depends only on the first order spherical harmonics. The scheme employed decomposes the problem space into boxes of variable size. It is called the *oct-tree* method, as the whole space is first divided into octants, which are then refined by further such divisions, stopping when only one particle remains in a given box. For each box, a truncated multipole expansion is computed. The scheme has a tree structure in the sense that if box *A* is divided, the information for box *A* is also retained. In this way, the interaction for a distant particle is computed from the largest reasonable box, and thus achieves a considerable saving in computational time.

This method has also been used to do vortex particle motion, a bubble hit by a shock wave, two stars (or bucky balls) colliding, and the flow on the surface of a sphere (by the panel method). Note is made that there must always be a fixed point in the last problem since inversion through the origin is not possible for flow.

Presentation by Mike Warren

The subject of this discussion was the dynamical motion of an *N*-body problem, interacting, for example, under the force of gravity.* One of the key aspects in doing computations on this problem is the data structure. The panelist reported that he first divided the model space into octants, and then each octant into smaller octants in a hierarchical manner. This process of refinement stops when the number of particles in each box becomes small enough. The interaction of a small box with the rest of the system is then represented by a multipole expansion of the interaction potential. (This type of hierarchical method can also be applied to computer-monitor pixels for image compression problems. If we have a large high-definition picture which we wish to shrink, we can divide the original into boxes corresponding to the final pixels and use a majority rule or whatever to assign a value to the pixel in the new image.) In this hierarchical method it is important to characterize the errors and to develop criteria necessary to derive the least set of boxes

* See also the first presentation by Mike Warren in this section.

to give that error or less. Each decimal place costs a factor of two or three in time. For an accuracy of about one part in one thousand, there is a crossover for a system of about 10,000 particles between the box method and doing each particle individually.

It is very difficult to break this problem down in a suitable manner for a parallel machine. This panelist has used successfully a one-dimensional list.* It is based on classical studies of space-filling curves. Two were mentioned, the Morton order and the Peano-Hilbert space-filling curve. The Morton order was used and there is a simple algorithm to produce it. One takes the x, y, z coordinates of a particle and interleaves the bits $1, b_1^x, b_1^y, b_1^z, b_2^x, b_2^y, b_2^z, b_3^x, \dots$ to form a number associated with each particle and then rank orders these numbers. The initial 1 bit was described as a “stack-holder” bit. The list is then chopped into a number of sections equal to the number of processors employed. There are some big spatial jumps between neighboring members of this list, but they occur with low enough frequency so that it was reported not to be a serious problem.** It was not reported how often the particles were reassigned to processors during the course of a calculation. Most of these calculations were done on a paragon computer. This method is called a spatial oct-tree method. It has applications to, for example, galactic clusters, star collisions, mock-redshifts, and comet impacts.

Presentation by Rajan Gupta

The subject of this discussion was QCD. There are at first sight at least 4 mesoscopic scales. They correspond to the b, c, s and l quarks and are 5–10 GeV, 2–4 GeV., 1–2 GeV, and 0.1–1.5 GeV, respectively. So this problem might appear to belong in the multiple-mesoscopic scale panel.† However, consider, for example, π and ρ interactions. These are mediated by gluons, and integrals of the form

$$\int \frac{dp}{p}$$

occur. It is these loop integrals which introduce an infinite number of scales. It was noted that every decade makes the same contribution to such an integral. The perturbative content of this theory is just taken over a range from an infrared cutoff given by $\alpha(p) \sim 1/\ln(p/\Lambda)$ to an ultraviolet cutoff above which (for large p) the content is computed by nonperturbative methods. Therefore, we can sum up this part of the contributions from perturbation theory. The *modus operandi* is to use the perturbation theory for scales in the low energy range 0–5 GeV and a nonperturbative lattice treatment for scales above this range (shorter spatial range). One of the major questions which arises is, “Is there a self-consistent way of matching these two parts?” There are a couple of ways, but there are errors in both. Work on an appropriate formalism to do this matching is in progress.††

* See also an alternate procedure given in the presentation of M. Sahota in Section 2.

** We do know that neither 2- nor 3-space can be well ordered, and this problem may be a reflection of that theorem.

† See Section 4.

†† One member of the audience suggested the use of a two-point Padé approximant in the interpolation region.

Presentation by George A. Baker, Jr.

In order to introduce another type of infinitely-many-mesoscopic-scale problem, the panelist described briefly the Ising model. In this model there is a space lattice of spins which point either up or down. These spins have a spin-spin interaction $J s_{\vec{r}} s_{\vec{r}+\vec{e}}$, where \vec{e} is a fundamental, nearest-neighbor lattice vector. If the two interacting spins are parallel, the interaction is J , and if they are antiparallel, $-J$. Note that any such configuration of spins can be decomposed into clusters of parallel spins with boundaries across which the spins are antiparallel. The distribution of cluster sizes sets the scale or scales of this type of problem. If $J > 0$ there is a tendency for the spins to align, which is in competition with the tendency toward random orientation caused by the temperature. The statistical mechanics of this model are controlled by the partition function,

$$Z = \sum_{s_{\vec{r}}=\pm 1} e^{-E/kT},$$

where k is Boltzmann's constant, E is the total energy which is the sum over all the bonds of the system of the bond energies given above, and T is the absolute temperature. There are many quantities of physical interest. The panelist chose to discuss just one, the two-spin correlation function,

$$\langle s_{\vec{0}} s_{\vec{r}} \rangle \propto \xi^{0.5(3-d)+\eta} \frac{e^{-r/\xi}}{r^{0.5(d-1)}}$$

in the limit as $r \rightarrow \infty$. This is a version of the Ornstein-Zernike form. Here, ξ is the correlation length, d is the spatial dimension, and η is a critical exponent characterizing the spin-spin correlation function at the critical temperature. For temperatures different from the critical temperature, $\xi < \infty$, and it sets the scale. The critical (or Curie) temperature is the lowest temperature at which there is no spontaneous magnetization. Below this temperature, the spins can be on average polarized up or down. As this temperature is approached, clusters of indefinitely large size with either up or down polarization occur.

The next idea is the **idea of scaling**. The idea here is that the details of the microscopic behavior don't matter! When $K = J/kT \rightarrow K_c$, at the critical temperature, as we have just remarked, $\xi \rightarrow \infty$, and the two-spin correlation function (for fixed r) goes over to the form

$$\langle s_{\vec{0}} s_{\vec{r}} \rangle \propto \frac{1}{r^{d-2+\eta}}.$$

In this limit, the distribution of cluster sizes (which sets the scales) behaves like a power law and does not define a single mesoscopic scale, but rather an infinity of scales. When we are close to the critical point, we have a continuum of scales up to the correlation length which provides a cutoff, but at the critical point there is no such cutoff. The approach to the critical point is called the "scaling region." Here, let

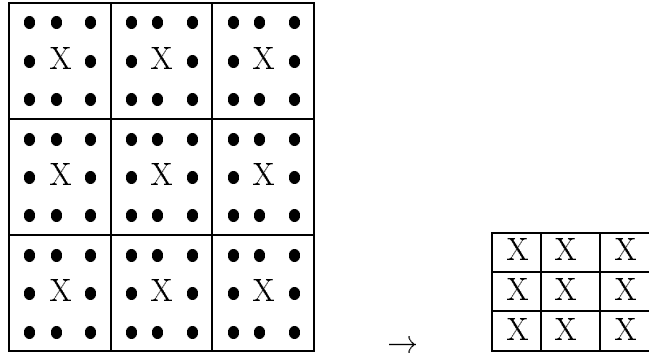
$$\vec{x} = \vec{r}/\xi, \quad \text{and} \quad \sigma_{\vec{x}} = \xi^a s_{\vec{r}},$$

which rescales the distances and the amplitude of the spins. Then we set

$$\langle \sigma_{\vec{0}} \sigma_{\vec{x}} \rangle \rightarrow F(x) \underset{x \rightarrow \infty}{\asymp} \frac{Ae^{-x}}{x^{0.5(d-1)}},$$

where the power of x in the denominator might be different. We still need to get from the microscopic scale to this limit!

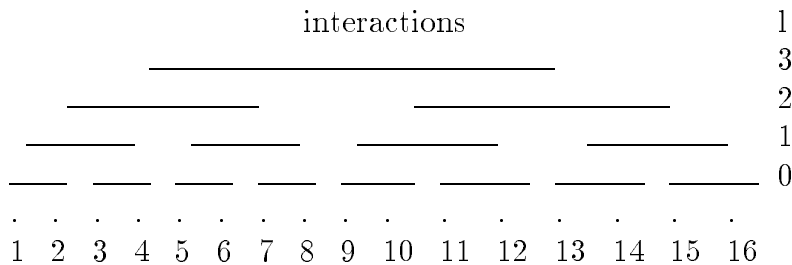
We now come to the **idea of scale-scale interaction** (thanks to Ken Wilson). The insight is that the physics is in the interaction between one length scale and its neighboring length scales. To exploit this insight, one seeks equations which result from the systematic reduction in the number of degrees of freedom. (We start from the microscopic scale for example.)



In the above figure, we have outlined blocks of nine spins. They are all the same but the one in the center is denoted by X for emphasis. The mapping envisioned is to replace each block by a single spin, as at the right which is an appropriately scaled version of the average block spin. The spin-spin interactions are no longer just between nearest neighbor pairs, but are adjusted to keep the answers correct. Without going into details, these arguments can lead to the definition of a mapping \mathcal{R} in the space of Hamiltonians, and we can look to see if it has a fixed point.

$$\mathcal{R}\mathcal{H}^* = \mathcal{H}^*.$$

An example of these ideas is the Hierarchical model. The interactions are illustrated by horizontal lines in the following figure.



The usual Ising model Hamiltonian is

$$-J \sum_j \nu_j \nu_{j+1} - mh \sum_j \nu_j = \frac{1}{2} \sum_j (\nu_j - \nu_{j+1})^2 - J \sum_j \nu_j^2 - mh \sum_j \nu_j.$$

In the model, we keep the $(\nu_1 - \nu_2)^2, (\nu_3 - \nu_4)^2, \dots$ terms for the zero level ($l = 0$). In the next level, we replace

$$(\nu_3 - \nu_2)^2 \mapsto \left[\frac{1}{2}(\nu_3 + \nu_4) - \frac{1}{2}(\nu_2 + \nu_1) \right]^2, \dots,$$

and so on, as indicated by the figure for $l = 1$. In the successively higher levels, in like manner we make a substitution of successively larger block averages. The argument here is that this change shouldn't be too bad, since $\nu_1 \approx \nu_2$ and $\nu_3 \approx \nu_4$ near the critical point because of long-range correlations. In more formal terms, let us define for ν_1, \dots, ν_{2^L} ,

$$\begin{aligned} s_{m,0} &= (\nu_{2m-1} - \nu_{2m})/\sqrt{2}, \\ \hat{s}_{m,0} &= (\nu_{2m-1} + \nu_{2m})/\sqrt{2}, \quad m = 1, \dots, 2^{L-1}, \\ &\vdots \\ s_{m,l+1} &= (\hat{s}_{2m+1,l} - \hat{s}_{2m,l})/\sqrt{2}, \quad m = 1, \dots, 2^{L-2-l}, \\ \hat{s}_{m,l+1} &= (\hat{s}_{2m+1,l} + \hat{s}_{2m,l})/\sqrt{2}, \quad l = 0, \dots, L-2, \end{aligned}$$

which defines 2^L new variables in terms of the ν_j . The Hamiltonian for the hierarchical model is then

$$\mathcal{H} = J \sum_{l=0}^{L-1} 2^{-l(2-\eta)} \sum_{m=1}^{2^{L-1-l}} s_{m,l}^2 - \frac{1}{2} J \left(\frac{1 - 2^{L(\eta-3)}}{1 - 2^{\eta-3}} \right) \sum_j \nu_j^2,$$

where the parameter η introduces a weighting of the different interaction levels so as to correspond to the above usage of η .

Now, following the renormalization group ideas, we first integrate over the $s_{m,l}$ for level $l = 0$, then $l = 1, \dots$. Let us pick the initial spin distribution as

$$f(\nu) = \exp \left[-\frac{1}{2}(a\nu^2 + b\nu^4) \right], \quad \text{where } a < 0, \quad \text{and } b > 0.$$

Performing the above mentioned integrations, we are led to the scale-scale recursion relations:

$$\begin{aligned} I_l(x) &= \int_{-\infty}^{+\infty} dy \exp \left[-Ky^2 - \frac{1}{2}Q_l(x+y) - \frac{1}{2}Q_l(x-y) \right], \quad \text{and} \\ Q_{l+1}(x) &= -2 \ln \left[I_l \left(2^{(1-\eta)/2} x \right) / I_l(0) \right]. \end{aligned}$$

The initial conditions are

$$Q_0(x) = P(x/\sqrt{2}), \quad \text{and} \quad \exp \left[-\frac{1}{2}P(x) \right] = f(x) \exp \left[\frac{1}{2}K \left(\frac{1 - 2^{L(\eta-3)}}{1 - 2^{\eta-3}} \right) x^2 \right].$$

The partition function then reduces to

$$Z = \prod_{l=0}^{L-1} \left\{ (2^{2-\eta})^{2^{L-2-l}} [I_l(0)]^{2^{L-1-l}} \right\} \\ \times \int_{-\infty}^{+\infty} \exp \left\{ mh\beta 2^{L/2} \hat{s}_{1,L-1} - \frac{1}{2} Q_L \left(\frac{\sqrt{2} \hat{s}_{1,L-1}}{2^{(2-\eta)L/2}} \right) \right\} \frac{d\hat{s}_{1,L-1}}{2^{(2-\eta)L/2}},$$

where $\beta = 1/kT$, h is the magnetic field, and m is the magnetic moment. Notice that the scale-scale recursion relations are solved by all the Q_l 's equal to quadratic functions. In the cases where $K \neq K_c$, the Q_l tend to such a fixed point, and these are called the high-temperature or low-temperature fixed points. Here the susceptibility $\chi \propto 1/Q''(0)$ is finite. In the case in which $K = K_c$, the Q 's tend to a fixed point Q^* and $\chi \propto 2^{L(2-\eta)}$ which goes to infinity. If we expand about K_c ,

$$Q_l(x, K) = Q_c(x) + (K - K_c)q_l(x) + o(K - K_c),$$

and we expect that $q_l \approx 2^{l\zeta} Q_c$. From ζ we can compute other critical indices. The critical index for χ is $\gamma = (2 - \eta)/\zeta$ and that for ξ is $\nu = 1/\zeta$.

The question is: *To what extent can these scale-scale interaction ideas be usefully employed in any (or all) the other problems of this initiative? Can they be used to move off the microscopic scale?*

6. Turbulence

Presentation by Charles Zemach

This presentation is on the subject of fluid turbulence in general. By way of introduction, several view graphs were shown displaying density profiles of rather wavy plumes of smoke from a rectangular building. These pictures show three principal attributes: (1) variations down to the smallest length scale, (2) unpredictability in time, and (3) mixing is rapid. In addition, view graphs were shown of the results when the previously mentioned pictorial information was digitized and averaged over about 100 to 1,800 frames. These results were quite smooth and regular. One question is to understand this average smoothness. Flow can be described by the Navier-Stokes equation,

$$\frac{d\vec{u}}{dt} = \frac{\partial\vec{u}}{\partial t} + (\vec{u} \cdot \vec{\nabla})\vec{u} = -\frac{\vec{\nabla}(p)}{\rho} + \frac{\mu}{\rho}\nabla^2\vec{u},$$

starting from an initial condition $\vec{u}(x, t_0)$ for some initial time t_0 . In this equation, the nonlinear term in the velocity field \vec{u} is called the advective term, and the term involving the viscosity μ is called the dissipative term. This term is so called because its action is to spread out and dissipate the initial velocity field. The pressure is p and ρ is the density, which may sometimes be regarded as a constant. The advective term tends to destabilize the problem by causing any initial irregularities to grow worse and without the dissipative term could lead to “catastrophe time.” It is the competition between these two terms which determines the nature of the solution. This competition is described by the Reynolds’ number,

$$\frac{\rho(\vec{u} \cdot \vec{\nabla})\vec{u}}{\mu\nabla^2\vec{u}} \approx \frac{\rho UL}{\mu} \approx \text{Re}.$$

This equation has built-in instability, and we get a statistical distribution driven by an explicit equation.

The total energy in the system is the mean energy, that is the energy of the mean flow, plus the turbulent energy. The Fourier transform of the turbulent energy gives a characteristic power spectrum. Starting from the low frequencies (large-scale behavior), we see a scaling law so that $\log E(\vec{k}) \propto \log |\vec{k}|$. The spectrum reaches a peak at a value of $|\vec{k}|$ which corresponds to the size of the dominant eddies. As $|\vec{k}|$ increases further, we come into the region called the inertial range. Here the spectrum decays like $E(\vec{k}) \propto |\vec{k}|^{-5/3}$. It is called the inertial range because it is in this range that the turbulent flow interacts with the mean flow. The flux over the inertial range is a constant. Above a limiting value, the dissipative wave length, k_d (Kolmogoroff), the spectrum drops off exponentially fast. It is in this region that the energy is converted into heat.

What one wants for this problem is a set of reliable codes which predict the flows, including turbulence. Modern turbulence theory started in the 1960s. We can now do $(512)^3$ to $(1024)^3$ grids which are satisfactory up to Reynolds’ numbers 100–300. There are real, important problems with Reynolds’ numbers of the order of a million, however.

Presentation by Charlie Doering

The work reported was done in collaboration with Peter Constantino and Mac Hyman. The speaker said that when you have chaos on many scales, you have turbulence. First, an example of fluid flow was considered. Suppose we have a hot lower surface and a cold upper surface, separated by height h . Then there will be convective transport of heat upward. The Rayleigh number is $\mathcal{R} = g\alpha\Delta Th^3/\nu\kappa$, where g is the acceleration due to gravity, α is the isothermal expansion coefficient, ΔT is the difference in temperature between the upper and lower surfaces, and ν is the viscosity. Stability is equivalent to the statement that the eigenvalues of the linearized operator have a positive real part which in turn is equivalent to the real part of a particular quadratic form being positive. For the definite models, the time behavior is characterized by $e^{-\lambda t}$. When $\lambda > 0$, the mode is stable, and when $\lambda < 0$, it is unstable. We were shown plots of \mathcal{R} vs horizontal wave number. There is a **U**-shaped curve of neutral stability. Above this curve is the unstable region and below it is the stable region. The minimum point occurs at the critical Rayleigh number \mathcal{R}_c and the critical wave number k_c . A second plot was presented in the λ - k plane. Here again we saw **U**-shaped curves of constant Rayleigh number. For $\mathcal{R} < \mathcal{R}_c$, the curves lie completely above the $\lambda = 0$ line. For $\mathcal{R} = \mathcal{R}_c$, the curve is tangent to it, and for $\mathcal{R} > \mathcal{R}_c$ the curves intersect the line twice each, with part of the curve below that line.

Deep in the turbulent regime, nonlinear effects take over, and the true problem doesn't look like this linearized version. However, these modes may still have some relevance.

At low Rayleigh numbers, there is no flow and there is a linear temperature gradient in the vertical direction. As the Rayleigh number increases, you get convective heat flow by means of rolls. By the time the Rayleigh number is approximately equal to, or a bit greater than, the critical Rayleigh number, the temperature profile has developed marked boundary layer effects. The temperature gradient dT/dz is high near the top and bottom surface, and much lower in the center of the sample. When the Rayleigh number is much greater than \mathcal{R}_c , the central region is almost isothermal and all the temperature change takes place in the boundary layers. There are now descending blobs of cold fluid and ascending blobs of hot fluid.

The Nusselt number is defined as $\mathcal{N} = \langle |\vec{\nabla} T|^2 \rangle$, where $T(\vec{x}, t)$ is the exact solution for the temperature profile. How thick is the boundary layer? One way to approach this question is the method of marginal stability. The idea here is that the thickness is such that the Rayleigh number is just equal to the critical Rayleigh number. Thus,

$$\mathcal{R}_c = \mathcal{R}_{\text{boundary}} = \frac{g\alpha \left(\frac{\Delta T}{2}\right) \delta^3}{\nu\kappa} = \frac{1}{2} \mathcal{R} \left(\frac{\delta}{h}\right)^3.$$

Therefore,

$$\frac{\delta}{h} = \left(\frac{2\mathcal{R}_c}{\mathcal{R}}\right)^{1/3} \propto \mathcal{R}^{-1/3}.$$

This kind of argument can be made rigorous. Choose a temperature profile, $\tau(z)$, then there is a theorem,

THEOREM. If $\tau(z)$ is marginally stable (the lowest eigenvalue is zero) on average (time average, when recast as a quadratic form), then \mathcal{N} equals the heat transport computed from τ (i.e., $\int_0^h \tau'(z)^2 dz$).

COROLLARY. If $\tau(z)$ is marginally or more stable, then \mathcal{N} is less than or equal to the heat transport computed from τ .

One can use this corollary and the variational calculus to determine \mathcal{N} .

What we find for each $\mathcal{R} > \mathcal{R}_c$ is that there exists a profile such that the curve in the $\lambda-k$ plane just touches the $\lambda = 0$ at one distinct value of k , which is marginally stable. We could just keep the modes that lie within the curve. As we crank up \mathcal{R} , the speaker said, it turns out that you get two distinct modes that touch the line of marginal stability ($\lambda = 0$). For a very high \mathcal{R} , you get many such tangent points which lead to highly degenerate, multiple scales of wave numbers.

Presentation by Shi-Yi Chen

Title: Passive Scalar Turbulence and Anomalous Diffusion

The work reported was done in collaboration with Nian Zheng Cao and Robert H. Kraichnan. Shi-Yi said that the theoretical study of passive scalar turbulence is significant because (i) turbulent advection of various quantities is of great importance in a variety of fluid flows, *including the migration of pollution in ground water, atmospheric and ocean pollutant dispersion*, chemical mixing processes, and combustion processes; (ii) improved modeling of stochastic diffusion is important both for applications to fields like those named and for the insight it can provide, in partnership with basic theory, into fundamental dynamics of turbulent processes; and (iii) from the point of view of dynamical systems theory, stochastic diffusion is a prime example of a complicated, distributed system in a state of strong statistical disequilibrium. The methods developed in recent years for the treatment of dynamical systems with small numbers of degrees of freedom have not been effective for turbulence problems. This is a fundamental theoretical challenge.

Next we were treated to a picture of the wake of a grounded tanker. People would like to know where and how fast the leaking oil goes. After that we saw a picture of the simulation structure on many different scales. Initially, there was a Gaussian distribution of temperatures. The advection and diffusion were said to be about equal, and there was flow taking place underneath the visible surface. Colored noise, stochastic Gaussian, and a fractal dimension of 1.36 were mentioned. Also shown was a picture of diffuse interstellar clouds, which is a real compressive diffusion problem. The fractal dimension was estimated to be about 1.32–1.325.

Chen now gave the equation of motion for a passive scalar temperature T as

$$\left(\frac{\partial}{\partial t} + \vec{u}(\vec{x}, t) \cdot \vec{\nabla} \right) T(\vec{x}, t) = \kappa^2 \nabla^2 T(\vec{x}, t) + f(\vec{x}, t),$$

where \vec{u} is the solenoidal velocity field, κ is the molecular diffusivity, and f represents the forcing term. We are interested in the structure functions. Let $\Delta T(\vec{x}, \vec{x}', t) \equiv T(\vec{x}', t) - T(\vec{x}, t)$. For the case of interest, the velocity field fluctuates randomly in time with a

correlation time which is very short compared with the convective and diffusive time scales. We define the 2nth order structure function as

$$S_{2n}(r) = \langle \Delta T(\vec{x}, \vec{x}', t)^{2n} \rangle, \quad \text{where } r = |\vec{x} - \vec{x}'|,$$

where n is a positive integer and $\langle \cdot \rangle$ denotes an ensemble average. The exact evolution equations for the structure functions are

$$\frac{\partial S_{2n}(r)}{\partial t} - \frac{2}{r^{d-1}} \frac{\partial}{\partial r} \left(r^{d-1} \eta(r) \frac{\partial S_{2n}(r)}{\partial r} \right) = \kappa J_{2n}(r),$$

where d is the spatial dimension and $\eta(r)$ is the two-particle eddy-diffusivity defined by

$$\eta(r) = \frac{1}{2} \int_0^t \langle \delta_{\parallel} u(\vec{r}, t) \delta_{\parallel} u(\vec{r}, t') \rangle dt',$$

with $\delta_{\parallel} u(\vec{r}, t) \equiv [\vec{u}(\vec{x}, t) - u(\vec{x} + \vec{r}, t)] \cdot \vec{r}/r$. The velocity field is switched on at $t = 0$, and $T(\vec{x}, t = 0)$ is a Gaussian field. We have the definition

$$J_{2n}(r) \equiv 2n \langle [\Delta T(\vec{r})]^{2n-1} \mathcal{H}[\Delta T(\vec{r})] \rangle,$$

where

$$\mathcal{H}[\Delta T(\vec{r})] = \langle (\nabla_x^2 + \nabla_{x'}^2) \Delta T(\vec{r}) | \Delta T(\vec{r}) \rangle = - \langle \nabla_{x'}^2 T' - \nabla_x^2 T | T' - T \rangle,$$

and $\langle \cdot | \Delta T(\vec{r}) \rangle$ denotes the ensemble average conditioned on a given value of $\Delta T(\vec{r})$.

The next problem addressed is the common one of closing a hierarchy of equations, specifically those for the J_{2n} . To this end, Chen gave a “refined similarity hypothesis,” *i.e.*,

$$\Delta T(\vec{r}) \frac{\partial \Delta T(\vec{r})}{\partial t} \sim \Delta T(\vec{r}) (\nabla^2 + \nabla'^2) \Delta T(\vec{x}, \vec{x}', t).$$

Then if we forget about the temperature and make a hand-waving argument, (a different rigorous argument exists)

$$\frac{\partial \Delta T(\vec{r})^2}{\partial t} \sim \Delta T(\vec{r})^2.$$

If we expand \mathcal{H} in ΔT , we have

$$\mathcal{H} \sim f_1(r) \Delta T + f_3(r) (\Delta T)^3 + \dots, \quad \mathcal{H}[\Delta T(\vec{r})] \sim \Delta T(\vec{r}) = f_1(r) \Delta T(\vec{r}),$$

which is a truncation to the first order in ΔT . This ansatz agrees very well with simulations.

$$f_1(r) = \frac{\langle \Delta T \mathcal{H} \rangle}{S_2(r)} = \frac{A(r)}{S_2(r)},$$

where $A(r) = \nabla^2 S_2(r) - \nabla^2 S_2(r)|_{r=0}$. The ansatz now is

$$\mathcal{H}[\Delta T(\vec{r})] = A(r)/S_2(r) \Delta T(\vec{r}), \quad J_{2n}(r) = 2n S_{2n}(r) A(r)/S_2(r).$$

Applying the last equation in the case $n = 1$ gives $J_2(r) = 2A(r)$ which in turn we have expressed in terms of $J_2(r)$. Thus the previously given partial differential equation for S_2 is closed (still depends of η of course). Once it is solved, then all the other $J_{2n}(r)$ are explicitly given by the ansatz in terms of S_{2n} which leads to explicit equations for the rest of the S_{2n} etc. Shi-Yi pointed out that this “linear ansatz” implies the formula

$$C_{2n}(r) \equiv \frac{J_{2n}(r)S_2(r)}{nJ_2(r)S_{2n}(r)} \equiv 1.$$

The speaker next assumed that there is a scaling range where

$$\eta(r) \propto r^{\zeta(\eta)} \quad (0 < \zeta(\eta) < 2), \quad S_{2n}(r) \propto r^{\zeta_{2n}}, \quad f_1(r) \propto r^{z_1},$$

and $\eta(r)$ is considered a given. Using the equation of motion for S_{2n} and power counting, we can obtain

$$\zeta_2 = 2 - \zeta(\eta), \quad z_1 = -\zeta_2, \quad \text{and} \quad \zeta_{2n} = \frac{1}{2}\sqrt{4nd\zeta_2 + (d - \zeta_2)^2} - \frac{1}{2}(d - \zeta_2),$$

where d is the spatial dimension. When $n \gg 1$, $\zeta_{2n} \approx \sqrt{nd\zeta_2}$. This behavior represents anomalous scaling as regular scaling is expected to yield $\zeta_{2n} = n\zeta_2$.

Chen told us that there were a number of computer simulation results which had been run on the CM5 on an 8192^2 grid in physical (not momentum) space. The initial field T was a Gaussian field. We saw some plots of C_{2n} , which should be unity. For $\zeta_2 = 0.5$, they were not so bad, but for $\zeta_2 = 1.0$ there were large departures. It is hard to tell whether the ansatz is violated or the inertial range is violated. When $\zeta_2 = 1$, the scaling exponent for J_{10} was not bad, but for smaller n they were not so good. The comparison of the direct numerical simulation with the solution of the equations is fairly close. We saw a graph in which it was clear that the anomalous scaling was a better description for large n of the scaling exponents than was the regular scaling.

The speaker said that he had plans for future work on diffusion in porous media, where the small-scale dynamics of the velocity is important and for future work on turbulent diffusion in compressible fluids.

7. General Methods

Presentation by Bruce J. Berne

Title: Symplectic Methods

(This presentation was made on Jan. 11, 1995, to a CNLS High Performance Computing Workshop. It seems relevant to this initiative and so is included.)

The sort of problems which are being considered in this talk are stiff vibrations such as are seen in polyatomic fluids and path integrals. Here small time steps are required to follow the stiff part which implies that millions of time steps are necessary to follow the soft part. This sort of problem also occurs in disparate mass systems* such as e, p, H diffusion, a dilute system of light particles in a dense system of heavy particles. Also mentioned were superionic conductors, the Lagrangian methods of Carr-Parinello,** and systems with long- and short-range forces.

In molecular dynamics where we have Newton's equations of motion,

$$m_i \frac{d^2 \vec{r}_i}{dt^2} = \vec{F}_i(\vec{r}_1, \dots, \vec{r}_N),$$

and so the Liouville theorem applies. These equations are too hard to solve exactly so the Verlet algorithm has been used (actually the velocity Verlet due to H. Andersen),

$$\begin{aligned} \vec{r}_i(\Delta t) &= \vec{r}_i(0) + \vec{v}_i(0)\Delta t + \frac{\Delta t^2}{2m_i} \vec{F}_i(0), \text{ and} \\ \vec{v}_i(\Delta t) &= \vec{v}_i(0) + \frac{\Delta t}{2m_i} [\vec{F}_i(0) + \vec{F}_i(\Delta t)]. \end{aligned}$$

Here energy is not conserved, but it is time reversal invariant and symplectic. (The Jacobian of the phase space transformations referred to in the Liouville theorem is unity.) The solution using this algorithm moves in an energy shell.

Another way to generate these equations is through a derivation based on the Liouville operator,

$$iL = \dot{x} \frac{\partial}{\partial x} + F \frac{\partial}{\partial p} = iL_1 + iL_2,$$

where we have written one term for each degree of freedom. The propagator is given by

$$\begin{pmatrix} x(\Delta t) \\ p(\Delta t) \end{pmatrix} = e^{iL\Delta t} \begin{pmatrix} x(0) \\ p(0) \end{pmatrix}.$$

Since L_1 and L_2 do not commute, we resort to the Trotter formula,[†]

$$e^{(iL_1+iL_2)t} = \left[e^{iL_1 t/2p} e^{iL_2 t/p} e^{iL_1 t/2p} \right]^p + O(t^3/p^3).$$

* See, for example, the presentation by Lee Collins, Section 4.

** See the discussion of Lee Collins in Section 4.

† Higher-order versions have been discovered by M. Suzuki and are very effective for some problems.

We can think of $\Delta t = t/p$ as a single time step. Since L is Hermitian, e^{iL} is unitary, and we write, for a single step,

$$\begin{pmatrix} x(\Delta t) \\ p(\Delta t) \end{pmatrix} = \left[e^{iL_1 t/2p} e^{iL_2 t/p} e^{iL_1 t/2p} \right] \begin{pmatrix} x(0) \\ p(0) \end{pmatrix},$$

which we can rewrite by the definitions as

$$\begin{pmatrix} x(\Delta t) \\ p(\Delta t) \end{pmatrix} = \exp\left(\frac{\Delta t}{2} F \frac{\partial}{\partial p}\right) \exp\left(\Delta t \dot{x} \frac{\partial}{\partial x}\right) \exp\left(\frac{\Delta t}{2} F \frac{\partial}{\partial p}\right) \begin{pmatrix} x(0) \\ p(0) \end{pmatrix}.$$

In this form, we have re-expressed the Trotter version of the propagator in terms of shift operators (by Taylor's theorem). From it we get directly the aforementioned velocity Verlet algorithm. If we interchange the roles of L_1 and L_2 , then we get the position Verlet algorithm, which is

$$\begin{pmatrix} x(\Delta t) \\ \dot{x}(\Delta t) \end{pmatrix} = \begin{pmatrix} x(0) + \frac{\Delta t}{2} [\dot{x}(0) + \dot{x}(\Delta t)] \\ \dot{x}(0) + \frac{\Delta t}{m} F [x(0) + \frac{\Delta t}{2} \dot{x}(0)] \end{pmatrix}.$$

Consider the case of light and heavy particles. Let L_x represent the fast degrees of freedom and L_y the slow degrees of freedom. As above, we can express

$$e^{i(L_x + L_y)\Delta t} \approx e^{iL_y t/2p} e^{iL_x t/p} e^{iL_y t/2p}.$$

We next break down $e^{iL_x \Delta t}$, by again employing the Trotter formula, so that we get

$$e^{iL_x \Delta t} = \left[\exp\left(\frac{\delta t}{2} F \frac{\partial}{\partial p}\right) \exp\left(\delta t \dot{x} \frac{\partial}{\partial x}\right) \exp\left(\frac{\delta t}{2} F \frac{\partial}{\partial p}\right) \right]^n,$$

where $\delta t = \Delta t/n$, and we have used, $iL_x = \dot{x} \frac{\partial}{\partial x} + F_x \frac{\partial}{\partial p}$, $F_x = F_{xx} + F_{xy}$. The idea here is take a lot of time steps for the fast degrees of freedom relative to the number taken for the slow degrees of freedom. This method is not the same, it was said, as holding the heavy particles fixed while the light ones move. It was emphasized that this method is by its structure simplectic.

Another application of these techniques is for short- and long-range forces. A force can be decomposed into short- and long-ranged forces by use of a switching function since $F(R) = S(R)F(R) + [1 - S(R)]F(R)$ will do the job if $S(0) = 1.0$ and drops rapidly to zero at some appropriate value of R . This procedure saves the recomputation of all the forces at every time step, which is a very time consuming part of the calculations. A factor of 100 improvement in speed was reported. This procedure has been used in reversible RESPA. Here, we write

$$iL = \dot{x} \frac{\partial}{\partial x} + F_s \frac{\partial}{\partial p} + F_l \frac{\partial}{\partial p} = iL_s + F_l \frac{\partial}{\partial p}.$$

We can now express the propagator

$$G_{lsl}(\Delta t) \approx e^{i(F_l \Delta t/2) \frac{\partial}{\partial p}} e^{iL_s t} e^{i(F_l \Delta t/2) \frac{\partial}{\partial p}}.$$

Following the method expounded above, we use the Trotter formula again to re-express the short-range portion as

$$e^{iL_s \Delta t} = \left[\exp \left(\frac{\delta t}{2} F_s \frac{\partial}{\partial p} \right) \exp \left(\delta t \dot{x} \frac{\partial}{\partial x} \right) \exp \left(\frac{\delta t}{2} F_s \frac{\partial}{\partial p} \right) \right]^n,$$

where again $\delta t = \Delta t/n$. Thus, for stiff degrees of freedom with long-range forces, we get by combining the above

$$G_{xyx}(\Delta t) = G_{lsl}^{(x)} \left(\frac{\Delta t}{2} \right) G_{lsl}^{(y)}(\Delta t) G_{lsl}^{(x)} \left(\frac{\Delta t}{2} \right).$$

This procedure has been applied to a crystalite of bucky balls, with a factor of forty increase in speed. Here, the need is for the lattice vibrations as well as the small stuff in the bucky balls.

Under the rubric of path integral methods, the speaker discussed a polymer chain. He discretized the imaginary time required in his calculations, and here there is a quadratic potential between the beads which gets stiffer as the number of points increases. The effective Hamiltonian* is given by

$$\mathcal{H}_{\text{eff}} = \sum_{t=1}^P \left\{ \frac{p_t^2}{2m} + \frac{mP}{2\beta^2 \hbar^2} (x_t - x_{t+1})^2 + \frac{1}{P} V(x_t) \right\}.$$

One problem here is that the system becomes nonergodic as P gets big. The speaker discussed the use of BGK dynamics here and hybrid Monte Carlo was also mentioned.

Presentation by Clint Scoval

Title: Symplectic Methods

In discussing large problems, parsimony is important as one does not wish to deal with too many variables. Furthermore, if a system has certain symmetry properties, it is highly desirable that they be conserved in any numerical simulation procedure. This presentation is concerned with Hamiltonian systems. Such a system is defined by (1) a Hamiltonian, $\mathcal{H} = H(\vec{p}, \vec{q})$, (2) the symplectic structure $W = \sum dq_i \wedge dp_i$, and (3) Hamilton's equations of motion

$$\dot{\vec{q}} = \vec{\nabla}_{\vec{p}} H, \quad \text{and} \quad \dot{\vec{p}} = -\vec{\nabla}_{\vec{q}} H.$$

The symbol \wedge denotes the wedge product.** By symplectic is meant that the volume in phase space is conserved. This property is a consequence of Liouville's theorem for

* This problem seems to bear some formal resemblance to that discussed by Fred Cooper in Section 4, although they are clearly distinct problems.

** One of the problems addressed by the multiscale initiative is that often different people are discussing intrinsically the same problem in different language which totally stifles communication. An example may be the wedge product, about which some of us

Hamiltonian systems. According to a theorem of Darboux, all Hamiltonians systems have the structure (2) just noted.

The important properties of such a system are that (i) the Hamiltonian is independent of time and so it is a constant, and (ii) the flow map of Hamilton's equations of motion is a canonical transformation (*i.e.*, symplectic). More explicitly, if Q, P are the time translations of q, p in the two-dimensional case $dQ \wedge dP = dq \wedge dp$ or the Jacobian,

$$\frac{\partial\{Q, P\}}{\partial\{q, p\}} = \frac{\partial Q}{\partial q} \frac{\partial P}{\partial p} - \frac{\partial Q}{\partial p} \frac{\partial P}{\partial q} = 1,$$

which corresponds to area preservation, or $\sum dq_i \wedge dp_i$ is constant in higher dimensions which corresponds to volume preservation, and has a different class of bifurcations.

are perhaps inadequately informed. The wedge product will define a Grassman algebra Λ . Let $B(\epsilon_1, \dots, \epsilon_n)$ be the 2^n basis vectors of a 2^n dimensional vector space over the real numbers, where the $\epsilon_i = 0$ or 1. Then any vector in this space can be written as

$$\alpha = \sum_{\epsilon} a(\epsilon_1, \dots, \epsilon_n) B(\epsilon_1, \dots, \epsilon_n).$$

The wedge product $\alpha \wedge \beta = \gamma$ is then defined by

$$c(\epsilon_1, \dots, \epsilon_n) = \sum_{\mu_i + \nu_i = \epsilon_i \pmod{2}} \delta \begin{pmatrix} \mu_1, \dots, \mu_n \\ \nu_1, \dots, \nu_n \end{pmatrix} a(\mu_1, \dots, \mu_n) b(\nu_1, \dots, \nu_n),$$

where

$$\delta \begin{pmatrix} \mu_1, \dots, \mu_n \\ \nu_1, \dots, \nu_n \end{pmatrix} = \begin{cases} 0 & \text{if } \mu_i = \nu_i = 1 \text{ for any } i, \\ \prod_{i=1}^n (-1)^{\nu_i(\mu_i + \mu_{i+1} + \dots + \mu_n)}, & \text{otherwise.} \end{cases}$$

The wedge product, together with the vector space defines the Grassman algebra. This product has been shown to be both associative and distributive, but not commutative, and so Λ is a linear associative algebra. The basis elements satisfy the identities

$$B(\mu_1, \dots, \mu_n) \wedge B(\nu_1, \dots, \nu_n) = \delta \begin{pmatrix} \mu_1, \dots, \mu_n \\ \nu_1, \dots, \nu_n \end{pmatrix} B(\mu_1 + \nu_1, \dots, \mu_n + \nu_n),$$

where the additions $\mu_i + \nu_i$ are again mod 2. Note that since $B(0, \dots, 0) \wedge \alpha = \alpha$, it acts as the identity operator in this algebra. If we define,

$$B(0, \dots, 0) = 0, \quad \text{and} \quad B(0, \dots, 1, \dots, 0) = E_i \text{ for } i = 1, \dots, n,$$

then the E_i and their wedge products

$$B(\epsilon_1, \dots, \epsilon_n) = \prod_{\{i|\epsilon_i=1\}} E_i$$

The speaker reported major stability results as the KAM (Kolmogorov, Arnold, Moser) theorem which he said implied that phase space is foliated by tori, and the Nekhoroshev theorem which he said says that if the energy is invariant if perturbed, then the energy is an adiabatic invariant. He showed some of his results for the Fermi-Pasta-Ulam system integrated by a symplectic method. Aside from a small, high-frequency fluctuation, it maintained the total energy quite accurately with no drift, such as was displayed by a fourth order Runge-Kutta method.

The most significant result for symplectic methods reported was a theorem due to Ge Zong:

THEOREM. *Suppose the Hamiltonian system corresponding to the Hamiltonian \mathcal{H} has no other integrals of the motion besides H . Let $\phi(t)$ be a symplectic integral, consistent to first order with \mathcal{H} 's Hamiltonian system, such that $\phi(t)$ preserves \mathcal{H} exactly. Then $\phi(t)$ travels along the orbits of \mathcal{H} 's Hamiltonian system, but possibly with the wrong speed.**

The speaker said that this theorem implies that if the energy is well preserved, it is a good indication of accuracy (for symplectic methods). Further examples were reported. The usual maps of the Hénon-Heiles problem showed clear curves when a symplectic method was used, but noticeably fuzzy ones otherwise.

Finally, Scovel discussed some simple ways to construct symplectic methods. First, he discussed local separation algorithms. Consider the case where $H(q, p) = \frac{1}{2}p^2 + V(q)$ which can be separated into two simple cases. (Spectral tracking) Consider $\frac{1}{2}p^2$. The flow

span the space, where $\mathbf{\Lambda}$ is like \prod but denotes a wedge product. One further operation is useful. We define

$$\alpha^* = \sum_{\epsilon} a(\epsilon_1, \dots, \epsilon_n) B(1 - \epsilon_1, \dots, 1 - \epsilon_n).$$

It is now useful to consider the sub-algebra of the E_i , $\vec{A} = \sum_{i=1}^n a_i E_i$. In this algebra, the usual dot product can be re-expressed as $\vec{A} \cdot \vec{B} = (A \wedge B^*)^*$, when we remember that the E_0 plays the role of unity. In the three-dimensional case, $\vec{A} \times \vec{B} = (A \wedge B)^*$. The volume of a parallelepiped whose edges are parallel to \vec{A}_i can be expressed by the wedge product as

$$v(\vec{A}_1, \dots, \vec{A}_r) = \left| \mathbf{\Lambda}_{i=1,r} A_i \right| = \sqrt{\det(A_i \wedge A_j^*)^*} = \sqrt{\det(\vec{A}_i \cdot \vec{A}_j)},$$

where $|A|$ is the length of the vector in the $B(\epsilon_1, \dots, \epsilon_n)$ representation and the last expression is the usual one for such a volume (due to Lagrange). This last result brings us at last, after a lengthy digression, to the aspect of the wedge product which is used in this presentation. [This explanation of the wedge product is based on G. Berman, Am. Math. Monthly **68**, 112 (1961).]

* Generalizations of this theorem were not discussed, but from the opening remarks, I presume that it is the general wisdom that if all the constants of the motion are exactly preserved by a symplectic method, then the system is expected to follow the same orbit as the original Hamiltonian system.

map here is

$$m_1(t) : \begin{array}{l} q \mapsto Q = q + tp, \\ p \mapsto P = p. \end{array}$$

Next consider $V(q)$. Here the flow map is

$$m_2(t) : \begin{array}{l} q \mapsto Q = q, \\ p \mapsto P = p - tV'(q). \end{array}$$

Now each of m_1 and m_2 is symplectic and so, therefore, is the composition $m_1 \circ m_2$, and it agrees to first order. Following the methods of Suzuki and collaborators, the method

$$S_2(t) = m_1\left(\frac{1}{2}t\right) \circ m_2(t) \circ m_1\left(\frac{1}{2}t\right)$$

is second order, and

$$S_4(t) = S_2(\alpha t) \circ S_2((1 - 2\alpha)t) \circ S_2(\alpha t)$$

is fourth order. These increases in the accuracy really cut down the energy error fast. The speaker described quite a number of known applications for these methods.

The relevance to multiscale problems is that the problem can be broken into sub-problems corresponding to fast and slow time scales* and by using symplectic integration on each scale, a much greater overall efficiency is allowed.

Presentation by Rajiv Kalia

Title: On Combining Different Techniques

Kalia first described the nature of the work undertaken and the facilities available to his group. Of that work, he discussed generally the morphology and fracture of porous materials, structural transformations in SiO_2 glass at high pressures, thermal transport in Si_3N_4 glass, and some work in progress. First he discussed methods for molecular dynamics on a parallel MIMD (multiple instruction, multiple data) machine. He justified the need for large-scale computation by pointing out that in porous materials there are structural correlations of the order 10–100 Å which require a molecular dynamics box of ten times that size, or a million to a billion particles. They are currently at the million particle level. Mention was also made of Nanophase ceramics. In this case for a realistic simulation, at least 1,000 clusters of about 1,000 atoms each are required. Furthermore, in problems with long-range Coulomb and three-body interactions, large computing resources are also required. Of the order of 10^4 to 10^6 time steps are needed.

In the molecular dynamics method, the fundamental equation is just Newton's second law of motion, $m_i \frac{d^2 \vec{r}_i}{dt^2} = -\vec{\nabla}_i V(\{\vec{r}_j\})$, and the physical properties are obtained from the particle trajectories. The interatomic potentials used are of the form

$$V = \sum_{i < j} V_2(\vec{r}_{ij}) + \sum_{i < j < k} V_3(\vec{r}_i, \vec{r}_j, \vec{r}_k),$$

* As described by Bruce Berne, see previous presentation.

where

$$V_2 = \frac{H_{ij}}{r^{\eta_{ij}}} + \frac{Z_i Z_j}{r} - \frac{\alpha_i Z_j^2 + \alpha_j Z_i^2}{2r^4}, \quad \text{and} \quad V_3 = B_{jik} f(\vec{r}_{ij}, \vec{r}_{ik}) (\cos \theta_{jik} - \gamma_{jik})^2.$$

With interactions of long-range Coulomb character, there are of the order of N^2 interaction terms. The desire is to reduce the number of these terms. The method employed to carry out this reduction is the cell multipole method. Also, the three-body potentials here are restricted to be of the form of separable interactions, *i.e.*,

$$v_{jik}(\vec{r}_{ij}, \vec{r}_{ik}) = \sum_{\alpha} v_{\alpha}^{(3)}(\vec{r}_{ij}) v_{\alpha}^{(3)}(\vec{r}_{ik}).$$

As the interactions are normally symmetric, the approximation here is that only a finite number of terms are kept in the sum over α .

The fast multipole method used by the speaker is designed for a system with a relatively uniform density, as distinguished from that for astrophysical problems.* Here the system is divided in half in each direction to yield 8 smaller boxes, then each new box is again divided into eighths, and so on down to the effective interaction length for the box size. Now the potential felt by a particle is taken as the sum of the interactions with the particles in its own and nearest-neighbor boxes (27 boxes) plus the multipole expansion of the field due to particles in the distant boxes. The boxes are combined in a hierarchical manner so that only $O(N)$ operations** are required. That is to say, the distant boxes are grouped into the largest “parent box” that is completely filled with distant boxes. The multipole expansion has the form

$$V_A^{\text{pole}}(\vec{R}) = \frac{Z}{R} + \frac{\mu_{\alpha} R_{\alpha}}{R^3} + \frac{Q_{\alpha\beta} R_{\alpha} R_{\beta}}{R^5} + \dots, \quad \vec{R} = \vec{r} - \vec{r}_A,$$

where summation over repeated indices is implied and \vec{r}_A is the reference point (usually the center) for the distant box A . The multipole expansions of 8 children boxes are combined to give that for a parent box (next level up in the hierarchy) by the formulas

$$Z^{(l-1)} = \sum_k Z_k^{(l)}, \quad \text{and} \quad \mu_{\alpha}^{(l-1)} = \sum_k (\mu_{\alpha,k}^{(l)} + Z_k^{(l)} R_{\alpha,k}), \dots$$

Finally, again to speed up the computations, the sum over the multipole expansions for the distant boxes is expanded in a Taylor series about the center of the box under consideration, C_0 , as

$$\sum_A V_A^{\text{pole}}(\vec{r} - \vec{r}_A) = V^{(0)} + V_{\alpha}^{(1)} r_{\alpha} + V_{\alpha\beta}^{(2)} r_{\alpha} r_{\beta} + \dots = V^T(\vec{r}),$$

where \vec{r} and \vec{r}_A are relative to the center of the box C_0 . To further improve efficiency, the Taylor series coefficients are also grouped by level, as were the multipole expansions

* See the presentations of Mike Warren, Section 5.

** It seems to me that it is $O(N \log N)$.

above, by simply summing up the coefficients for the children to give that for the parent box and then repeating back up the hierarchical chain. The appropriate modification to take account of periodic boundary conditions was noted briefly and is called the reduced cell multipole method.

The next point of methodology discussed is the multiple-time-step method. Here the forces on the particles are divided into primary and secondary, and the primary forces are updated at every time step. The secondary forces and their first l_{\max} time derivatives are updated every l_{\max} time steps. In between updates, a Taylor expansion in the time since the last update to order l_{\max} is used.

Modern parallel computers require that thought be given to how to distribute the work among the different central processor units. The volume is divide into p subsystems of volume Ω/p each. The internode communication involves data motion in the surface layers.* These procedures have been implemented on the 512-node Intel Touchstone Delta and the 128-node IBM SP1 for $8232p$ particles, where p is the number of processors. The speaker found a parallel efficiency of 92% with 8% communications on the Delta running at 4.8 sec/time step for 4.2 million SiO_2 particles. The speed on the SP1 is 4.8 times faster.

Next, the speaker reported a variety of results. First there was his study of amorphous silica. He described molecular dynamics simulations of silica glasses under uniform dilation and the occurrence of “percolating pores” by which is meant a pore of system spanning size. He first discussed the morphology of (nonpercolating) pores. The radius of a pore is defined by

$$R^2 = \frac{1}{N_S} \sum_{i=1}^{N_S} |\vec{r}_i - \vec{r}_0|^2, \quad \text{and} \quad \vec{r}_0 = \frac{1}{N_S} \sum_{i=1}^{N_S} \vec{r}_i,$$

where the \vec{r}_i are the particles on the surface of the pore. If V is the volume of the pore, then the fractal dimension of the pore, d_f , is defined by the scaling relation $R \propto V^{1/d_f}$. The pore interface width or roughness is defined by

$$w^2 = \frac{1}{N_S} \sum_{i=1}^{N_S} (|\vec{r}_i - \vec{r}_0| - R)^2,$$

and the scaling relation $w \propto V^\mu$ defines the index μ . One can also define the average pore size as

$$V_{\text{av}} = \frac{\sum_V V^2 n(V)}{\sum_V V n(V)},$$

where $n(V)$ is the number of pores of volume V . Here we expect the scaling relation $V_{\text{av}} \propto |\rho - \rho_c|^{-\gamma}$, where ρ_c is the percolation threshold density and γ is a critical exponent. Kalia’s simulation studies give the results, (at a density of 1.44 g/cm^3) $\mu = 0.31$, $d_f = 2.6$. He also estimates that $\rho_c = 1.40 \pm 0.04$ and $\gamma = 1.89 \pm 0.15$. By way of reference, $\gamma = 1.8$ as estimated numerically for three-dimensional percolation. With regard to pore percolation,

* See the discussion on domain decomposition in the presentations of Mike Warren, Section 5, and M. Sahota, Section 2.

Kalia found for the correlation length, $\xi \propto |\rho - \rho_c|^{-\nu}$ and the pore size distribution, $n(s) \propto s^{-\tau}$, that $\nu = 0.9 \pm 0.2$, and $\tau = 2.18 \pm 0.13$.

He next reported that internal fracture surfaces have a roughness exponent of 0.87 ± 0.02 for this case. This exponent is computed from $g(\sigma) = \langle [h(y+y_0, z+z_0) - h(y_0, z_0)]^2 \rangle^{0.5}$, where $h(y, z)$ is the surface height and $\sigma = \sqrt{y^2 + z^2}$. The scaling relation $g(\sigma) \propto \sigma^\alpha$ defines the roughness exponent α . These results conform well with experimental measurements on a number of materials which have suggested a universal value of $\alpha \approx 0.8$, although there are other experiments at variance with this idea.

In his studies, Kalia considered structural phase transformations in amorphous silica at high pressure. As an indicator of this transition, he pointed out the disappearance of the first sharp diffraction peak in the structure factor $S(q)$, related to the loss of medium range order. There was also the appearance of a new peak in $S(q)$. The structural transformation goes from a tetrahedral network (at a normal density of 2.2 g/cm³) to an octahedral network as the pressure increases.

Finally, he reported some results on thermal transport in Si₃N₄ glass. He has computed the thermal conductivity and said it is a good thermal insulator at $T = 1,200^\circ\text{C}$. This work also relates to the experimental measurements on silica and carbon aerogels which indicate that $\lambda \propto \rho^{1.5}$. He indicated that work is in progress on nanoclusters of silica nitride. Also work is in progress on nanophase materials. I understood these to be described as sintered solids which are very fine grained materials with very special mechanical properties.

Presentation by George Baker:

Title: Quick-Solve, Stable, Implicit Differencing Scheme

The problem illustrated in this presentation is the numerical solution of

$$\nabla^2 \theta = \frac{\partial \theta}{\partial t}.$$

Historically, the first idea was to write a difference approximation of the form

$$\theta_{\vec{r}}^{n+1} = \theta_{\vec{r}}^n + \Delta t \left(\frac{\theta_{\vec{r}+\vec{\delta}}^n - 2\theta_{\vec{r}}^n + \theta_{\vec{r}-\vec{\delta}}^n}{\delta^2} \right).$$

The superscripts indicate the time step, and the subscripts the lattice point. This method is called an ‘‘explicit’’ one. The trouble with it is well known. It is only stable when

$$\Delta t < 2(\Delta x)^2,$$

which considerably limits the size of the time step.

Instead one could center the time derivative and the spatial difference in the same place and write

$$\theta_{\vec{r}}^{n+1} - \frac{1}{2} \Delta t \left(\frac{\theta_{\vec{r}+\vec{\delta}}^{n+1} - 2\theta_{\vec{r}}^{n+1} + \theta_{\vec{r}-\vec{\delta}}^{n+1}}{\delta^2} \right)$$

$$= \theta_{\bar{r}}^n + \frac{1}{2} \Delta t \left(\frac{\theta_{\bar{r}+\bar{\delta}}^n - 2\theta_{\bar{r}}^n + \theta_{\bar{r}-\bar{\delta}}^n}{\delta^2} \right).$$

This method is called implicit because the values of θ at the advanced time are not given explicitly, but only implicitly through the solution of a linear system of equations. It is, however, unconditionally stable and is the popular Crank-Nicolson method.

Next there was a discussion of implicit differencing schemes in one dimension. The speaker promised to show how they can be extended to higher dimensions for which the exact (numerically speaking) solution to the difference equations could be obtained in a time proportional to the number of mesh points (for a rectangular lattice).

To analyze stability, the recent method of A. Iserles was used. The discretized numerical equation can be written as (the one-dimensional case is used here for illustration)

$$\sum_{j=-\tau}^{\tau} \beta_j u_{l-j}^{(n+1)} = \sum_{j=-\sigma}^{\sigma} \alpha_j u_{l-j}^{(n)}$$

for mesh $\Delta x = h$ and time step Δt . Let $\hat{u}(\theta)$ be the Fourier transform,

$$\hat{u}(\theta) = \sum_{l=-\infty}^{\infty} u_l e^{i l \theta h}, \quad -\frac{\pi}{h} < \theta < \frac{\pi}{h}$$

$$u_l = \frac{h}{2\pi} \int_{-\pi/h}^{\pi/h} \hat{u}(\theta) e^{i l \theta h} d\theta.$$

If we Fourier transform the difference equation we get

$$\sum_{l=-\infty}^{\infty} \sum_{j=-\tau}^{\tau} \beta_j e^{i j \theta h} u_{l-j}^{(k+1)} e^{i(l-j)\theta h} = \sum_{l=-\infty}^{\infty} \sum_{j=-\tau}^{\tau} \alpha_j e^{i j \theta h} u_{l-j}^{(k)} e^{i(l-j)\theta h},$$

or

$$P(z) \hat{u}^{(k+1)}(\theta) = Q(z) \hat{u}^{(k)}(\theta),$$

where

$$P(z) = \sum_{j=-\tau}^{\tau} \beta_j e^{i j \theta h}, \quad Q(z) = \sum_{j=-\sigma}^{\sigma} \alpha_j e^{i j \theta h}, \quad \text{and} \quad z = e^{i \theta h}.$$

Therefore,

$$\hat{u}^{(k+1)}(\theta) = r(z) \hat{u}^{(k)}(\theta), \quad \text{where} \quad r = \frac{Q}{P}.$$

Now if we Fourier transform the original differential equation, we get

$$\frac{\partial}{\partial t} \hat{u}(\theta, t) + -\theta^2 \hat{u}(\theta, t).$$

Therefore,

$$\hat{u}(\theta, t + \Delta t) = e^{-\theta^2 \Delta t} \hat{u}(\theta, t).$$

If we define the Courant number as $\mu = \Delta t / (\Delta x)^2$, then we need

$$r(z) \approx e^{-\theta^2 \Delta t} = e^{-\mu(\theta \Delta x)^2} = e^{\mu(\ln z)^2}.$$

If we want an approximation of the order $(\Delta x)^p = h^p$, this is equivalent to $O((z - 1)^p)$. Thus we require,

$$r(z) - e^{\mu(\ln z)^2} = O((z - 1)^p),$$

which are just the equations for Padé approximants. The Crank-Nicolson method (discussed above) gives

$$r(z, \mu) = \frac{z + \mu(z - 1)^2 / 2}{z - \mu(z - 1)^2 / 2},$$

which is an approximation of order 3. The little-known Crandall method, derivable by Padé methods, is

$$r(z, \mu) = \frac{z + \left(\frac{1}{12} + \frac{\mu}{2}\right)(z - 1)^2}{z + \left(\frac{1}{12} - \frac{\mu}{2}\right)(z - 1)^2}$$

and is of order 5, with only the same amount of work to use as for the Crank-Nicolson!

In this formalism, the stability conditions (for A -acceptability*) are that

$$|r(e^{i\theta}, \mu)| \leq 1, \quad \text{for } 0 \leq \theta \leq 2\pi,$$

which is the von Neumann condition, and the condition that $r(z, \mu)$ has an equal number of poles inside and outside the unit circle, $|z| = 1$. An additional stability condition is required for L -stability** or stiff-stability. It is

$$r(z = -1, \mu) = e^{-\pi^2 \mu} \approx 0.$$

This property is particularly important in this initiative because we are normally not much interested in the behavior of the microscopic scale and would be happy to see it die quickly and quietly so we can concentrate on the longer time scales.

Iserles has proven that all schemes based on diagonal Padé approximants are A -stable for every $\mu \in \text{cl}\{\mu \in \mathcal{C} : \text{Re}(\mu) > 0\}$. Thus Crandall's method is an A -stable (but not L -stable) one.

* A -acceptability means that no Fourier component grows in time.

** L -stability includes A -stability and in addition requires that the high-frequency components decay more and more rapidly with increasing frequency. Note that this behavior is expected from the solution given for the Fourier transform of the differential equation.

I have found the following new scheme which satisfies $r(-1, \mu) = 0$:

$$r(z, \mu) = \frac{1 + a(z-1) + b(z-1)^2 + c(z-1)^3}{1 + a(z-1) + d(z-1)^2},$$

where

$$a = 1 + \frac{\mu - \frac{1}{3}}{1 + 4\mu}, \quad b = \frac{1}{12} + \frac{\mu}{2} + \frac{\mu - \frac{1}{3}}{1 + 4\mu}, \quad c = \frac{\mu(\mu - \frac{1}{3})}{1 + 4\mu}, \quad \text{and} \quad d = b - \mu,$$

which is order 4, and both A - and L -stable, (at least for $0 \leq \mu < \infty$). It is unsymmetrical as it involves 3 spatial points at the advanced time and 4 at the current time. As it only involves the inversion of tridiagonal matrices, it is no more work than the Crank-Nicolson method, and (a) it is more accurate, order 4 versus order 3, and (b) L -stable, which Crank-Nicolson is not. Compared to the Crandall scheme, it is (a) less accurate, order 4 versus order 5, but it is L -stable.*

The key to the quick-solve methods is the Baker-Oliphant idea of a factorizable difference scheme. I will treat the Crandall scheme here. For one dimension we have explicitly

$$\begin{aligned} & \sum_{i'} \left[\left(\frac{1}{12} - \frac{\mu}{2} \right) (\delta_{i, i'+1} + \delta_{i, i'-1}) + \left(\frac{5}{6} + \mu \right) \delta_{i, i'} \right] u_{i'}^{n+1} \\ &= \sum_{i'} \left[\left(\frac{1}{12} + \frac{\mu}{2} \right) (\delta_{i, i'+1} + \delta_{i, i'-1}) + \left(\frac{5}{6} - \mu \right) \delta_{i, i'} \right] u_{i'}^n + O((\Delta x)^6), \end{aligned}$$

where u_i^n is an exact solution of $\partial^2 u / \partial x^2 = \partial u / \partial t$.

For 2 dimensions, we have

$$\begin{aligned} & \sum_{i', j'} \left[\left(\frac{1}{12} - \frac{\mu}{2} \right) (\delta_{i, i'+1} + \delta_{i, i'-1}) + \left(\frac{5}{6} + \mu \right) \delta_{i, i'} \right] \\ & \times \left[\left(\frac{1}{12} - \frac{\mu}{2} \right) (\delta_{j, j'+1} + \delta_{j, j'-1}) + \left(\frac{5}{6} + \mu \right) \delta_{j, j'} \right] u_{i', j'}^{n+1} \\ &= \sum_{i', j'} \left[\left(\frac{1}{12} + \frac{\mu}{2} \right) (\delta_{i, i'+1} + \delta_{i, i'-1}) + \left(\frac{5}{6} - \mu \right) \delta_{i, i'} \right] \\ & \times \left[\left(\frac{1}{12} + \frac{\mu}{2} \right) (\delta_{j, j'+1} + \delta_{j, j'-1}) + \left(\frac{5}{6} - \mu \right) \delta_{j, j'} \right] u_{i', j'}^n + O((\Delta x)^2), \end{aligned}$$

where again $u_{i, j}^n$ is an exact solution of the partial differential equation, and we have taken $\Delta y = O(\Delta x)$ and $\Delta t = \mu(\Delta x)^2$. This is a 9-point difference scheme.

* This scheme has some practical drawbacks. Subsequently the speaker has devised better schemes based on the idea of the quadratic (Padé) approximant, at least for spatial dimension less than five.

The same product method works for $d = 3, \dots$ and the equations

$$B_{l,m,n}^{i,j,k} \theta_{i,j,k}^{\nu+1} = A_{l,m,n}^{i,j,k} \theta_{i,j,k}^{\nu}$$

factor as

$$\hat{B}_l^i \bar{B}_m^j \tilde{B}_n^k \theta_{i,j,k}^{\nu+1} = A_{l,m,n}^{i,j,k} \theta_{i,j,k}^{\nu},$$

where \hat{B} , \bar{B} , and \tilde{B} are each tridiagonal matrices and can be solved by the usual factorization method followed by forward and back substitution:

$$\begin{pmatrix} a_1 & a_2 & 0 & \dots \\ c_2 & a_2 & b_2 & \dots \\ 0 & c_3 & a_3 & \dots \\ \vdots & \vdots & \vdots & \ddots \end{pmatrix} = \begin{pmatrix} \alpha_1 & 0 & 0 & \dots \\ \gamma_2 & \alpha_2 & 0 & \dots \\ 0 & \gamma_3 & \alpha_3 & \dots \\ \vdots & \vdots & \vdots & \ddots \end{pmatrix} \begin{pmatrix} 1 & \beta_1 & 0 & \dots \\ 0 & 1 & \beta_2 & \dots \\ 0 & 0 & 1 & \dots \\ \vdots & \vdots & \vdots & \ddots \end{pmatrix}$$

The number of operations in this solution method is of the order of the number of mesh points used, in any number of dimensions.

I have programmed this procedure for the $D = 2$ case. It runs as advertized. One sample run was on a 700×700 mesh which has approximately 0.5×10^6 mesh points. It was advanced 300 time steps. For $\mu \approx 1166$, the dominant mode decays by a factor of $10^{-1/49}$ per time step. It ran just fine, but with μ this large, the time scale is distorted. It takes about 8 microseconds per cycle point on a SPARC 20 (or a Pentium 90 PC).

There are various generalizations which are straightforward to implement. Adding a constant times θ and a source term is simple. Generalization involving a nonconstant factor, nonlinearity, a variable diffusion constant, etc., usually require the addition of a small iteration loop at each time step. The cases the speaker had tried required about 15 iterations initially, but this number decreased to about one or two at large times.

Presentation by Gregory Beylkin (Applied Mathematics, University of Colorado)

Title: A Multiresolution Strategy for Reduction of PDEs and Eigenvalue Problems

The work reported here was done jointly with Nicholas Coult. The speaker said that in the homogenization problem, the coefficients of the partial differential equations (PDEs) change across many scales, and the influence of the fine scales on a coarse scale is nonlinear. The approaches in classical homogenization theory have been formal asymptotics using small parameters and weak limits. Here multiresolution homogenization will be discussed. Instead of the classical requirement of a small parameter or a weak limit, the present approach studies the transition between two adjacent scales. For this method to work well there must be a "preservation of form" and fast algorithms. The only requirement on the "form of the equations" is that it is such that it may be used recursively.*

* This idea is at the heart of the renormalization group approach, where the smallest scales are successively eliminated and the equations governing the larger scales are modified appropriately.

Beylkin next began a formal description of his multiresolution analysis. Consider a chain of subspaces,

$$\dots \subset \mathcal{V}_2 \subset \mathcal{V}_1 \subset \mathcal{V}_0 \subset \mathcal{V}_{-1} \subset \mathcal{V}_{-2} \dots, \quad \bigcap_j \mathcal{V}_j = \{0\} \text{ and } \overline{\bigcup_j \mathcal{V}_j} = L^2(\mathcal{R}^d).$$

In addition he defined the “detail” subspaces by

$$\mathcal{V}_{j-1} = \mathcal{V}_j \oplus \mathcal{W}_j \quad \text{i.e.,} \quad \mathcal{W}_j = \mathcal{V}_{j-1} \setminus \mathcal{V}_j.$$

The next important concept which he introduced is the nonstandard representation of operators. To this end, consider the projection operators, P_j which projects onto \mathcal{V}_j and Q_j which projects onto \mathcal{W}_j . If we are given the operator S , we can define from it the operators

$$S_j = P_j S P_j,$$

$$A_{S_j} = Q_{j+1} S Q_{j+1}, \quad B_{S_j} = Q_{j+1} S P_{j+1}, \quad C_{S_j} = P_{S_j} S Q_{j+1}, \quad \text{and} \quad T_{S_j} = P_{j+1} S P_{j+1}.$$

Note that $T_{S_j} = S_{j+1}$. If we use the identities

$$S_0 - S_n = \sum_{j=1}^n (S_{j-1} - S_j), \quad \text{and} \quad P_{j-1} = P_j + Q_j,$$

then we have

$$S_0 - S_n = \sum_{j=0}^{n-1} (A_j + B_j + C_j).$$

Next suppose that $S_j \vec{x} = \vec{f}$, then we can express this equation as

$$\begin{pmatrix} A_{S_j} & B_{S_j} \\ C_{S_j} & T_{S_j} \end{pmatrix} \begin{pmatrix} \vec{d}_x \\ \vec{s}_x \end{pmatrix} = \begin{pmatrix} \vec{d}_f \\ \vec{s}_f \end{pmatrix}.$$

The name \vec{s} is for the smoothed part, and the name \vec{d} is for the detailed part. The variables \vec{d}_x may be formally eliminated so that the above equation becomes

$$R_{S_j} \vec{s}_x = \vec{s}_f - C_{S_j} A_{S_j}^{-1} \vec{d}_f, \quad R_{S_j} \equiv \left(T_{S_j} - C_{S_j} A_{S_j}^{-1} B_{S_j} \right).$$

In the case the S_j are finite matrices, R_{S_j} is also a matrix with $\frac{1}{4}$ times as many elements as S_j had, so the number of unknowns is reduced and the form is preserved.*

* To make more transparent what is going on here, consider the 8×8 matrix

$$S_j = \begin{bmatrix} -2 & 1 & 0 & 0 & \dots \\ 1 & -2 & 1 & 0 & \dots \\ 0 & 1 & -2 & 1 & \dots \\ 0 & 0 & 1 & -2 & \dots \\ \vdots & \vdots & \vdots & \vdots & \ddots \end{bmatrix}.$$

The speaker then reported some general results that he and his coworkers have obtained. First, there was theorem on the preservation of spectral bounds:

THEOREM 1. *Let S_j be a self-adjoint positive-definite operator on \mathcal{V}_j ,*

$$m\|\vec{x}\|^2 \leq (S_j\vec{x}, \vec{x}) \leq M\|\vec{x}\|^2, \quad \forall \vec{x} \in \mathcal{V}_j,$$

where $0 < m \leq M \leq \infty$. Then

$$R_{S_j} = R_{S_j}^\dagger, \quad \text{and} \quad m\|\vec{x}\|^2 \leq (R_{S_j}\vec{x}, \vec{x}) \leq M\|\vec{x}\|^2, \quad \forall \vec{x} \in \mathcal{V}_{j+1}.$$

Next Beylkin discussed the case of a matrix version of the nonstandard representation. Suppose that A_j, B_j, C_j, T are represented by the matrices, $\alpha^j, \beta^j, \gamma^j, \tau^j$ with the matrix elements,

$$\begin{aligned} \alpha_{k,k'}^j &= \int \int K(x, y) \psi_{j,k}(x) \psi_{j,k'}(y) dx dy, \\ \beta_{k,k'}^j &= \int \int K(x, y) \psi_{j,k}(x) \phi_{j,k'}(y) dx dy, \\ \gamma_{k,k'}^j &= \int \int K(x, y) \phi_{j,k}(x) \psi_{j,k'}(y) dx dy, \quad \text{and} \\ \tau_{k,k'}^j &= \int \int K(x, y) \phi_{j,k}(x) \phi_{j,k'}(y) dx dy, \end{aligned}$$

where the ψ 's span \mathcal{W}_j and the ϕ 's span \mathcal{V}_j , $K(x, y)$ is the kernel of T_{j-1} and satisfies the conditions

$$|K(x, y)| \leq \frac{1}{|x - y|}, \quad |\partial_x^M K(x, y)| + |\partial_y^M K(x, y)| \leq \frac{C_0}{|x - y|^{1+M}},$$

The nonzero diagonals wrap around, so that the matrix is a circulant. If we transform \vec{x} into the Haar basis, $d_1 = (x_1 - x_2)/\sqrt{2}$, $s_1 = (x_1 + x_2)/\sqrt{2}$, $d_2 = (x_3 - x_4)/\sqrt{2}$, $s_2 = (x_3 + x_4)/\sqrt{2}$, ..., then the above $2n \times 2n$ matrix transforms into the $n \times n$ matrix

$$R_{S_j} = \begin{bmatrix} -\frac{48}{17} & -\frac{1}{2} & -\frac{3}{17} & -\frac{1}{3} \\ -\frac{1}{2} & -\frac{17}{48} & -\frac{2}{17} & -\frac{17}{3} \\ -\frac{3}{17} & -\frac{1}{2} & -\frac{48}{17} & -\frac{1}{2} \\ -\frac{1}{2} & -\frac{3}{17} & -\frac{1}{2} & -\frac{48}{17} \end{bmatrix},$$

which illustrates for $n = 4$ that the circulant form is preserved, but not the number of nonzero diagonals.

The first matrix is the standard difference representation of $\Delta x^2 \frac{d^2}{dx^2}$ with periodic boundary conditions. The reduced matrix represents $-\frac{37}{17} + \Delta x^2 (\frac{1}{2} \frac{d^2}{dx^2} + \frac{12}{17} \left\{ \frac{d^2}{dx^2} \right\}_2)$, where $\left\{ \frac{d^2}{dx^2} \right\}_2$ is the difference operator over an interval of $2\Delta x$ instead of Δx .

as well as a “weak cancellation condition,”

$$\left| \int_{I \times I} K(x, y) dx dy \right| \leq C|I|,$$

for all dyadic intervals I . With these preliminaries, he gives a theorem on the rate of decay of the representation for the nonstandard form.

THEOREM 2. *If the wavelet* basis has M nonvanishing moments, then for any K satisfying the above named conditions, the matrices $\alpha^j, \beta^j, \gamma^j, \tau^j$ satisfy*

$$|\alpha_{k,k'}^j| + |\beta_{k,k'}^j| + |\gamma_{k,k'}^j| \leq \frac{C_M}{(1 + |k - k'|)^{M+1}}$$

for all integers k, k' .

The next theorem tells us that this estimate for the rate of decay is also satisfied by the matrix representing the reduced operator, R .

THEOREM 3. *Let us assume that the operator T and the wavelet basis satisfy the conditions of Theorem 2. Let R_j be the reduced operator on some scale j , where the reduction started on some scale n , $n \leq j$ for $n, j \in \mathcal{Z}$, and let $A_{R_j}, B_{R_j}, C_{R_j}$ be its blocks. Then the bi-infinite matrices $\alpha^{r,j}, \beta^{r,j}$ and $\gamma^{r,j}$ representing these blocks satisfy*

$$|\alpha_{k,k'}^{r,j}| + |\beta_{k,k'}^{r,j}| + |\gamma_{k,k'}^{r,j}| \leq \frac{C_M}{(1 + |k - k'|)^{M+1}}$$

for all integers k, k' .

These theorems demonstrate the importance of using high-order wavelets in the reduction procedure. They show that the nonstandard form for a wide class of operators has fast off-diagonal decay and that the rate of decay is controlled by the number of vanishing moments of the wavelet basis. These theorems also show that the reduction procedure preserves the rate of decay on all scales and therefore results in sparse matrices for computational purposes.

At this point, Beylkin said that the LU -decomposition, i.e., the factoring of the matrix into a low-left triangular and an upper-right triangular matrix provides a fast algorithm

* For those people who are not familiar with wavelets: Like the Fourier transform, the discrete wavelet transform is a linear operation which changes the basis vectors in the vector space. There are, of course, extensions to infinite dimensional spaces. The wavelet transforms are invertible and orthogonal. What makes a wavelet basis interesting is that individual wavelet functions are quite localized in space and have a characteristic scale. The whole set of wavelets runs through the whole range of scales. Their advantage is that the large class of computations which take advantage of sparsity become computationally fast in an appropriate wavelet basis. A wavelet transformation maps a vector into a smooth part and a detailed part. The transformation has the property that a constant, a linear term, and so on, up to the “order” of the wavelet transformation contribute zero to the detailed part.

for the reduction process. By fast he means of $O(N)$ or $O(N \ln N)$ for an $N \times N$ matrix. The reason this order is obtained was said to be because of the sparsity of the original matrix of this character. Presumably, there are only of order N non-negligible elements by the above theorems. When the matrix is factored in this way, it is a straightforward identity that the product of the lower-right block of L times the lower-right block of U is just the reduced matrix, R , we have seen before. He also remarked at this point that the multigrid method, dear to the hearts of some in the audience, is an iterative method and that wavelets give a direct method. He also claimed that the wavelet methods work in higher dimensions.

Turning to the eigenvalue problem, Beylkin showed how his methods were applicable for the positive definite, self-adjoint case. He considered

$$\begin{pmatrix} A_{S_j} & B_{S_j} \\ B_{S_j}^\dagger & T_{S_j} \end{pmatrix} \begin{pmatrix} \vec{d} \\ \vec{s} \end{pmatrix} = \lambda \begin{pmatrix} \vec{d} \\ \vec{s} \end{pmatrix}.$$

By use of the reduction process, we can rewrite this equation as

$$T_{S_j} \vec{s} = \lambda \vec{s} + B_{S_j}^\dagger G(\lambda) B_{S_j} \vec{s},$$

where

$$G(\lambda) = (A_{S_j} - \lambda I)^{-1}, \quad G(\lambda) - G(0) = \lambda G(\lambda) G(0), \quad \text{and} \quad G(0) = A_{S_j}^{-1}.$$

Thus, using the definition of R_{S_j} we obtain

$$\begin{aligned} R_{S_j} \vec{s} &= \lambda \vec{s} + \lambda B_{S_j}^\dagger A_{S_j}^{-1} G(\lambda) B_{S_j} \vec{s}, \quad \text{and} \\ R_{S_j} \vec{s} &= \lambda \left(I + B_{S_j}^\dagger A_{S_j}^{-2} B_{S_j} \right) \vec{s} + \lambda^2 B_{S_j}^\dagger A_{S_j}^{-2} G(\lambda) B_{S_j} \vec{s}. \end{aligned}$$

These results suggest three approximations to the eigenvalue equations,

$$T_{S_j} \vec{s} = \lambda_T \vec{s}, \quad R_{S_j} \vec{s} = \lambda_R \vec{s}, \quad \text{and} \quad L_{S_j}^{-1} R_{S_j} (L_{S_j}^\dagger)^{-1} \vec{z} = \lambda_Y \vec{z},$$

where L_{S_j} is a lower-left triangular matrix obtained by Cholesky decomposition as

$$I + B_{S_j}^\dagger A_{S_j}^{-2} B_{S_j} = L_{S_j} L_{S_j}^\dagger, \quad \text{and} \quad \vec{z} = L_{S_j}^\dagger \vec{s}.$$

The last result is for what he calls a modified reduced operator. It preserves better accuracy for the smaller eigenvalues. Beylkin now relates a theorem which quantifies the errors in these approximations.

THEOREM 4. *Given an eigenvector x of S_j such that $S_j x = \lambda x$, $\|x\|_2 = 1$, $d = Q_{j+1} x$, and $\|d\|_2^2 \ll \frac{1}{2}$, there exist real $\lambda_T, \lambda_R, \lambda_Y$ as defined above, such that*

$$\begin{aligned} |\lambda_T - \lambda| &\leq C_d \|B_{S_j}\|_2 \|d\|_2, \quad |\lambda_R - \lambda| \leq C_d \|B_{S_j}\|_2 \|d\|_2 \left(\frac{\lambda}{m_A^j} \right), \\ |\lambda_Y - \lambda| &\leq C_d \|B_{S_j}\|_2 \|d\|_2 \left(\frac{\lambda}{m_A^j} \right)^2, \end{aligned}$$

where

$$C_d = \frac{3 - \|d\|_2^2}{\sqrt{1 - \|d\|_2^2}}, \quad \text{and} \quad \|x\|^2 m_A^j \leq (A_{S_j} x, x)$$

defines m_A^j .

It was explained that the splitting of the eigenvalue spectrum induced by the reduction process leaves the large eigenvalues with A_{S_j} and the small ones with R_{S_j} so that, for low-lying states of S_j , the ratio λ/m_A^j is quite small and thus the second and third approximations show progressively greater improvement.

The speaker then showed some examples of the results of these procedures on an original $1,024 \times 1,024$ matrix representation of the operator

$$\frac{d}{dx}(2 + \cos \pi n x) \frac{d}{dx}.$$

For a single reduction procedure using wavelets with 12 vanishing moments, the three approximate results became more accurate than his computational accuracy limit of about 10^{-12} for the first 64, 100, and 130 eigenvalues respectively. For the results after four reductions (leaving just a 64×64 matrix) the same accuracy with λ_R was obtained for the first 14 eigenvalues. The importance of using higher-order wavelets was also demonstrated by showing how much more poorly the fourth and eighth order versions did. Further results using random coefficients were shown. Here, while there is a similar pattern, the obtained accuracy is not so great, as might have been expected. These methods effectively obtain a fast algorithm for computing small eigenvalues of elliptic operators in $O(N)$ operations, which N is the size of the discretization on the finest scale.

Finally, the speaker showed us a diagram of how sparse a waveletized matrix gets for the kernel $1/\tan(\theta_i - \theta_j)$. One point of the bounds on the size of the matrix elements is that it eliminates having to compute the elements where they are known, *a priori*, to be insignificant. Timing tables were given for several examples. They showed, particularly for $N \gtrsim O(100)$, very significant speedups compared to the standard direct methods.

Presentation by David Kinderlehrer (Carnegie Mellon University)

Title: Variational Methods for Understanding Meso- and Microstructure in Nonlinear Solids

In this lecture, the speaker used the term microstructure for what we have been customarily calling mesostructure, and mesostructure for what we basically have regarded as macroscopic structure. Please bear these notational differences in mind as in these notes I will use his terminology. His approach is to start with equations which describe what we have been calling macroscopic behavior and to try to incorporate features into them which relate to microscopic features of the system in order to attempt to produce a description of mesoscopic behavior.

To start with, we saw a slide intended to illustrate what was meant by microstructure. It showed what appeared to be a crystalline solid filled with many grains having one or another of several distinct orientations. He then propounded the question “what can we

know about microstructure?” with the unstated but implied limitation on the level of detailed calculations that can be included in his frame of reference. He was interested in devising a consistent framework which can suggest limitations on the microstructures for specific materials and can accommodate interactions among length scales. In particular, he was thinking of reversible phase transitions, such as a crystal which can be oriented with its long axis back and forth or side to side equally well, and a concomitant dramatic response to small loads. He said the issue was to describe the average picture while capturing essential energetic and kinematic properties. He showed pictures on a slide which illustrated an extremely lumpy energy surface in “configuration space.” In his view, reversible phase transitions were movements between different energy minima of equal energy.

He next spent a little time on a phenomenological theory based on lattice considerations. Here the language employed is that of continuum mechanics. The stored energy is denoted by $W(\overleftrightarrow{F}, \theta)$, where $\overleftrightarrow{F} = \overleftarrow{\nabla} \vec{y}$ is the deformation gradient and y is the deformation of the original space Ω , and θ is the temperature. He expresses frame indifference and symmetry by the relation $W(\mathbf{Q} \overleftrightarrow{F} P, \theta) = W(F, \theta)$, where \mathbf{Q} refers to a rotation of the Cartesian coordinate frame and $P \in \mathbf{P}$ is a member of the symmetry group of the crystal and refers to invariance under such a transformation. In this theory, the energy surface in the nine-dimensional \overleftrightarrow{F} space changes as a function of temperature going, for example, from a single minimum for a configuration corresponding to a simple cubic lattice to an energy surface corresponding to multiple minima at low temperatures. The potential well structure is such that the existence of a transformation strain U_1 implies the existence of a set of strains, $\{U_i\}$, given by $P^T U_1 P$ for all $P \in \mathbf{P}$, and in turn to the potential wells $SO(3)U_i$. So $W(\overleftrightarrow{F}, \theta) = \min W = 0$ exactly on $\cup SO(3)U_i$ which leads to a very rough and nonconvex energy surface. So far, the speaker said, there is still missing in his picture, surface energy (on grain boundaries, for example), more details for the finer structure of the Bravais lattice, polarizations, magnetizations, shifts, *etc.*

To make progress in this framework, the speaker next introduced a variational framework, and his notion of weak convergence (which seems to be that the sequence tends to a limit cycle rather than to an individual limit). If y^k is a “minimizing sequence,” then using a device of Y. L. Young from control theory for representing measures for the local spatial averages of the minimizing sequence, he obtains a family of probability measures, $\nu = (\nu_x)_{x \in \Omega}$ which are the density distribution of values of the deformation gradient. When one determines the minima of the energy density W according to the crystallography of the material, then it leads to a variational condition for the minimizing sequence, *e.g.*,

$$\overleftarrow{\nabla} \vec{y}^k \rightarrow \overleftarrow{\nabla} \vec{y},$$

$$\int_{\Omega} W(\overleftarrow{\nabla} \vec{y}^k) dx \rightarrow \inf_A \int_{\Omega} W(\overleftarrow{\nabla} \vec{\eta}) dx = |\Omega| \min W.$$

Now we also have

$$\int_{\Omega} \int_M W(\overleftrightarrow{\lambda}) d\nu_x(\overleftrightarrow{\lambda}) = |\Omega| \min W \Rightarrow \text{support}(\nu) \subset \{W = \min W\},$$

which is a variational condition and says in the speaker's words that "the only set that can be charged by this measure lives in the bottom of the potential wells."

Some quantities are continuous with respect to this weak convergence, so there are equations between the limit of a function and the function of the limit. For example,

$$\overleftarrow{\nabla} \vec{y} = \int_M \overleftrightarrow{\lambda} \, d\nu_x(\overleftrightarrow{\lambda}), \quad \text{adj } \overleftarrow{\nabla} \vec{y} = \int_M \text{adj } \overleftrightarrow{\lambda} \, d\nu_x(\overleftrightarrow{\lambda}), \quad \det \overleftarrow{\nabla} \vec{y} = \int_M \det \overleftrightarrow{\lambda} \, d\nu_x(\overleftrightarrow{\lambda}),$$

as well as some relations involving the minors of these determinants. These results together with the variational conditions were reported to give extremely strong restrictions on the deformations which can participate in a microstructure.

At the end of the lecture, the speaker presented some examples in orthorombic CuAlNi and terfenol-D. The twinning relation of the crystallographic theory of martensite was discussed.

Presentation by Misha Shashkov

Title: High-Quality, Finite-Difference Schemes for PDE's

The motivation for this approach is that a great many of the equations of practical mathematical physics can be expressed in terms of the differential operators, div , grad , curl . These operators have certain invariance properties whose preservation is important so that the solutions of the equations preserve various physically relevant properties. Among these might be conservation of energy and momentum, symmetries of the solution, and non-divergence of particular fields.* The plan is to develop a theory of the discrete analog of vector analysis. The discrete versions of the first order operators will be denoted as DIV , GRAD , CURL . The sort of applications that are envisioned are to the heat equation, magnetic fields, Langvin gas, gas dynamics in Eulerian form, Lagrangian fluid dynamics, and porous media flow.

The basis of the analysis in the construction of the discrete version of vector and tensor analysis is the idea of the preservation of certain identities. Various types of grids are considered in 2 and 3 dimensions, namely, logically rectangular grids, triangular and Voronoi grids, and rectangular grids with local refinement. Use is made of the notions of the discrete analogs of line integral, potential vector, flux of a vector through a surface, and the circulation of a vector along a contour.** The procedure is to introduce a definition of, say, GRAD which is called the "prime operator", and from it to construct, by insisting that Gauss' theorem holds, DIV . In a similar manner, by insisting that Stokes' theorem holds, one may construct CURL . There is a problem when one tries to compose the first order operators in a straightforward way to get, say, grad div . For example, the natural range of DIV is cell-centered values and the natural domain of GRAD is nodal values. Thus one

* For other important preservation property considerations, see the first two presentations in this section.

** This approach bears some relation to Courant's approach to calculus. Courant takes the integral as fundamental and the derivative as a deduced concept.

cannot in a natural way compose these two operations. In addition, the operators satisfy, for example, the identity,

$$\int_V \phi \operatorname{div} \vec{W} dV + \int_V \vec{W} \cdot \vec{\operatorname{grad}} \phi dV = \oint_{\partial V} \phi \vec{n} \cdot \vec{W} dS,$$

which is a version of integration by parts, and where V is an arbitrary volume, ϕ and \vec{W} are arbitrary scalar and vector functions, ∂V is the surface of V , and \vec{n} is its normal vector. The discrete analog of this identity and the discrete analog of other such integral identities are used to derive discrete versions of the second order operators. All of these operators, as well as the nonprime, first-order operators are called derived operators.*

An illustration in one dimension was given of how the definition of DIV when substituted into the above identity leads to a definition of GRAD:

$$\sum p_{i,j} (\operatorname{DIV} \vec{W})_{i,j} + \sum_{i,j} (\vec{W} \cdot \operatorname{GRAD} p)_{i,j} V_{i,j} = \sum_{\text{boundary}} p_{i,j} (\vec{W} \cdot \vec{n})_{i,j} S_{i,j}.$$

The first term on the left-hand side can be re-expressed as

$$\begin{aligned} \sum p_{i+\frac{1}{2}} \left(\frac{u_{i+1} - u_i}{h_{i+\frac{1}{2}}} \right) h_{i+\frac{1}{2}} &= \sum (p_{i+\frac{1}{2}} u_{i+1} - p_{i+\frac{1}{2}} u_i) = \\ &= \sum (p_{i-\frac{1}{2}} - p_{i+\frac{1}{2}}) u_i + \text{boundary terms,} \end{aligned}$$

so the representation for $\operatorname{GRAD} p$ is taken to be $p_{i-\frac{1}{2}} - p_{i+\frac{1}{2}}$. The need to know how to approximate the divergence of tensors was mentioned.

The application to Lagrangian fluid dynamics was discussed. It was reported that conservative finite-difference schemes will be constructed that will be free from nonphysical grid distortions of cells such as "hourglassing," "herringbone," and "geometrical error," which can lead to the overlapping of grid cells or to decreasing accuracy. Examples of the computer results for the "bubble problem" were shown.** The use of artificial viscosity was mentioned. Various other applications were also discussed.

* There are yet other difficulties. The speaker points out that one cannot define CURL so that the orthogonal decomposition of vector fields $\vec{A} = \operatorname{GRAD} \phi + \operatorname{CURL} \vec{B}$, $\operatorname{DIV} \operatorname{CURL} \equiv 0$, and $\operatorname{CURL} \operatorname{GRAD} \equiv 0$ all hold simultaneously. Thus the definition of the derived operators is not unique, but it depends on which of the identities hold and which do not.

** The famous bubble problem is described in a previous footnote. Does it really become a torus? The reported results stopped short of torus time.

8. Applications

First Presentation by Bryan Travis

In environmental science, there are a number of scales. There is the macroscopic scale, which is measured in kilometers. There is interest in diffusion and permeability over scales of this size. For example, there are spills of various organic pollutants, such as oil or a solvent like CCl_4 . It is of interest how fast these spills permeate the ground. The ground itself has many layers, and the penetration of the aquifer is of particular interest. There appear to be two mesoscopic scales in this problem. One scale is the pore size (μm 's) in soil-like materials, and the other scale is an unusually large one, *i.e.*, the laboratory scale (cm's). In addition of course, there is the microscopic scale, which is approximated here by flow equations, so there was no explicit reference to this scale. In this area, there is interest in the structure over a wide range of scales, from micrometers to tens of kilometers. The data sampling is usually sparse, and the workers in this area have not been able to give analytic solutions to their model equations. As we saw in the ocean model problems* subgrid dynamics is important here as well. In addition, the problems of non-Fickian (not \sqrt{t}) diffusion and scale-dependent dispersion occur.

The governing equations concern the flow or movement of water, air, *etc.*, in bulk materials. There is the case of saturated (the space between the grains is filled with water) material where the governing equation is

$$\vec{\nabla} \cdot \bar{k}(\bar{x}) \vec{\nabla} \bar{p} = \dot{s},$$

where k is the permeability, p is the pressure, the overbar denotes a local average, and the overdot is the time derivative. Extreme examples of the various types of media considered might be sand and fractured granite. In the case of “unsaturated” systems, we denote the fractional degree of saturation by σ and the equations are

$$\frac{\partial(\epsilon\bar{\sigma})}{\partial t} - \vec{\nabla} \cdot \left(\frac{k(\bar{\sigma})}{\mu} \right) (\vec{\nabla} \bar{p}_c(\bar{\sigma}) + \vec{g}) = \dot{s},$$

where now k is the relative permeability and p_c is the capillary pressure. The transport equations for following species are

$$\frac{\partial(\epsilon\bar{\sigma}\bar{C})}{\partial t} + \vec{\nabla} \cdot \vec{u}\bar{C} = \vec{\nabla} \cdot D^* \vec{\nabla} \bar{C} + R(\bar{C}),$$

where D^* is the dispersion and C is the solubility.

The quantities involved, \bar{k} , $\bar{\sigma}$, \bar{p} , D^* *etc.*, can be obtained from theoretical models and laboratory or field experiments. There are various approaches to the problem of modeling porous media. One approach is to treat it like a bundle of tubes. Another approach is to consider it in terms of a representative elementary volume. Yet another is to study the correlation functions between velocity and fluctuations. Then again there is dual porosity,

* See the discussion by M. Hyman, Section 3.

dual permeability (for fractures), and finally there is explicit modeling using, for example, the lattice Boltzmann method run on the CM5. Various slides were shown illustrating the behavior of some of these quantities. The capillary pressure used in the above equations was displayed in crushed tuff and increases as the degree of water saturation decreases. The argument given was that when there is no capillary pressure then there is complete saturation as there are no capillary surfaces. The opposite limit of zero saturation was not discussed. Consequently, the permeability of water increases with increasing saturation, while that of air decreases. Dispersivity increases with scale for reasons which were not made clear to me. Most of the current theories assume a “simple” system. However, environmental concerns, such as oil recovery, agriculture, *etc.*, involve (i) multiphase flow, (ii) thermal effects, (iii) chemistry, (iv) bacterial action, and (v) physical effects such as colloids, flocs, porosity and permeability alterations, *etc.*

A key feature here from the multiscale competency point of view is that each of these phenomena acts primarily at some particular length and time scale, but its effects couple into the other scales. It is a question of general interest how these types of effects propagate to the other scales.

An interesting discussion was given of the mid-ocean ridge hydrothermal systems. These are of considerable environmental interest for several reasons. First and foremost, it was said that one-quarter of the earth’s energy comes up through the mid-ocean ridges! In addition, there is the influence on the geochemistry of the sea floor and deposition of minerals on and beneath the sea floor. The computations reported were in the magma and its earthen overlayer. As the magma rises, it mixes with the silicate material of the sea floor, and there develop little plumes of porosity. This effect is a result of the silica chemistry, which makes a significant difference as was illustrated in a slide.

Finally, we heard a brief discussion of stochastic modeling in hydrology. The concern is the prediction of ground water and contaminant flow with at best highly imperfect knowledge of the spatial distribution of the hydraulic conductivity. The goal of these efforts was described as the deduction of the hydraulic head or the concentration covariance from the estimated hydraulic conductivity covariance. Monte Carlo and perturbation methods have been used. In 1984 Cushman proposed that the covariance structure of heterogeneities depends on the scale of observation. Results on forward transport solutions at just two scales were shown. An attempt to compare the results of computations with experiments was reported. An actual oil-saturated sandstone was thin-sliced and put in a glass sandwich. The geometry of the pore space was taken directly from a digitized photomicrograph. Computations were made on this geometry and compared with the introduction of a slug of water into the system.

Second Presentation by Bryan Travis

This talk began with a brief review of the speaker’s earlier August 19, 1994, talk for the benefit of those present who had missed that talk.*

Travis said that his group works on the numerical modeling of flow and transport in complex media, enhanced oil recovery, and the cleanup of subsurface contamination.

* See the immediately preceding presentation for this background information.

Unsolved or partially solved problems in the area of porous media are the following: (i) structure at all scales, (ii) stochastic models, and how to integrate them, (iii) multi-phase constitutive relations, (iv) complex processes involving chemical, biological and/or physical (e.g., flocculation) features, (v) faster, more accurate solutions for ADR (advection-diffusion-reaction) equations and nonlinear differential equations with multiple time scales and variable coefficients, (vi) inverse problems (i.e., given the flow, what is the structure?), (vii) optimization of resource use in the presence of uncertainty, and (viii) what are the fundamental governing equations—Darcy’s law ($\vec{u} = -(k/\mu)\vec{\nabla}P$) vs other approaches, e.g., that of W. Gray.

In the complex process problems there can be feedback, from other features, which affects the porosity structure, thereby causing considerable complication. In the numerical simulation of an oil reservoir, a finite element method is used. Each cell is 1 to 10 meters in size, roughly, and tens of thousands of cells are used. Even so, the size of the some relevant aspects of the structure is smaller than the grid size.*

The various scales in this problem are the pore size (μm), the laboratory size (cm) and the field size (km). Flow here refers to the movement of water, air, and sometimes oil through the bulk material. The transport equations are

$$\frac{\partial(\epsilon\bar{\sigma}\bar{C})}{\partial t} + \vec{\nabla} \cdot \vec{u}\bar{C} = \vec{\nabla} \cdot D^*\vec{\nabla}\bar{C} + R(\bar{C}),$$

where the overbar denotes a local average, t is time, \vec{u} is the velocity field, D^* is the dispersion, and C is the solubility. There was considerable discussion about D^* which enters the equation as if it were a diffusion term. It was explained that in the language of this specialty, diffusion refers to molecular diffusion, and that the dispersion is a turbulent diffusion by the pores and grains, and that this dispersive process is just modeled by a diffusion-like term. There have been a lot of laboratory studies of dispersion. $D_{||}$ will denote the observed dispersion, and D_d will denote the molecular diffusion. Further, we define the Pecklet number, $Pe = ud/D_d$. We saw a log-log plot of $D_{||}/D_d$ vs Pe . The results were apparently well fit by

$$\frac{D_{||}}{D_d} \approx A Pe + 1,$$

where A is a constant, for *nice* materials. For heterogeneous materials, one requires a “diffusion tensor.”

The question was raised as to what were the major phenomena, what was the problem to be solved. The answer was to clean up contaminates, and to do so one needs to know where the contaminate plume is going and what its structure is. Heterogeneity is a major problem. Stochastic modeling is used, and the results from many runs are analyzed. An example was given of forward transport under a pressure gradient. Fingering was evident in the flow. This behavior creates a sampling problem as one can be seriously misled if the test bore lies between the fingers, and somewhat misled if it hits a finger.

* We have seen this problem in other contexts. See the presentation of Mac Hyman, Section 3.

The various relevant properties seem to vary depending on the scale on which they are measured.* Pump test wells, slug test wells, core samples, air permeability measurements, and geologic mapping were mentioned as approaches to this problem. In order to treat computationally the embedding of multiple scales of heterogeneity, an approach of multi-level grid refinement is being used.

Another problem encountered in this work is that of multiple phases. The two-phase case is not too bad as only about three coefficients are needed to fit the constitutive relations to an adequate extent for their purposes. In the case of three phases, around twenty coefficients are required. One problem of concern to the speaker's group is an air-water-gas-oil system. The approach they have used to treat these systems is (1) measure a few values and interpolate and (2) to interpolate between phases.

The problem of the fundamental governing equations is not as straightforward as one might think. Consider for example a system composed of water, air, and rock granules. Because of surface tension, drops of water stick to the surfaces of the rock granules, which, depending on the previous state of the system and the velocity of flow of the air through the system, may open or close various passageways to the flow of air. Thus, according to Bill Gray of Notre Dame, whose approach is based on first-principles thermodynamics, the dynamics depend not only on A , the interfacial area (per unit volume at the local spot), and the volume fraction of water, but also on how the water is distributed in the pores. A lattice Boltzmann approach is being tried to compare with Gray's theory. The "Lattice Boltzmann Permeabilitymeter" is a joint project with Mobil Oil and is the winner of a 1994 R & D 100 award.

An interesting example was described of an approach to clean up TCE (tri-chloro-ethelene) contamination of an air-water-rock system. It seems that there is a certain bacterium which metabolizes methane. In the process, it produces mmo; however mmo also decomposes TCE. The scheme is to introduce the bacterium, and to pump in methane, which stimulates the production of mmo, and the excess mmo decomposes the TCE.

In order to study this sort of problem numerically, a numerical code for bioremediation simulations was developed called TRACR3D with Microbial Processes or TRAMP. The general layout of the transport differential equations is

$$\begin{aligned} \mathcal{L}_i(C_i) \equiv & \frac{\partial[C_i(\epsilon\sigma + \epsilon f H^i) + \rho_b C_{si}]}{\partial t} + \vec{\nabla} \cdot [(\vec{u}_w + H^i \vec{u}_g) C_i] \\ & - \vec{\nabla} \cdot [\epsilon(\sigma D_w^i + f H^i D_g^i) \vec{\nabla} C_i] - B_i(C_1, C_2, \dots, C_N) = 0, \end{aligned} \quad (1)$$

$$\frac{dC_{si}}{dt} = (K_d^i C_i - C_{si})/T_i, \quad (2)$$

where C_i is the concentration of species i in the water, C_{si} is the concentration of species i sorbed onto the soil grains, ϵ is the porosity, σ is the water saturation, f is the air saturation, H^i is the Henry's law coefficient, ρ_b is the matrix bulk density, K_d^i is the equilibrium sorption coefficient, \vec{u}_w is the water-phase velocity, \vec{u}_g is the gas-phase velocity,

* Presumably, this observation reflects different material properties (e.g., pores, grains, cracks, etc.) of the bulk material which have various characteristic sizes. Appropriate characterization would facilitate a comprehensive theoretical treatment.

D_w^i is the water-phase diffusivity, D_g^i is the gas-phase diffusivity, B_i is the nonlinear term describing reactions between species i and the other components, t is the time, and T_i is the time constant for sorption.

The modus operandi for solving these equations is as follows. First, we approximate \mathcal{L}_i by a finite-difference operator, \mathcal{L}_i^d . Then a two-step iterative process is employed at each time level. First, we split the operator

$$\mathcal{L}_i^d = \hat{\mathcal{L}}_i^d + \tilde{\mathcal{L}}_i^d,$$

where we define

$$\begin{aligned} \tilde{\mathcal{L}}_i^d = & A_i^{n+1} \tilde{C}_i^k - A_i^n C_i^n - Q_i^n + \frac{\Delta t}{\Delta \Omega} \sum_{s=1}^6 (u_w + H^i u_g)_s \tilde{C}_{is} \Delta A_s \\ & - \sum_{s=1}^6 \epsilon (\sigma D_w^i + f H^i D_g^i)_s \frac{\Delta A_s}{\Delta x_s} (\tilde{C}_{is} - \tilde{C}_s) - \frac{\epsilon \sigma}{2} \rho_w (B_i^n + \tilde{B}_i^{k-1}) \Delta t, \end{aligned}$$

and

$$\hat{\mathcal{L}}_i^d = A_i^{n+1} C_i^{n+1} - A_i^{n+1} \tilde{C}_i^k - \frac{\epsilon \sigma}{2} \rho_w \Delta t (B_i^{n+1} - \tilde{B}_i^{k-1}).$$

In these equations, the superscript n refers to the time level n , and $n+1$ refers to the next time point, $t^{n+1} = t^n + \Delta t$. The current time step is denoted by Δt , and the overscript, $\sim k$, refers to an intermediate value between time levels n and $n+1$. Note that the overscripted terms cancel in the sum \mathcal{L}_i^d . The area of the s -th face of a grid cell is denoted by ΔA_s , and $\Delta \Omega$ is the grid cell volume. The notation Δx_s is the distance between cell centers on the s -th face of each grid cell, ρ_w is the water density, and \sum_s represents the summation over the faces of a grid cell. The Q_i^n represents an expression which involves the diffusion into and out of the soil particles and which only involves quantities evaluated at the previous time level, t_n . It originated with the terms involving C_{is} . These were eliminated by use of equation (2) and the resulting terms at time level t_n were gathered together and called Q_i^n , with the other terms retained in the equations. Finally, we define

$$A_i = \epsilon \sigma + \epsilon f H^i + \rho_b K_d^i \left(1 - \frac{T_i}{\Delta t} (1 - e^{-\Delta t/T_i})\right).$$

The solution of equations (1) and (2), as approximated and reformulated, is accomplished by setting $\tilde{\mathcal{L}}_i^d$ and $\hat{\mathcal{L}}_i^d$ each to zero. From the knowledge at previous times, $\tilde{\mathcal{L}}_i^d = 0$ is solved for \tilde{C}_i^k . This step emphasizes the transport processes in (1). Then $\hat{\mathcal{L}}_i^d = 0$ is solved. This step emphasizes the reactions between species. In this equation, \tilde{B}_i^{k-1} is evaluated using the \tilde{C}_i^{k-1} values. The initial conditions for each time step are $\tilde{C}_i^{k-1} = C_i^n$. In order to solve self-consistently for the C_i^{n+1} , the term B_i^{n+1} must be evaluated at the advance time t_{n+1} . To accomplish this solution, we expand B to linear order in a Taylor's expansion. Thus we take

$$\hat{\mathcal{L}}_i^d \approx A_i^{n+1} C_i^{n+1} - A_i^{n+1} \tilde{C}_i^k - \frac{\epsilon \sigma}{2} \rho_w \Delta t \left(B_i^k - \tilde{B}_i^{k-1} + \sum_j \frac{\partial \tilde{B}_i^k}{\partial C_j} (C_j^{n+1} - \tilde{C}_j^k) \right).$$

This approximation to the $\hat{\mathcal{L}}_i^d = 0$ is iterated in each cell until the change in the C_j^{n+1} falls below a prescribed tolerance, usually of the order of 10^{-12} to 10^{-15} . Note that the solution at each step involves the solution of a set of N , simultaneous, linear equations for the variables C_j^{n+1} , $j = 1, \dots, N$. Currently, $N = 6$. Next $\tilde{\mathcal{L}}_i^d = 0$ is resolved with the converged values just obtained used to compute the values of \tilde{B}_i^{k-1} in that equation. This process is continued until convergence on Eq. (1) is occurs. The procedure then starts over for the next time step.*

Presentation by Alan Bishop

Title: Nonequilibrium Phase Transitions (and Phases)

The topic of this talk is the subject of a project funded out of the Director's reserve and will involve a focal group and an interior/exterior seminar series. The other participants are Fred Cooper, Emil Mottola, Salman Habib, and Wojiceh Zurek. The aim of this project is a combined experiment-theory -simulation strategy to determine the physical principles, the underlying structure, and the dynamics of nonequilibrium phase transitions and phases. A further aim, in tune with our multiscale theme, is "closing the loop" of the interplay between the microscopic scale, the mesoscopic scale, the macroscopic scale, and experiments by means of a modeling-validation-prediction method. The phrase "interdisciplinary synergism and impact" was used to summarize the following impacts:

heavy-ion physics, AOT	:	quark-gluon plasma
ion beam	:	storage ring/proton radiography
materials science, MST, P	:	texture, aging, deformation, failure
condensed matter, T, STC	:	HTC, surfaces/films, complex fluids
bioscience	:	protein structure/dynamics, biominetics
chemistry, CMS	:	polymers, reaction diffusion
ocean dynamics, CNLS, HMFC	:	eddies, vortices
astronomy	:	plasmas
cosmology	:	early universe

The topics to be focused on were reported to be space (1,2, and 3 dimensions) and time, with the study encompassing both open and closed systems.

* It is my impression that the spatial dependence of the problem is hidden in Q_i^n so that this procedure is an explicit difference scheme. If the linear approximation applied to $\hat{\mathcal{L}}_i^d$ were applied directly to \mathcal{L}_i^d , then by the solution of the N , simultaneous, linear equations in each cell for the different species concentrations, we would have a straightforward explicit difference approximation to the problem. The problem which arises is the nonlinear dependence of B on the C 's at the forward time. It is for this reason, and perhaps there are stability concerns which were not mentioned, that the elaborate iteration scheme was used. It is often the case that higher-order schemes like adaptive step size, Runge-Kutta for nonlinear ordinary differential equations can provide efficient procedures. Perhaps those of us who specialize in such matters can make some useful suggestions here.

- TOPOLOGICAL (esp. “Kosterlitz-Thouless”) : e.g., condensed matter/materials
flux order/flow
surface morphology/growth
fracture/friction
shear bands/deformation zones
- “LANDAU-GINZBURG” coarse-grained : solid-solid PTs
annealing/quenching/ripening
nucleation/spinodal
complex fluids/multiphase flow
granular flow
- LOW T, QUANTUM : mesoscopic
quantum tunneling/PTs
- “NONEQUILIBRIUM” : time and opportunity [theory, simulation, experiment (spallation neutrons)]
AFM/STM, ultrafast(picoseconds), HMFC

The speaker then summarized the topics as being described by “nonlinear, quantum chaos, stochastic, nonadiabatic, glassy, multiscale ... history.” In more detail, Alan then talked about the inter-relation between nonlinear and nonequilibrium. In his view, it is competing interactions that are important here, *e.g.*, coupled fields, time scales, spatial scales, noise, and disorder. All these taken together lead to mesoscopic-scale phenomena such as textures*, landscapes**, self-assembly, patterns, glassy†, stick-slip, and metastability. One idea is to use statistical or average measures of the mesoscale phenomena and to try to relate them to macroscopic functionalities such as pattern recognition and collective structures. A problem here is to identifying a structure out of a noisy background.

Bishop then moved on to a discussion of collective coherent structures and internal noise. He raised the question of how to move from the Kuramoto-Sivashinski equation,

$$\partial_t h = -\nu \partial_x^2 h - \kappa \partial_x^4 h - \frac{\lambda}{2} (\partial_x h)^2$$

to a noise Burgers equation

$$\partial_t h = \nu_{\text{eff}} \partial_x^2 h + \frac{\lambda_{\text{eff}}}{2} (\partial_x h)^2 + \eta(x, t).$$

He showed a figure of spatio-temporal chaos produced by KS (Kuramoto-Sivashinski) dynamics. Here the cellular patterns are slowly changing in time.

Next, the speaker turned to a discussion of “mound” morphology or, more formally, the modeling and simulation of surface growth. Included in this topic are (i) roughing/smoothing/melting transitions (molecular beam epitaxy), (ii) deposition/emission (particle flux) and surface diffusion, (iii) kinetic/thermodynamic/thermodynamic stability, (iv)

* See the presentation by Pieter Swart in Section 4.

** See the presentation by Hans Frauenfelder in Section 4.

† See the presentation by David Sherrington in Section 3.

reaction-diffusion, *e.g.*, biomineralization, (v) Langevin/kinetic dynamics, and (vi) solid-on-solid *etc.* The work of Villain, Plischke and Zangwill was alluded to. An important governing equation is, for example,

$$\frac{\partial h}{\partial t} = \nu \nabla^2 h + \lambda (\vec{\nabla} h)^2 - \kappa \nabla^2 (\nabla^2 h) + \sigma \nabla^2 [(\vec{\nabla} h)^2] + \dots + \mathbf{F} + \eta,$$

where h refers to the height, and $\kappa \geq 0$. Special cases are the Edwards-Wilkinson equation, $\lambda = \kappa = \sigma = 0$ and the KPZ equation, $\kappa = \sigma = 0$. It seems that pyramids, mounds, hillocks *etc.* occur. Some pictures of actual occurrences on iron and some results produced by MBE (molecular beam epitaxy) were shown. Multiple space/time scales enter into this problem. The work of H. E. Stanley on noisy reduced models was mentioned here. The occurrence of disorder in the step height was also mentioned. The example of the random phase sine-Gordon model was cited, as well as the problems of the random-field XY model, pinned charge-density waves, spin glasses, and vortex pinning in superconductors. In this area, attention was focused on the Hamiltonian,

$$H = \frac{1}{2} \sum_{\langle i, j \rangle} (k_i - k_j)^2 - V_0 \sum_i \cos(k_i - k_i^0) + \text{dynamics, forcing terms } \dots,$$

where $\langle i, j \rangle$ means nearest neighbor pairs, and the k_i^0 are quenched random variables. It is of interest to investigate the ergodic and nonergodic regions in temperature and potential strength, V_0 , space.

At this juncture, the attention of the audience was drawn to the work of C. M. Zaremba *et al.* on the topic of the critical transitions in the biofabrication of abalone shells and flat pearls. A couple of nice schematic diagrams were shown to illustrate the structure of abalone shells and abalone flat pearls. It seems that, by changing the protein which nucleates the growth, it is possible to change the growth patterns.

A further illustration was given by a side-by-side comparison of the experimental results of Kwok *et al.* and the computer simulation of Dominguez *et al.* of the voltage-current characteristics (at three temperatures) over the region where a melting transition with internal fields occurred. The two results were qualitatively very similar. It was explained that the linear regime is because the flux lines order among themselves and flow together.

As a final illustration, we saw pictures of twin and tweed textures in perovskite oxides. The ordering of changes is the underlying driving force.

In summary Bishop said that the basic topic of this effort is “what is the nonlinear, nonequilibrium, statistical mechanical principles of mesoscopic self-organization?”* He

* Certainly, this theme is one that has been repeatedly considered in this ongoing series of multiscale seminars. It is particularly germane to the class of topics where there is one spatially dispersed mesoscopic scale. Strictly speaking, for the examples of twin and tweed textures, one must add an additional step or steps as there is more than one mesoscopic scale. It appears that each one drives the next one, just as the microscopic-scale behavior drives the first mesoscopic-scale behavior.

points out that the answer to this question is relevant far beyond what one might suppose, as it has potential applications in biology, oceanography and cosmology. The proposal is to approach these problems by combining our detailed knowledge of both materials science and solid state physics to illuminate the answer to this question.

Presentation by David Sharp

Title: Multiscale Science for Science Based Stockpile Stewardship

Dave Sharp began his talk by making a few remarks on how to present scientific ideas to administrators. He recommend not using technical jargon (unless you know your audience is specialized in that area) and to keep the overhead transparencies clear and not have too many points on each one. His topic was to describe a multiscale project which has been funded for 5 years at a million dollars per year. He and Len Margolin are co-principal investigators for this project. Since not everyone in our seminar group may be familiar with all the members of the project and their special areas of expertise, here follows his list and brief description of the team members.

Fluids

- D. H. Sharp, theoretical and numerical fluid dynamics, multiphase flows, turbulence modeling, and applied mathematics
- F. H. Harlow, theoretical and numerical fluid dynamics, multiphase flows, and turbulence modeling
- T. T. Clarke, theoretical and numerical fluid dynamics, turbulence modeling, and direct numerical simulation
- C. S. Cranfill, numerical fluid dynamics, multiphase flows, turbulence modeling, weapons physics, and code development
- T. C. Wallstrom, numerical fluid dynamics, and applied mathematics

Materials

- L. G. Margolin, fluid dynamics, multiphase flows, constitutive modeling, weapons physics, and code development
- B. L. Holian, solid dynamics and fracture mechanics, and molecular dynamics models
- P. S. Lomdahl, solid dynamics and fracture mechanics, and molecular dynamics models
- J. E. Hammerberg, solid dynamics, molecular dynamics models, and nuclear weapons physics
- D. Tonks, solid dynamics, damage theory, and fracture mechanics

Dave said that the problem under consideration was the application of multiscale science to “mix” processes in nuclear weapons. Mix is a process in which distinct substances are combined into some aggregate material. Examples of mix are cream in coffee, and vegetable soup. In the case of cream in coffee, the mixture is at the molecular level. In the case of vegetable soup this is not the case, as lumps of vegetable remain in the soup. In our context here at Los Alamos, the mix results from shock compression of metal shells, which causes ejecta, spall, and hydrodynamic instabilities. We saw a nice slide from a Pegasus experiment by Danny Sorenson *et al.* of a tin cylinder imploding. Various ejecta were seen,

and a dependence on the preparation on the surface was pointed out. This feature is one which can change with the aging of the stockpile of nuclear weapons and has an important effect on the performance of nuclear weapons. Specifically, mix affects the thermonuclear burn, and hence the weapon's performance. A predictive science of weapons performance is not possible without a handle on the mix problem.

The amount of mix depends on the physical state of the weapon. The relevant factors are the following: (i) the degree of roughness of the metal surfaces, (ii) the metallurgical state (volume texture, *etc.*), and (iii) large-scale features such as the condition of joints and welds, *etc.* These factors may change as a result of aging or remanufacture. The speaker said that it is these issues which make this project relevant to a central part of the science-based stockpile stewardship mission. That mission is, namely, to assess safety, reliability, and performance of nuclear weapons in the absence of full-scale testing.

Sharp said that there are two objectives of this project. The scientific objective is to create and to validate predictive models for fluid and materials mix, based on micro-physical descriptions of key processes. The technology objective is to transfer key features of improved models to design and assessment codes. Here the output should meet the needs of the downstream user! Success is expected based on (i) past successes of the team in the subject area of this project, (ii) new ideas and new methods (multiscale science), and (iii) some shift of emphasis from deterministic prediction to stochastic prediction of outcomes (*i.e.*, yields, *etc.*) and their uncertainties.

Next the speaker discussed the Richtmyer-Meshkov instability. This phenomenon describes the following situation. A shock wave collides with a material interface and is refracted. The reflected wave may be either a shock or a rarefaction depending on the fluid parameters and the shock strength. The instability consists of the growth in time of perturbations at the material interface. In the case illustrated, the net result was a spike with a cap of mushroomlike cross section of a heavy gas being injected into the lighter gas. A key question is "what is the growth rate of this instability?" There has recently been a breakthrough in this regard. Agreement has been achieved between experiment and theoretical computations for the first time. This work used multiscale analysis of the motion of the interface in combination with the use of modern computer algorithms, such as front tracking and adaptive mesh refinement,* which can utilize this information.

Another important point here is "what is multiscale science?" This term is meant to refer to the analysis of problems whose solution is determined by the interaction of physical processes that occur on widely different scales of length and time. The main difficulty is that feasible computations do not allow the smallest-scale (microscopic) and the largest-scale (macroscopic) processes to be simultaneously resolved in a single calculation. A multiscale science solution starts with a detailed (frequently statistical) model of the small-scale processes. The next step** is a coarse-graining step to represent correctly and adequately the influence of the small-scale processes on the large-scale processes.

To tie things together, Sharp explained that mix is a multiscale problem. On the macroscopic scale, there are phenomenological models of complex materials and fluid phenomena. Examples are (i) multiphase and turbulent fluid flow and (ii) elasto-plastic flow

* See the presentations in Section 2.

** This step, in this area, is very widely sought after. It is, so to speak, the holy grail.

of real materials. On the microscopic scale, there are (i) the small-scale fluid structures like droplets, jets and vortices and (ii) texture, porosity, grain size distributions, voids, and microfracture in metals.

The research program for this project is built around the dramatic, recent progress in multiscale science. In the theoretical region, there are the renormalization group ideas*, there is progress on homogenization** and on closure relations. In the area of computer simulation, there are the front tracking methods, AMR and molecular dynamics. These are now capable of making the more refined computations necessary to validate the models. In the area of statistical physics, models are developed (or under development) for microphysics, microfractures, voids, the brittle-ductile transition, and small-scale fluid structures. Sharp said he has been developing a statistical mechanics of coherent structures like bubbles, grains, *etc.* First, identify the coherent structures; second, look at the interactions (bubble mergers); third, look at an ensemble of these, governed by two-bubble interactions; and fourth, develop the constituent equations. In this way, he hopes to develop useful statistical physics models.

The speaker told us that the expected benefits and impact of this project would be that a predictive theory of mix would allow us (i) to identify factors associated with aging and with the remanufacture that affect weapons performance, (ii) to estimate the importance of these factors quantitatively, and (iii) to use variance reduction methods in the remanufacturing of weapons that are less sensitive to the uncertainties in the identified factors. He further stated that this capability will provide a scientific basis for allocating future science-based stockpile stewardship resources so as to produce a maximum reduction in the uncertainties concerning weapons performance.†

Finally, Sharp drew our attention to the added value attributable to LDRD. Specifically, by the development of multiscale science essential for the science-based stockpile stewardship program, this LDRD project could lead the way toward (i) improved methods for risk assessment and risk management based on more reliable probabilistic estimates of the performance of complex technologies and (ii) enhanced capabilities in other important areas of basic and applied science within the Laboratory mission, such as environmental remediation, design of advanced materials, and climate modeling.

* See the presentation of George Baker in Section 5.

** See the presentation of Mac Hyman, Section 3.

† Presumably only in the areas impacted by mix effects.

This report has been reproduced directly from the best available copy.

It is available to DOE and DOE contractors from the Office of Scientific and Technical Information, P.O. Box 62, Oak Ridge, TN 37831. Prices are available from (615) 576-8401.

It is available to the public from the National Technical Information Service, US Department of Commerce, 5285 Port Royal Rd. Springfield, VA 22616.

Los Alamos
NATIONAL LABORATORY

Los Alamos, New Mexico 87545